UNIVERSIDADE FEDERAL DE SÃO CARLOS
CENTRO DE CIÊNCIAS EXATAS E DE TECNOLOGIA
PROGRAMA DE PÓS-GRADUAÇÃO EM ENGENHARIA QUÍMICA

Desenvolvimento de Reator Eletroquímico de Leito Particulado para Processo Hidrometalúrgico de Produção de Cobre

PEDRO HENRIQUE DE BRITTO COSTA

SÃO CARLOS - SP
2014

UNIVERSIDADE FEDERAL DE SÃO CARLOS
CENTRO DE CIÊNCIAS EXATAS E DE TECNOLOGIA
PROGRAMA DE PÓS-GRADUAÇÃO EM ENGENHARIA QUÍMICA

Desenvolvimento de Reator Eletroquímico de Leito Particulado para Processo Hidrometalúrgico de Produção de Cobre

Pedro Henrique de Britto Costa

Tese apresentada ao Programa de Pós-Graduação em Engenharia Química da Universidade Federal de São Carlos, como parte dos requisitos para a obtenção do título de Doutor em Engenharia Química.

Orientador: Prof. Dr. Luís Augusto Martins Ruotolo

SÃO CARLOS - SP
2014

Ficha catalográfica elaborada pelo DePT da Biblioteca Comunitária/UFSCar

C837dr

Costa, Pedro Henrique de Britto.
Desenvolvimento de reator eletroquímico de leito particulado para processo hidrometalúrgico de produção de cobre / Pedro Henrique de Britto Costa. -- São Carlos : UFSCar, 2014.
117 f.

Tese (Doutorado) -- Universidade Federal de São Carlos, 2014.

1. Engenharia eletroquímica. 2. Reator eletroquímico. 3. Eletrodo de leito pulsante. 4. Eletrodo de leito de jorro. 5. Eletrorrecuperação de cobre. 6. Hidrometalurgia. I. Título.

CDD: 660.297 (20ª)

MEMBROS DA BANCA EXAMINADORA DA TESE DE DOUTORADO DE PEDRO HENRIQUE DE BRITTO COSTA, APRESENTADA AO PROGRAMA DE PÓS-GRADUAÇÃO EM ENGENHARIA QUÍMICA DA UNIVERSIDADE FEDERAL DE SÃO CARLOS EM 22 DE AGOSTO DE 2014.

BANCA EXAMINADORA:

Luís Augusto Martins Ruotolo
Orientador, UFSCar

Eliane Bezerra Cavalcanti
UNIT

Alexandre Argondizo
UNIFESP

José Mario de Aquino
UFSCar

José Carlos Gubulin
UFSCar

Dedico este trabalho aos meus pais
Pedro Alexandrino (in memorian) e Maria Helena,
com todo meu amor e gratidão por
tudo o que fizeram por mim ao longo desses anos
e à Clarice pelo amor e companheirismo
em todos os momentos.

AGRADECIMENTOS

Agradeço aos meus pais Pedro Alexandrino (*in memorian*) e Maria Helena por todo o suporte, apoio e carinho. São meus exemplos de dignidade, determinação e perseverança. Ao meu pai por ter sido a melhor pessoa que conheci e por ter feito o máximo que pôde para me proporcionar tudo. À minha mãe pela força magnífica em momentos extremamente difíceis, além de sempre me encorajar a tomar as decisões mais difíceis. Minha gratidão e admiração por vocês é eterna!

À Clarice, por compartilhar sua vida comigo e me permitir compartilhar da minha. Pela força, compreensão, carinho e amor ao longo desses anos. A vida não é simples, muito menos fácil, mas ao seu lado, ela se torna muito mais simples e fácil. Te amo!

Ao Prof. Luís Augusto pelo exemplo de dedicação e paixão pelo que faz. Agradeço também a todo o ensinamento a mim dispensado ao longo destes muitos anos de orientação, que como fruto surgiu uma grande amizade.

Aos Professores Gubulin e Alexandre Argondizo pelas importantes sugestões e contribuições realizadas durante este trabalho. Ao Prof. Edenir pelas importantes contribuições no planejamento de experimentos.

Ao Engenheiro Tone Takayama Filho, da Votorantim Metais Zinco, por ter nos recebido tão bem na Votorantim e pelas contribuições com o trabalho.

A todos os amigos do LATEA, que fiz ao longo de todos esses anos.

A todos os amigos do ITEMM e da Moura.

Aos funcionários do Departamento de Engenharia Química, em especial ao Oscar e ao Adílson pela prestação de socorro nos momentos imprevistos e à técnica Alyne pela ajuda no laboratório e análises de MEV.

Ao Programa de Pós Graduação em Engenharia Química da UFSCar e em especial às funcionárias da secretaria da pós-graduação por toda a atenção.

Ao Conselho Nacional de Desenvolvimento Científico e Tecnológico - CNPq pela bolsa de estudo e recursos concedidos para a pesquisa.

À Coordenação de Aperfeiçoamento de Pessoal de Nível Superior - Capes e à Fundação de Amparo à Pesquisa do Estado de São Paulo - FAPESP pelos recursos concedidos para a pesquisa.

A todos que de alguma forma participaram da realização deste sonho.

Muito obrigado!!!

NOMENCLATURA

Letras latinas

C_s	Concentração de eletrólito suporte	$[ML^{-3}]$
C_{ac}	Concentração de ácido sulfúrico	$[ML^{-3}]$
CE	Consumo energético	$[L^2T^{-2}M^{-1}]$
CE	Current efficiency	[-]
e	Espessura do reator	[L]
E	Potencial de eletrodo	$[L^2MT^{-3}I^{-1}]$
E_{cell}	Potencial de célula	$[L^2MT^{-3}I^{-1}]$
EC	Eficiência de corrente	[-]
EC	Energy consumption	$[L^2T^{-2}M^{-1}]$
F	Constante de Faraday	$[ITN^{-1}]$
i	Densidade de corrente elétrica	$[IL^{-2}]$
i_0	Densidade de corrente de troca	$[IL^{-2}]$
I	Corrente elétrica	[I]
I_{lim}	Corrente limite	[I]
m_{cf}	Mass deposited on the current feeder	[M]
R	Constante universal dos gases	$[ML^2T^{-2}\theta^{-1}N^{-1}]$
t	Tempo	[T]
t_f	Tempo de leito fluidizado	[T]
t_p	Tempo de leito fixo	[T]
T	Temperatura	[θ]
v	Velocidade de escoamento	$[LT^{-1}]$
x	Direção no sentido do campo elétrico	[L]

Y	Rendimento espaço-tempo	$[ML^{-3}T^{-1}]$
Y	Space-time Yield	$[ML^{-3}T^{-1}]$
z	Número de elétrons envolvidos na reação	[-]

Letras gregas

α_C	Coeficiente de transferência de carga catódico	[-]
α_A	Coeficiente de transferência de carga anódico	[-]
η	Sobrepotencial	$[L^2MT^{-3}I]$
ϕ_s	Potencial elétrico na solução	$[L^2MT^{-3}I^{-1}]$
ϕ_m	Potencial elétrico na fase sólida	$[L^2MT^{-3}I^{-1}]$

Abreviaturas em português

ELF	Eletrodo de leito fluidizado
ELJ	Eletrodo de Leito de Jorro
ELP	Eletrodo de Leito Pulsante
ELV	Eletrodo de Leito Vórtice
MEV	Microscopia Eletrônica de Varredura
RDH	Reação de Desprendimento de Hidrogênio

Abreviaturas em inglês

CCRD	Central Composite Rotatable Design
DSA®	Dimensionally Stable Anode
FFD	Full Factorial Design
HER	Hydrogen Evolution Reaction
PBE	Pulsed-bed electrode
RSM	Response Surface Methodology
SEM	Scanning Electron Microscopy

LISTA DE FIGURAS

LISTA DE TABELAS

RESUMO

Os processos hidrometalúrgicos atuais para produção de metais tais como zinco, cobre, níquel e cobalto, entre outros, empregam grandes tanques de eletrodeposição que demandam uma grande área devido à baixa corrente elétrica que deve ser aplicada para a obtenção de um depósito de qualidade. Neste projeto de pesquisa propõe-se o desenvolvimento de um novo equipamento para a eletrorrecuperação de metais a partir do extrato lixiviado do minério visando superar as limitações apresentadas anteriormente. Os equipamentos propostos, denominados reatores eletroquímicos tridimensionais de eletrodo de leito pulsante (ELP) e de eletrodo de leito de jorro (ELJ), são compostos por pequenas partículas que proporcionam uma área superficial específica elevada em pequenos volumes de equipamento, permitindo-se assim que valores de corrente elevados possam ser aplicados, diminuindo assim a necessidade de grandes tanques de eletrorrecuperação. Os diferentes eletrodos foram analisados em função da eficiência de corrente (EC), consumo energético (CE) e rendimento espaço-tempo (Y) do processo de eletrodeposição. No reator com ELP foram realizados planejamentos estatísticos para se determinar a condição otimizada do processo além de se conhecer qual a influência de cada variável independente no processo. Para isto foram realizados experimentos variando-se a densidade de corrente elétrica (i), o tempo de leito fixo (t_p), o tempo de leito fluidizado (t_f), a concentração de eletrólito suporte (C_s) e a espessura do reator (e). Verificou-se que o tempo de leito fluidizado apresenta efeito negativo no processo, devendo ser reduzido ao mínimo valor possível, que seja suficiente para realizar sua função de movimentar e homogeneizar as partículas, evitando aglomeração e curto-circuito. Verificou-se que um valor de t_f igual a 2 s é suficiente para isto, desde que o pulso seja realizado de forma a misturar as partículas, evitando um curto-circuito. Durante o estado de leito fixo, melhores taxas de eletrodeposição de metais foram obtidas e, por esta razão, a variável t_p deve ser maximizada. A i também deve ser maximizada para reduzir, ou mesmo impedir, a existência de zonas anódicas durante a fluidização do leito. Uma vez estabelecido que os baixos valores de EC foram atribuídos à existência de zonas anódicas, ficou evidente a necessidade de se reduzir a concentração de ácido sulfúrico (eletrólito suporte) ao limite mínimo de 100 g L^{-1}, sendo que valores menores causam um aumento demasiado do potencial de célula e como consequência um crescimento dendrítico do eletrodepósito de cobre sobre a partícula, provocando o curto-circuito do sistema devido ao contato de eletrodepósito com o contra-eletrodo. Por fim, a condição ótima foi encontrada através do uso de técnicas estatísticas. Uma condição necessária para se melhorar a performance

do reator eletroquímico foi a diminuição da espessura do reator, de maneira a melhorar a distribuição do sobrepotencial no eletrodo, diminuindo zonas de dissolução anódica. A condição ótima obtida para a eletrorrecuperação de cobre em ELP foi de 2600 A m^{-2}, t_p = 54 s,116 g L^{-1} de H_2SO_4 e espessura de 2,4 cm, proporcionando 100% de *EC*, 1,7 kWh kg^{-1} de *CE* e 76 kg $m^{-3}h^{-1}$ de *Y*, valores superiores aos obtidos no processo convencional da indústria hidrometalúrgica. A partir da experiência adquirida com o ELP, decidiu-se estudar a utilização do ELJ, uma vez que este reator também apresentaria características hidrodinâmicas promissoras para a eletrorrecuperação de cobre. Desta forma, foram estudadas as variáveis independentes densidade de corrente elétrica (*i*), concentração de eletrólito suporte (C_s), pH, temperatura do eletrólito (T) e espessura do eletrodo (e) sobre a *EC*, *CE* e *Y* do processo. No caso do ELJ foi utilizado como eletrólito suporte o sulfato e sódio e estudou-se o efeito do pH sobre o processo. Verificou-se que, da mesma forma que o observado para o ELP, a densidade de corrente deve ser maximizada para se evitar zonas anódicas, soluções mais concentradas de ácido favorecem a *EC* e diminuem o potencial de célula, melhorando o *CE*, pHs menores também diminuem o potencial de célula, entretanto interferem de forma negativa na *EC*, sendo que pHs menores que 1,0 devem ser evitados; a temperatura do eletrólito atuou de forma negativa, interferindo mais na reação de dissolução do que na de eletrodeposição. No caso do ELJ, a espessura do eletrodo não apresentou grandes melhorias no processo. A condição ótima obtida foi: 1,8 mol L^{-1} de Na_2SO_4; pH 1,0; T = 40 ºC e *e* = 2,1 cm, que proporcionou 97% de *EC*, 2,7 kWh kg^{-1} de *CE* e 109 kg $m^{-3}h^{-1}$ de *Y*. Com exceção do consumo energético, o ELJ apresentou valores bastante superiores aos encontrados na indústria, inclusive superiores aos obtidos no ELP, uma vez que operou a 100% de *EC* para diversas condições e apresentou rendimento muito superior ao do ELP. Todavia, comparando-se com as necessidades da indústria hidrometalúrgica, o ELP apresentou resultados mais favoráveis do que o ELJ, uma vez que um dos interesses principais da indústria é reduzir o custo do processo, ou seja, a característica mais importante para a indústria hidrometalúrgica de uma forma geral é o consumo energético do processo, de modo que uma diferença de apenas 100 mV no potencial de célula representa uma redução de custos considerável.

ABSTRACT

Typical hydrometallurgical processes for metal production such as zinc, copper, nickel and cobalt, among others, are carried out in huge electrochemical tankhouses since only low current densities can be applied in order to obtain a good deposit quality. In this work, the development of a new equipment was proposed for metal electrowinning from the leached ore extract aiming to overcome the limitations reported. The two pieces of equipment proposed are called three-dimensional electrochemical reactors with pulsed-bed electrode (PBE) and spouted-bed electrode (SBE), which are composed of small particles that provide a great improvement in specific surface area, using only a small amount of reactor volume, allowing high current densities to be applied, consequently diminishing the need for huge electrowinning tankhouses. An analysis and comparison of these two electrodes were based on the dependent variables current efficiency (CE), energy consumption (EC) and space-time yield (Y), that are considered the most important variables affecting electrochemical processes and reactors. Designs of experiments (DoE) were carried out in order to determine the best conditions achievable and also to obtain a deep understanding of the influences of each variable on the electrowinning process. In order to do that, the current density (i), time of packed bed (t_p), time of fluidized bed (t_f), sulfuric acid concentration (C_s) and electrode thickness (e) were studied. It was verified that time of fluidized bed has a negative effect on the process and must be reduced to its minimal value, which is 2 s, that is enough to recirculate and mix the particles in order to prevent from electrode clogging and also short-circuit. During the packed bed, best electrodeposition rates are achieved and it must be increased to its maximum possible value. Current density also must be increased in order to prevent from anodic zones during the fluidization step. Once established that low *CE* values are due to existence of anodic zones, it was clear the need of reducing acid concentration to its minimum value (100 g L^{-1}), since lower values would increase the cell potential (E_{cell}) and cause a dendritic growth that is the major cause of short-circuit. Finally, the best condition was obtained by the union of all this information, allied with the reduction of electrode thickness, in order to make the overpotential profile more even inside the electrode. Thus, the best condition for copper electrowinning using a PBE was 2600 A m^{-2} of i, 54 s of t_p, 116 g L^{-1} of H_2SO_4 and 2.4 cm of electrode thickness, providing 100% of EC, 1.7 kWh $kg^{-1}$of CE and 76 kg $m^{-3}h^{-1}$of Y. These values are considered much superiors to those found in the conventional copper electrowinning processes. From this experience, it was decided to study the copper electrowinning using a SBE which also have promising features in this field. In this way, the independent variables current density (i),

supporting electrolyte concentration (C_s), pH, electrolyte temperature (T) and electrode thickness (e) were studied. It was verified that, in accordance with the results of PBE, the current density must be increased in order to prevent from anodic zones; more concentrated supporting electrolytes improve *CE* and also decrease E_{cell}; low pH values also decrease E_{cell}, although values lower than 1.0 depreciate *CE*; and the electrolyte temperature have more impact in the dissolution rate than in the electrodeposition rate. In this case, the electrode thickness doesn't improve much, thus the best condition obtained for copper electrowinning into the SBE was: 1.8 M Na_2SO_4; pH 1.0; T = 40 ºC and e = 2.1 cm, could achieve 97% EC, 2.7 kWh kg^{-1} CE and 109 kg $m^{-3}h^{-1}$ Y. With exception to the energy consumption, the SBE presented a better performance than the conventional reactors used in industry, even better than the PBE, once it worked at 100% CE in many conditions imposed. It also presented very much higher Y values than the PBE. Even though, taking into account the hydrometallurgical industry needs, the PBE presented results that would attend those needs, once cost is the major issue in most of industry. Moreover, a difference of only 100 mV in cell potential is responsible for a big reduction in energy consumption and, consequently, cost of production.

1 INTRODUÇÃO

Os metais estão presentes na natureza na forma de óxidos e outros compostos em uma concentração geralmente baixa, todavia suficiente para tornar viável a extração do metal e sua comercialização. Dentre os procedimentos de extração dos metais não-ferrosos empregados atualmente, a hidrometalurgia é um processo bastante utilizado que oferece riscos menores ao meio ambiente, quando comparado à pirometalurgia.

A palavra hidrometalurgia é definida como a extração de um metal a partir do seu minério, obtendo-o portanto na sua forma metálica, em um processo em que a água executa um papel indispensável. Segundo (SALAS-MORALES; EVANS; NEWMAN et al., 1997), o processo é geralmente composto por três etapas: calcinação, lixiviação, que pode utilizar solução ácida ou básica, e recuperação química ou eletrolítica (grande maioria dos casos) (SALAS-MORALES; EVANS; NEWMAN et al., 1997). Entretanto muitas empresas utilizam outra sequência de etapas, como exemplo a Votorantim Metais Zinco, que utiliza as etapas lixiviação, flotação, purificação e eletrorrecuperação do metal, item este que se insere dentro da eletrometalurgia. Neste processo, a flotação é utilizada para aumentar a concentração do metal, no caso o zinco, e a purificação para reduzir, algumas vezes a traços, as impurezas prejudiciais ao processo eletrolítico (ALAM; TANAKA; KOYAMA et al., 2007, HERRERO; ARIAS; GÜEMEZ et al., 2010).

A pirometalurgia ainda é um processo bastante empregado, principalmente quando a produção do metal por rota hidrometalúrgica é impossível, devido a compostos insolúveis em água ou mesmo inviável economicamente. Para o cobre, a pirometalurgia, que utiliza temperaturas bastante elevadas para separar o metal do minério é uma rota muito utilizada, pois cerca de 80% das minas de cobre apresentam o composto $CuFeS_2$ como fonte de cobre, o qual não é solubilizado pela lixiviação tradicional (NORGATE e JAHANSHAHI, 2010). Portanto, mesmo gerando uma grande variedade de resíduos, entre eles gases de efeito estufa, em muitos casos a pirometalurgia é o único processo de produção do metal economicamente viável. Uma relevante vantagem da rota hidrometalúrgica consiste na utilização de temperaturas geralmente menores que 60 ºC, resultando em uma economia com relação aos processos supracitados(NORGATE e JAHANSHAHI, 2010).

O nascimento da hidrometalurgia moderna ocorreu em 1887 quando dois processos industriais foram desenvolvidos: o processo de tratamento do minério de ouro por cianetação e o Processo Bayer para a produção de alumina. O primeiro apresentou grande impulso na hidrometalurgia, uma vez que tanques extremamente grandes eram utilizados para lixiviar o minério de ouro com cianeto. O segundo e bastante conhecido Processo Bayer, ainda utilizado nos dias atuais, consiste na lixiviação básica da bauxita em um reator pressurizado e foi inicialmente desenvolvido para a indústria têxtil, tornando-se de suma importância na metalurgia extrativa após a invenção do processo eletrolítico do alumínio em 1886 (HABASHI, 2010).

As indústrias hidrometalúrgicas utilizam eletrodos planos em seus processos de metalurgia extrativa nos quais são aplicadas densidades de corrente da ordem de 300 A m^{-2} (JIRICNY; ROY e EVANS, 2002, PANDA e DAS, 2001, WIECHMANN; MORALES e AQUEVEQUE, 2010). Devido à pequena área superficial proporcionada por este tipo de eletrodo, células eletroquímicas extremamente grandes são requeridas para se obter uma elevada produtividade. Além destas limitações, existem outras desvantagens em se utilizar eletrodos planos, como a necessidade de remover o depósito do substrato, a intensa liberação de vapores ácidos devido ao tamanho das células eletroquímicas, que podem oxidar os contatos elétricos ou mesmo causar danos à saúde, além da necessidade de se utilizar um grande número de placas anódicas (CIFUENTES; ORTIZ e CASA, 2005, EVANS; DING; DOYLE et al., 2005, JIRICNY; ROY e EVANS, 2002, SAN MARTIN; OTERO e CRUZ, 2005, SHAKARJI; HE e GREGORY, 2011, SIGLEY; JOHNSON e BEAUDOIN, 2003, WIECHMANN; MORALES e AQUEVEQUE, 2010). Os eletrodos de PbO_2, geralmente usados nos processos de eletrorrecuperação, tem como principal desvantagem a baixa resistência à corrosão, principalmente durante a manutenção da célula ou remoção do eletrodepósito em que a solução ácida ataca o eletrodo no momento em que não há passagem de corrente elétrica, diminuindo sua vida útil, além de contaminar o depósito catódico devido à incorporação de chumbo (LAFRONT; ZHANG; GHALI et al., 2010, MOSKALYK; ALFANTAZI; TOMBALAKIAN et al., 1999). Aditivos químicos geralmente são utilizados na tentativa de minimizar este problema.

Neste contexto, o eletrodo tridimensional, em particular o eletrodo particulado, apresenta-se como uma alternativa para superar alguns dos problemas associados ao processo convencional. Altas densidades de corrente elétrica (até 4466 A m^{-2}) poderiam ser aplicadas nestes reatores particulados (EVANS; DING; DOYLE et al., 2005, JIRICNY; ROY e EVANS, 2002), sem prejudicar a qualidade do depósito, uma vez que estes eletrodos apresentam elevada área superficial, pela qual a corrente elétrica fornecida é distribuída no meio poroso

(COEURET, 1980, EVANS; DING; DOYLE et al., 2005, JIRICNY; ROY e EVANS, 2002). Além disto, caso as partículas sejam do mesmo material do metal a ser depositado, a etapa de remoção do depósito seria desnecessária, reduzindo bastante os custos com mão-de-obra e sem a necessidade de interrupções da produção (JIRICNY; ROY e EVANS, 2002). Devido à significativa redução do volume do reator, uma substituição do ânodo de chumbo por um que seja dimensionalmente estável poderia se tornar viável e reduzir, ou até mesmo eliminar, a necessidade de aditivos químicos (JIRICNY; ROY e EVANS, 2002, LUPI e PILONE, 1997).

A utilização de reatores tridimensionais também soluciona o problema de vapores ácidos, que podem ser facilmente canalizados e neutralizados, evitando sérios danos à saúde dos operários. Dentre os eletrodos de leito particulado, o de leito fixo tem sido bastante estudado, particularmente na área de tratamento de efluentes, em que a concentração de metais é baixa (EL-SHAKRE; SALEH; EL-ANADOULI et al., 1994, OLIVE e LACOSTE, 1979, RUOTOLO e GUBULIN, 2002, STANKOVIC e WRAGG, 1995). As principais características do leito fixo são a alta condutividade elétrica da fase sólida e o elevado valor do coeficiente de transporte de massa. Essas características promovem altos valores de eficiência de corrente, fazendo com que o leito fixo seja a configuração mais eficiente para a eletrodeposição de metais (EL-SHAKRE; SALEH; EL-ANADOULI et al., 1994, PLETCHER; WHITE; WALSH et al., 1991, RUOTOLO e GUBULIN, 2002, WIDNER; SOUSA e BERTAZZOLI, 1998). Entretanto, quando a concentração do metal é muito alta, o entupimento do eletrodo decorrente da deposição do metal nos seus poros ocorre muito rapidamente, impossibilitando a sua utilização em escala industrial (RUOTOLO e GUBULIN, 2002).

Dentre os eletrodos tridimensionais particulados destacam-se os de leito fixo, fluidizado, jorro e o pulsante, de modo que cada eletrodo apresenta vantagens e desvantagens de acordo com os objetivos de sua utilização e também com relação às variáveis operacionais.

Em um âmbito geral, este trabalho teve como objetivo o estudo da eletrorrecuperação de cobre em eletrodo de leito pulsante e em eletrodo de leito de jorro. Em linhas mais específicas, buscou-se avaliar a influência das variáveis operacionais de cada reator nas variáveis dependentes eficiência de corrente (EC), consumo energético (CE) e rendimento espaço-tempo (Y). As principais metas atingidas neste trabalho estão descritas a seguir:

Realizar triagem das variáveis operacionais do processo para entendimento dos efeitos que as mesmas apresentaram nas variáveis dependentes e entendimento dos fenômenos eletroquímicos;

- Determinar os parâmetros de acordo com os efeitos que as variáveis independentes mais importantes apresentaram sobre o processo;
- Otimizar o processo de eletrorrecuperação de cobre em eletrodo de leito pulsante;
- Estudar e comparar os processos de eletrorrecuperação de cobre em eletrodo de leito de jorro com o eletrodo de leito pulsante.

Organização da Tese

Neste subitem é descrito como a tese foi organizada.

O capítulo 2 apresenta uma revisão bibliográfica sobre os temas cinética eletroquímica de eletrodeposição de metais em soluções concentradas, inovações no processo hidrometalúrgico de eletrorrecuperação de metais e tipos de eletrodos tridimensionais que podem ser aplicados em eletrorrecuperação de cobre.

A triagem das variáveis operacionais do eletrodo de leito pulsante é abordada no capítulo 3. A importância deste capítulo foi a determinação, a partir de um número reduzido de experimentos, de quais variáveis são mais significativas no processo de eletrorrecuperação no ELP e, dependendo da faixa de operação, quais poderiam ser ignoradas nos estudos subsequentes.

O capítulo 4 apresenta um arranjo do planejamento composto central rotacional ortogonal, das variáveis selecionadas no capítulo 3, em busca das melhores condições operacionais do processo de eletrorrecuperação de cobre em ELP. Este capítulo apresenta ainda um estudo sobre a qualidade do depósito obtido, comparando-o com o depósito obtido no eletrodo plano, que simula o processo convencional, porém sem adição de produtos químicos.

O capítulo 5 apresenta os resultados da otimização do processo de eletrorrecuperação de cobre utilizando eletrodo de leito pulsante, através de um planejamento composto central rotacional realizado em um reator com menor espessura. Adicionalmente, neste capítulo é feita uma discussão acerca da utilização de eletrodos dimensionalmente estáveis como ânodos nos processos de eletrorrecuperação de metais.

O capítulo 6 apresenta um estudo sobre a utilização de um eletrodo de leito de jorro para a eletrorrecuperação de cobre e comparação destes resultados experimentais com os experimentos realizados com o ELP, de forma a se estudar mais uma alternativa de leito tridimensional aplicado ao processo de eletrorrecuperação de metais.

Finalmente, no capítulo 7 é feita uma discussão final de todos os resultados obtidos, comparando-se o ELP e o ELJ.

A Figura 1.1 apresenta um fluxograma mostrado como a tese foi organizada e as relações existentes entre os escopos de cada capítulo.

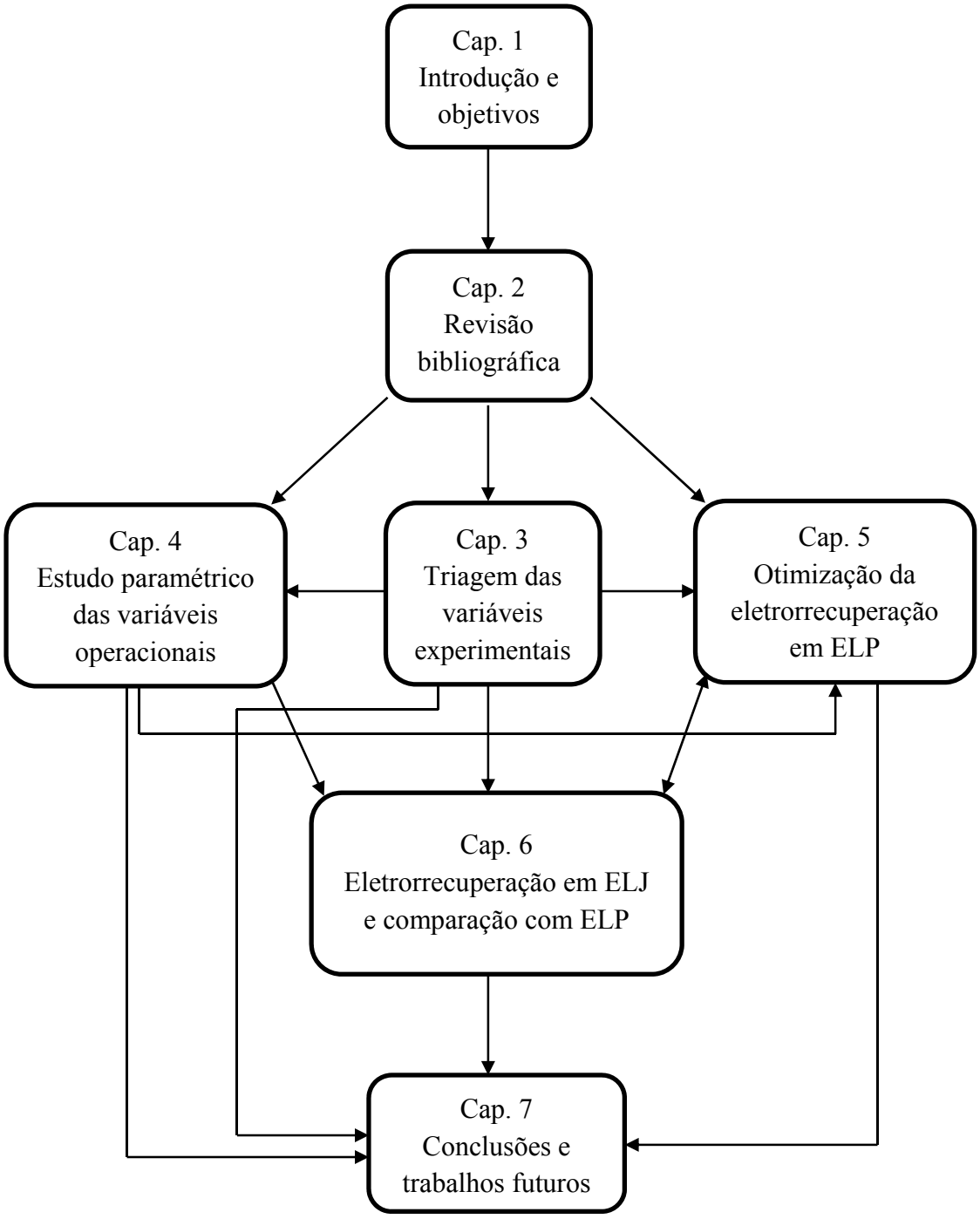

Figura 1.6. Fluxograma ilustrando a organização da tese e as relações entre os capítulos.

2 REVISÃO BIBLIOGRÁFICA

Neste capítulo são apresentados alguns dos conceitos fundamentais relacionados ao processo e reatores estudados nesta tese, além de uma revisão sobre o estado d'arte no tema de eletrorrecuperação de metais utilizando eletrodos tridimensionais particulados.

A eletroquímica é um processo em que o elétron é o principal agente da reação e pode ser entendido com um reagente "limpo", uma vez que não gera subprodutos tóxicos ou inutilizáveis na redução de compostos iônicos. Entretanto, muitas vezes este processo está associado a altos custos operacionais devido ao alto valor da energia elétrica nacional e ao desconhecimento, por parte das indústrias hidrometalúrgicas, de reatores eletroquímicos pouco utilizados, porém com alto potencial inovador. Neste sentido, foi depositada uma patente do reator eletroquímico de leito pulsante, utilizado neste trabalho, para despertar o interesse por parte das indústrias hidrometalúrgicas. Estes reatores apresentam custos operacionais e estruturais consideravelmente inferiores às células eletroquímicas convencionais, que nada mais são que tanques em que estão imersos e justapostos paralelamente diversos eletrodos planos. Desta forma, este capítulo é iniciado pela apresentação das principais vantagens que eletrodos tridimensionais poderiam proporcionar quando comparados a eletrodos planos.

2.1 Eletrodos bi e tridimensionais.

Os eletrodos bidimensionais, geralmente placas planas, são assim chamados porque a eletrodeposição e a distribuição de corrente e de potencial ocorrem somente em duas dimensões, o que torna simples a construção e operação dos reatores eletroquímicos. Entretanto, estes eletrodos apresentam pequena área superficial, que prejudica o transporte de íons metálicos à superfície do eletrodo em situações de baixa concentração de metais, inviabilizando sua utilização. Em soluções concentradas, a utilização deste tipo de eletrodo acarreta em baixo rendimento do reator, uma vez que baixos valores de densidade de corrente podem ser aplicados. Nos eletrodos tridimensionais, por outro lado, a reação ocorre na elevada área superficial proporcionada pelo volume poroso do eletrodo, conforme ilustrado na Figura 2.1. A corrente elétrica é distribuída no volume do eletrodo, permitindo a aplicação de correntes muito mais elevadas sem perder eficiência, como ocorreria no eletrodo plano devido às reações paralelas como a reação de redução da água, também conhecida como a reação de desprendimento de hidrogênio (RDH). Em soluções diluídas, o processo é geralmente

controlado pela transferência de massa, que pode ser consideravelmente melhorada pela utilização deste tipo de eletrodo. No entanto, eletrodos tridimensionais geralmente apresentam maiores problemas com distribuição de potencial e corrente do que os eletrodos bidimensionais; isto se deve primariamente à anisotropia dos eletrodos porosos e de leitos particulados com relação à condutividade do eletrodo, fluxo de eletrólito e concentração das espécies eletroativas (RUOTOLO, 1998).

São utilizados na área da Engenharia Eletroquímica, diversos tipos de reatores eletroquímicos, sendo eles compostos por eletrodos bi ou tridimensionais. A Figura 2.2 apresenta as principais classes desses eletrodos, de acordo com a geometria e fluidodinâmica.

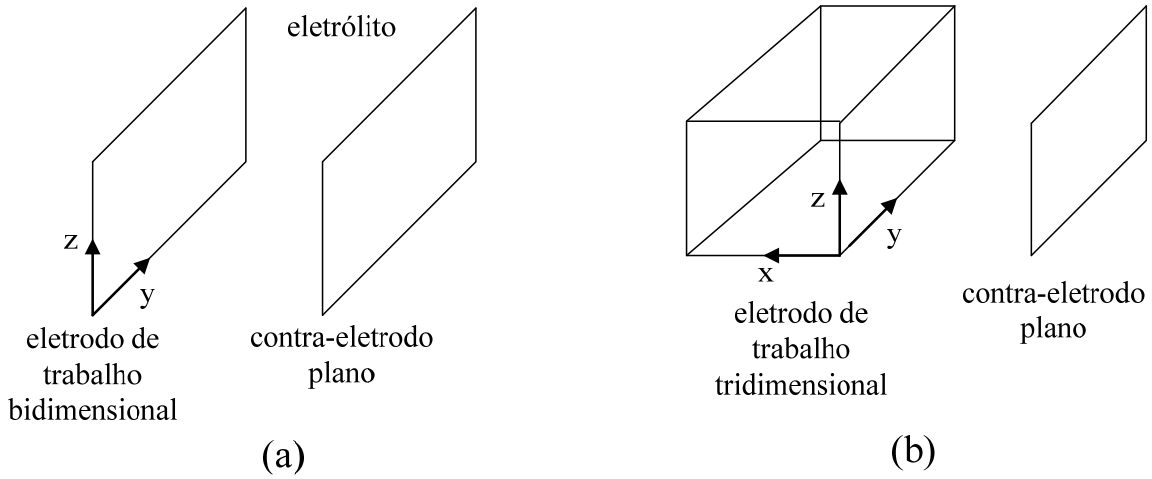

Figura 2.6. Eletrodos a) bidimensional e b) tridimensional.

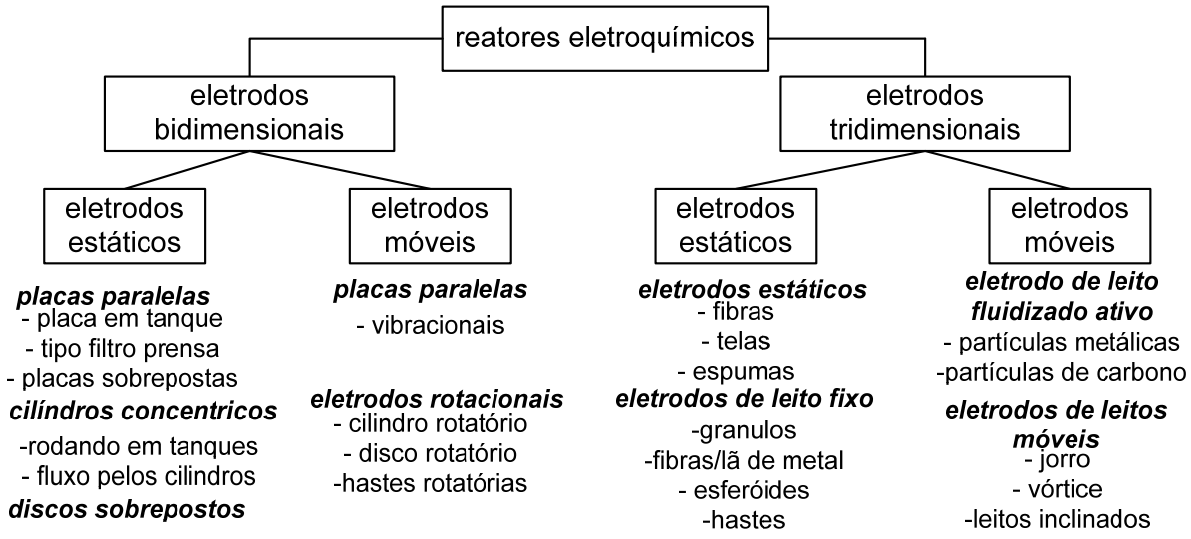

Figura 2.7. Classificação de reatores eletroquímicos em função da geometria do eletrodo e da fluidodinâmica (RAJESHVAR e IBANEZ, 1997).

Dentre os tipos de eletrodos apresentados na Figura 2.2, os que mais se destacam em uma possível utilização para a eletrorrecuperação de metais são os eletrodos tridimensionais particulados, cuja abordagem na utilização é detalhada a seguir.

Os eletrodos particulados de leito fixo apresentam boa condutividade da fase sólida, portanto, altas densidades de corrente podem ser aplicadas mantendo-se altos os valores de eficiência de corrente (EC) (BRITTO-COSTA e RUOTOLO, 2013, COEURET e PAULIN, 1988). Entretanto, isto só é válido para uma pequena fração de tempo, uma vez que rapidamente o material particulado começa a se aglomerar aumentando a perda de carga no reator até impedir a passagem do eletrólito (RUOTOLO, 1998).

No entanto, verifica-se na Figura 2.2 a existência de uma classe de eletrodos conhecida como leito móvel, que compreende os eletrodos de leito fluidizado (ELF), vórtice (ELV), jorro (ELJ) e também o pulsante (ELP), dentre outros. Estes eletrodos apresentam a vantagem de evitar o fechamento dos poros do meio, entretanto isto pode ocasionar menores valores de *EC* pelo fato de apresentar uma descontinuidade da fase sólida. Curiosamente no reator de leito fluidizado, quando utilizado em soluções diluídas, a descontinuidade da fase sólida é contrabalanceada pelo incremento no transporte de massa proporcionado pelo aumento da vazão do eletrólito, fazendo com que exista uma condição operacional que melhora a cinética de eletrodeposição e a eficiência de corrente(SILVA, 2000).

O eletrodo de leito de jorro (ELJ) apresenta uma configuração bastante promissora no processo hidrometalúrgico e pode ser basicamente caracterizado por duas regiões distintas, sendo que a primeira apresenta características eletroquímicas similares àquelas obtidas em um leito fixo, mas sem a aglomeração das partículas que é evitada pelo seu movimento descendente constante na região do ânulo. Na segunda região ocorre o arraste das partículas para a formação do jorro. Entretanto, para soluções muito ácidas, pode ocorrer a dissolução do metal na região central e do jorro, uma vez que estas partículas não estarão em contato constante e, consequentemente, poderão não estar catodicamente polarizadas (COEURET e PAULIN, 1988, EVANS; DING; DOYLE et al., 2005, JIRICNY; ROY e EVANS, 2002).

O eletrodo de leito pulsante (ELP), objeto de estudo deste trabalho, apresenta alternância entre os estágios de leito fixo e fluidizado com pulsos de vazão que impossibilitam a aglomeração das partículas. Adicionalmente, a principal característica deste leito é utilizar o

pulso apenas para se evitar essa aglomeração, de forma que a maior parte do tempo (em alguns casos maior que 90%) o leito encontra-se no estado de fixo, operando com altas densidades de corrente sem perder eficiência. Há estudos em que o leito pulsante operou com eficiências de corrente 25% superiores aos do leito fluidizado, justamente por manter a continuidade do meio poroso durante a maior parte do tempo, diminuindo a ocorrência de regiões com sobrepotencial menor que o potencial de dissolução do metal (BAREAU e COEURET, 1979, COEURET, 1980, HADZISMAJLOVIC; POPOV e PAVLOVIC, 1996).

Existem atualmente poucos estudos sobre a utilização do ELP na hidrometalurgia em escala laboratorial e nenhum estudo em escala piloto ou industrial. Com relação aos eletrodos pulsantes, foram encontrados na literatura apenas três métodos diferentes de se realizar os pulsos, são eles: pulso mecânico (GARFIAS-VASQUEZ; DUVERNEUIL e LACOSTE, 2004), pulso de vazão por válvulas paralelas com sistema de abre/fecha (COEURET e PAULIN, 1988) e pulso de vazão controlado por um inversor de frequência, que se constitui em um método bastante simples e atualmente acessível (ARGONDIZO, 2001).

Com relação à operação destes reatores, há dois modos de se configurar os fluxos de eletrólito e corrente elétrica em um reator eletroquímico, conforme ilustra a Figura 2.3. Na primeira, Figura 2.3 (a), os fluxos de eletrólito e corrente elétrica apresentam a mesma direção ("flow-through electrodes"), ao contrário da configuração de fluxos perpendiculares ("flow-by electrode"), Figura 2.3 (b). Os eletrodos de fluxos paralelos são pouco utilizados, uma vez que a distribuição irregular de corrente e potencial dificulta o aumento de escala. A configuração mais comumente utilizada é a de fluxos perpendiculares por apresentar um maior tempo de residência, possuir um perfil de potencial mais uniforme e uma maior taxa de reação por passo do eletrólito. Os reatores eletroquímicos utilizados neste trabalho que usavam eletrodos tridimensionais estavam configurados em *flow-by* (fluxos perpendiculares).

Os reatores eletroquímicos podem ser operados de duas maneiras distintas: 1) galvanostaticamente, ou seja, a corrente aplicada é mantida constante durante o processo, ou então 2) potenciostaticamente, em que o processo opera a potencial constante. O modo galvanostático, muito utilizado na indústria de galvanoplastia, torna o processamento mais rápido; entretanto, quando são atingidos baixos valores de concentração, ocorre uma diminuição da eficiência de corrente e um consequente aumento do consumo energético devido principalmente ao desvio de uma parcela da corrente para reações paralelas, como a de desprendimento de hidrogênio. No modo potenciostático é aplicado um potencial constante ao

eletrodo, implicando em maiores valores de eficiência de corrente instantânea ao longo do processo, o que faz diminuir o consumo energético instantâneo. Contudo, o tempo de processamento pode tornar-se demasiadamente longo nesse tipo de processo devido às bolhas que se acumulam na superfície do eletrodo (STANKOVIC e WRAGG, 1995).

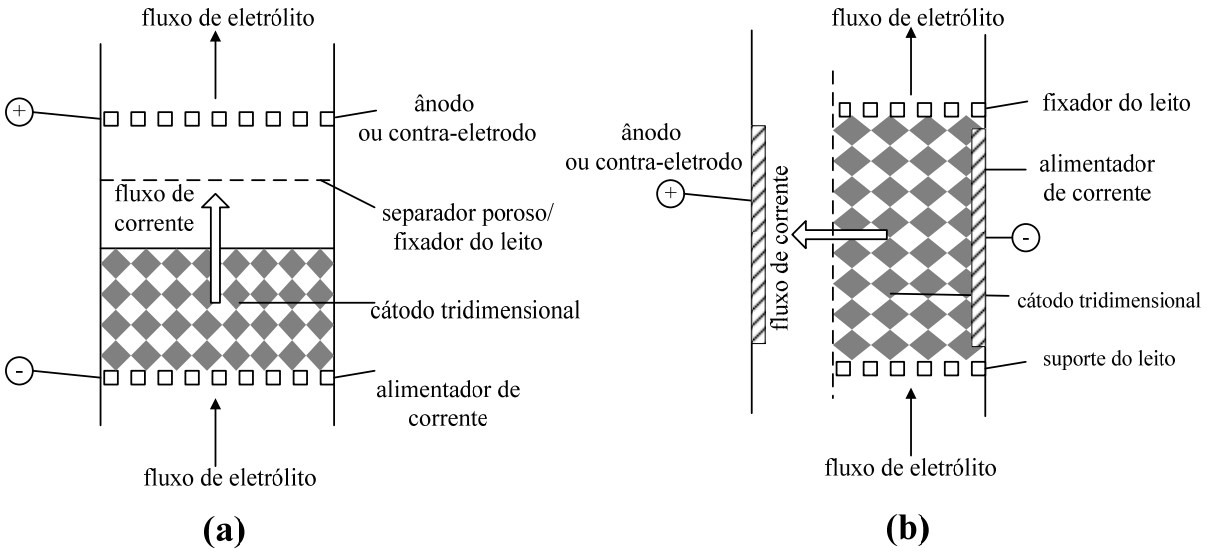

Figura 2.8. Diferentes configurações entre fluxos de corrente e eletrólito: a) eletrodo de fluxos paralelos; b) eletrodo de fluxos perpendiculares (PLETCHER e WALSH, 1990).

2.2 Eletroquímica: aspectos gerais

2.2.1 Cinética eletroquímica

Quando se injeta uma carga elétrica em um eletrodo através de uma fonte externa podem ocorrer três situações(TICIANELLI e GONZÁLEZ, 1998):

1. A carga é transferida na interface eletrodo/solução devido ao deslocamento do potencial de eletrodo do seu valor de equilíbrio através da passagem de uma corrente faradaica. Neste caso, a diferença de potencial através da interface depende da carga injetada, o que ilustra a forma de controlar externamente essa diferença. Neste caso, o eletrodo se diz polarizado.

2. A carga injetada escoa através da interface sendo transferida para alguma das espécies em solução. Assumindo que essa transferência seja infinitamente rápida, será observado que a diferença de potencial através da interface permanece inalterada. Neste caso, o eletrodo se diz *não-polarizado*. Um exemplo desta situação seria um eletrodo de cobre em equilíbrio com uma solução que contém íons Cu^{2+}. Os sistemas comprovadamente estáveis e

que mantêm o potencial inalterado durante o escoamento rápido de cargas injetadas são os mais indicados para serem usados como eletrodos de referência.

3. Quando é aplicada uma diferença de potencial dentro de um intervalo de valores que não induza a ocorrência de uma reação eletródica (corrente não-faradaica) diz-se que o eletrodo está *idealmente polarizado*. Nestas circunstâncias, os fenômenos estão apenas relacionados com a reacomodação de íons e/ou dipolos na superfície do eletrodo.

No caso de processos eletroquímicos de interesse industrial, a situação 1 é a mais importante e, neste caso, a curva de polarização, ou seja, a curva de corrente elétrica em função do potencial de eletrodo pode ser representada esquematicamente, para os casos mais simples, pela curva da Figura 2.4.

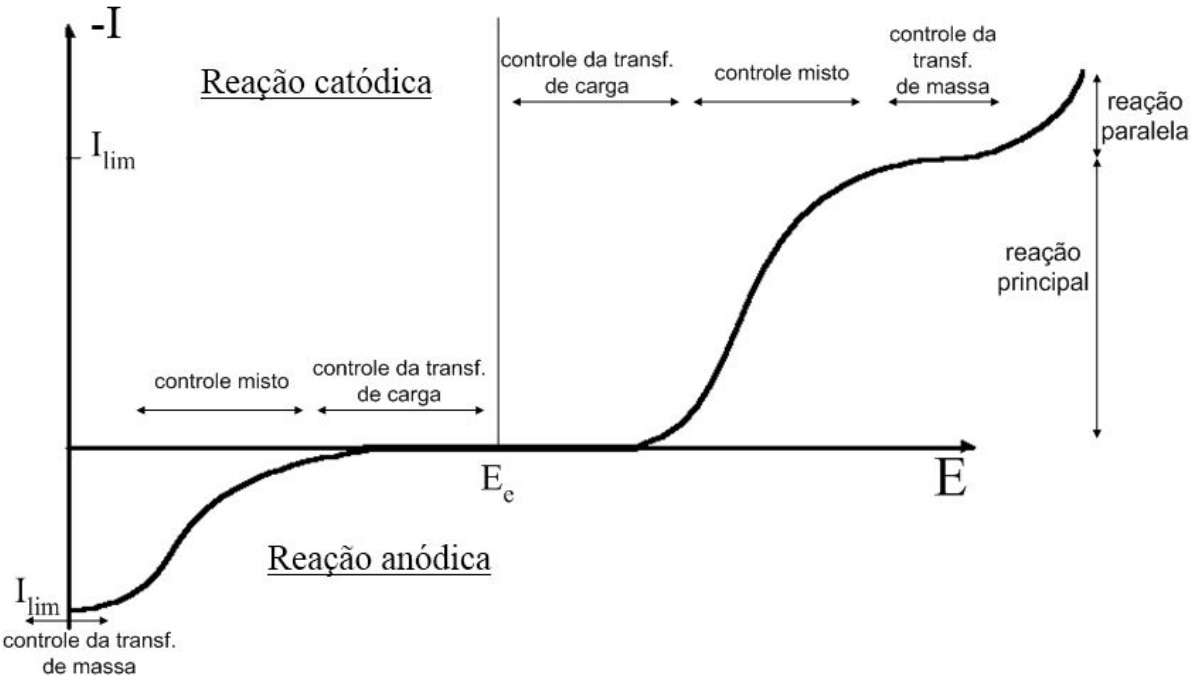

Figura 2.9. Curva de corrente em função do potencial.

Em uma reação eletródica simples do tipo $O + ze^- \Leftrightarrow R$, em que há a inter-conversão, sobre a superfície de um eletrodo inerte, de espécies reduzidas R e oxidadas O, é essencial disponibilizar o reagente na superfície do eletrodo e remover o produto formado com a finalidade de se manter uma corrente, ou seja, para garantir que ocorra a reação de transferência de elétrons (PLETCHER e WALSH, 1990). Neste caso, é possível desmembrar o processo em uma sequência de etapas básicas:

$$O_{bulk} \xrightarrow{\text{transporte de massa}} O_{eletrodo} \quad (2.1)$$

$$O_{eletrodo} \xrightarrow{\text{transferência de elétrons}(ne^-)} R_{eletrodo} \quad (2.2)$$

$$R_{eletrodo} \xrightarrow{\text{transporte de massa}} R_{bulk} \quad (2.3)$$

Uma vez que a taxa de redução e, consequentemente, a densidade de corrente catódica são determinadas pela velocidade total das três etapas, a etapa mais lenta determinará a taxa de reação. Portanto, para a compreensão das características das reações eletródicas é necessário conhecimento sobre transferência de massa e transferência de elétrons.

Considerando os dois mecanismos de transferência e a curva de polarização da Figura 2.4, em regiões de potencial próximos ao potencial de equilíbrio, há um excesso de espécies eletroativas na superfície do eletrodo, não sendo então a concentração o fator limitante da reação; nestes casos, o potencial é o fator determinante da taxa de reação e diz-se que o controle é ativado ou por transferência de elétrons. À medida que se caminha para potenciais mais anódicos ou catódicos, o fluxo mássico das espécies eletroativas para a superfície do eletrodo começa a ter um efeito cada vez mais significativo sobre a cinética da reação. Esta região é denominada de controle cinético misto, pois, tanto a transferência de elétrons quanto a transferência de massa exercem influência sobre a cinética. Aumentando-se ainda mais o potencial, atingir-se-á uma condição em que o fluxo mássico se iguala à taxa de transferência de elétrons para a espécie eletroativa de interesse e, nesta condição, sua concentração na superfície do eletrodo é zero. Nesta situação, denominada de corrente limite, são observadas as melhores taxas de reação e eficiência de corrente e o processo é controlado exclusivamente pelo transporte de massa da espécie eletroativa do seio da solução para a superfície do eletrodo (GOODRIDGE e SCOTT, 1995). O aumento do potencial para valores acima do potencial de corrente limite fará com que a parcela adicional de elétrons fornecida ao sistema seja desviada para reações paralelas, geralmente reações de decomposição do solvente.

No entanto, poucas das reações de interesse industrial são simples. Elas podem envolver transferências múltiplas de elétrons e, pelo menos, três tipos adicionais básicos de

estágios podem também ocorrer: reações químicas, adsorção e formação de fases(TICIANELLI e GONZÁLEZ, 1998). A seguir são descritos alguns desses fenômenos.

1. Reações químicas. As espécies formadas na reação de transferência de elétrons podem não ser estáveis no meio eletrolítico, elas podem ser intermediárias de uma reação química que formará os produtos observados.

2. Adsorção. A sequência de reações 2.1 a 2.3 assume que a transferência de elétrons ocorre na superfície do eletrodo, mas sem a formação de uma ligação entre a superfície e O ou R. Nem sempre isto é verdade e para que a reação ocorra pode ser necessário que reagentes, intermediários ou produtos sejam adsorvidos sobre a superfície do eletrodo.

3. Formação de fases. A reação eletródica pode envolver a formação de uma nova fase, como por exemplo, no caso de eletrodeposição de metais ou então na formação de produtos gasosos como o hidrogênio.

Uma vez que as reações eletródicas comumente envolvem a transferência de vários elétrons, as complicações 1 a 3 descritas acima ocorrem de maneira superposta, portanto, muitas situações complexas podem aparecer. Contudo, neste texto serão consideradas equações idealizadas, mas que geralmente são suficientes para o entendimento e reconhecimento das etapas fundamentais envolvidas nos processos eletrolíticos como um todo, presentes na maioria dos processos industriais de interesse prático.

2.2.2 Controle por transferência de elétrons

Quando uma reação é controlada pela transferência de elétrons (controle ativado) a taxa de reação não depende da concentração da espécie eletroativa na solução e, consequentemente, a variação da concentração em função do tempo será linear. Em um processo potenciostático, a corrente elétrica que circula pelo sistema é uma função do potencial de eletrodo e esta relação é expressa pela equação de Butler-Volmer (Equação 2.4). Uma dedução detalhada desta equação pode ser encontrada em VETTER (1967) e Rajeshvar e Ibanez (1997).

$$i = i_0 \left[exp\left(\frac{\alpha_A \cdot z \cdot F}{R \cdot T} \cdot E\right) - exp\left(-\frac{\alpha_C \cdot z \cdot F}{R \cdot T} \cdot E\right)\right] \quad (2.4)$$

Na Equação 2.4 o primeiro termo exponencial à esquerda corresponde à corrente parcial anódica e o segundo termo à corrente parcial catódica. A equação de Butler-Volmer é comumente escrita em função do sobrepotencial de eletrodo:

$$i = i_0 \left[exp\left(\frac{\alpha_A \cdot z \cdot F}{R \cdot T} \cdot \eta\right) - exp\left(-\frac{\alpha_C \cdot z \cdot F}{R \cdot T} \cdot \eta\right)\right] \quad (2.5)$$

Quando o sobrepotencial é muito negativo, ou seja, em um processo catódico, o primeiro termo exponencial da Equação 2.5 torna-se desprezível comparado ao segundo e, desta forma, pode-se escrever:

$$\log(-i) = \log(i_0) - \frac{\alpha_C \cdot Z \cdot F}{2{,}3 \cdot R \cdot T} \cdot \eta \quad (2.6)$$

De forma análoga, em um processo anódico o sobrepotencial é muito positivo e o segundo termo da exponencial torna-se negligenciável comparado ao primeiro.

$$\log(i) = \log(i_0) + \frac{\alpha_A \cdot Z \cdot F}{2{,}3 \cdot R \cdot T} \cdot \eta \quad (2.7)$$

As formas da equação de Butler-Volmer mostradas nas Equações 2.6 e 2.7 são conhecidas como equações de Tafel e são utilizadas para determinar experimentalmente os coeficientes de troca α_C e α_A e a densidade de corrente de troca (i_0).

2.2.3 Distribuição de Potencial em Eletrodo Tridimensional

Eletrodos tridimensionais geralmente apresentam maiores problemas com distribuição de potencial e corrente do que os eletrodos bidimensionais; isto se deve principalmente à anisotropia dos eletrodos porosos e de leitos particulados com relação à condutividade do eletrodo, fluxo de eletrólito e concentração das espécies eletroativas. Diante disto, o conhecimento da distribuição de potencial elétrico no interior de um eletrodo poroso é de fundamental importância para o entendimento dos fenômenos eletroquímicos que ocorrem neste tipo de eletrodo e, consequentemente, é importante para o projeto adequado do eletrodo poroso (RAJESHVAR e IBANEZ, 1997).

Existem diversos trabalhos que se dedicaram à modelagem e medição (DOHERTY; SUNDERLAND; ROBERTS et al., 1996, GUBULIN, 1998, PONTE; PONTE e GUBULIN, 1994) do perfil de potencial em eletrodos porosos. Embora os modelos matemáticos sejam bastante completos (e muitas vezes complexos), sua utilização de maneira quantitativa é bastante restrita devido à necessidade do conhecimento de diversos parâmetros que muitas vezes não são de fácil obtenção. Parâmetros elétricos, tais como a condutividade efetiva da solução eletrolítica e do eletrodo, e parâmetros hidrodinâmicos como a tortuosidade do meio poroso, muitas vezes são de difícil determinação, fazendo com que os perfis de potencial obtidos através de modelos sejam utilizados principalmente para uma análise qualitativa dos processos que ocorrem no interior do eletrodo.

Os modelos existentes levam em consideração o perfil de potencial elétrico na fase líquida e na fase sólida conforme mostrado na Figura 2.5(a). O potencial de eletrodo (E) consiste na diferença entre o potencial da fase sólida (ϕ_m) e o potencial da fase líquida (ϕ_s). Como a taxa de reação é uma função do sobrepotencial (η), existem, portanto, zonas com diferentes atividades eletroquímicas no interior de um eletrodo poroso, ao longo da direção do campo elétrico. De maneira geral, o perfil típico obtido em eletrodos de leito fixo tem comportamento similar ao mostrado na Figura 2.5(b), em que se observa uma maior atividade eletroquímica na região próxima ao contra-eletrodo. Em alguns casos, pode ocorrer também a dissolução da matriz porosa (NEWMAN, 1973).

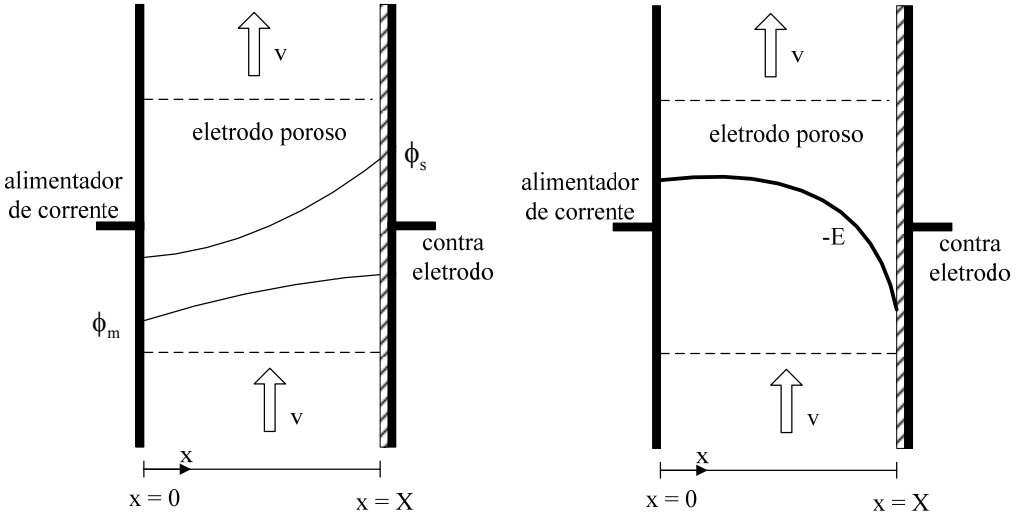

Figura 2.10. Perfil de potencial em eletrodo tridimensional.

3 ELETRORRECUPERAÇÃO DE COBRE UTILIZANDO ELETRODO DE LEITO PULSANTE

3.1 Introdução

Este capítulo versa sobre o emprego de um reator eletroquímico ELP para a eletrorrecuperação de cobre a partir de um eletrólito ácido que simulava concentrações típicas encontradas em processos reais da indústria hidrometalúrgica. Na literatura, apenas um trabalho foi encontrado sobre a utilização de ELP no processo de eletrorrecuperação de metais e este apresentava configuração de fluxos de corrente e eletrólito paralelos e mecanismo de pulsos realizado por meio de válvulas(COEURET e PAULIN, 1988). Neste trabalho, os pulsos do ELP foram gerados através do controle da rotação de uma bomba centrífuga, usando um módulo lógico e um conversor de frequência. De acordo com literatura, existem poucos trabalhos que relatam o uso de ELP para a eletrorrecuperação de metais e nenhum que utiliza esta configuração de eletrodos ou este método de gerar os pulsos de vazão.

Um planejamento fatorial fracionário foi utilizado a fim de se realizar uma triagem das variáveis operacionais que poderiam interferir no processo de eletrorrecuperação do cobre e desta forma determinar as melhores condições para maximizar a eficiência de corrente e o rendimento espaço-tempo, minimizando o consumo energético. Além disso, a distribuição de sobrepotenciais de eletrodo foi medida experimentalmente a fim de se determinar a possível existência de zonas anódicas no interior do eletrodo e que poderiam explicar os baixos valores de *EC* observados.

As curvas da variação de concentração de cobre em função do tempo de experimento, para diferentes condições experimentais são apresentadas. Além disso, são mostrados os perfis de sobrepotencial de eletrodo para o ELP, medidos durante a condição de leito fixo para as duas densidades de corrente estudadas. Utilizando um multímetro acoplado a um computador, mediu-se o comportamento do potencial de célula ao longo do tempo de eletrólise. Verificou-se que a diminuição do potencial de célula durante o processo de eletrodeposição foi devido, principalmente, ao aumento da temperatura do eletrólito causado majoritariamente pela operação de bombeamento. Adicionalmente, a influência da temperatura sobre o potencial de célula foi atribuído especialmente a uma redução da resistência ôhmica resultante do aumento

na condutividade do eletrólito. Voltametrias de varredura linear para soluções de cobre em diferentes temperaturas são apresentadas visando o entendimento da diminuição do potencial de célula em função do tempo de eletrólise. Finalmente, diagramas contendo os contrastes dos efeitos que cada variável independente apresentou na eficiência de corrente e as curvas de concentração-tempo obtidas variando os tempos de leito fixo e fluidizado fecham a discussão do trabalho.

3.2 Desenvolvimento

O desenvolvimento do Capítulo 3 é apresentado a seguir no artigo intitulado *Copper electrowinning using a pulsed bed three-dimensional electrode*, publicado no periódico internacional *Hydrometallurgy* 144–145 (2014) 15–22, apresentado a seguir.

Hydrometallurgy 144–145 (2014) 15–22

Contents lists available at ScienceDirect

Hydrometallurgy

journal homepage: www.elsevier.com/locate/hydromet

Copper electrowinning using a pulsed bed three-dimensional electrode

Pedro H. Britto-Costa [a], Edenir R. Pereira-Filho [b], Luís A.M. Ruotolo [a,*]

[a] Department of Chemical Engineering, Federal University of São Carlos, P.O. Box 676, 13565-905 São Carlos, SP, Brazil
[b] Department of Chemistry, Federal University of São Carlos, P.O. Box 676, 13565-905 São Carlos, SP, Brazil

ARTICLE INFO

Article history:
Received 12 June 2013
Received in revised form 17 January 2014
Accepted 19 January 2014
Available online 30 January 2014

Keywords:
Pulsed bed
Porous electrodes
Electrowinning
Flow rate pulses

ABSTRACT

This work concerns the electrowinning of copper from an acidic medium using a membraneless three-dimensional pulsed bed electrode (PBE). The effect of current density (i), packed bed time (t_p), and fluidized bed time (t_f) on current efficiency (CE), energy consumption (EC), and space-time yield (Y) was investigated using a fractional factorial design (FFD). The results showed that the most important variables affecting the electrodeposition process were i and t_p. Experiments using i greater than 3000 A m^{-2} and t_f lower than 2 s revealed that the process rapidly short circuited, mainly due to a non-uniform overpotential distribution inside the porous cathode. An important improvement of the reaction kinetics and EC was achieved by increasing t_p and decreasing t_f. The best values of CE (76.7%) and EC (2.5 kWh kg^{-1}) were obtained by applying 3000 A m^{-2}, with $t_f = 2$ s and $t_p = 60$ s. Although the CE value was lower than reported elsewhere, the EC value was within the range commonly found for industrial processes. The FFD results indicated ways by which copper electrowinning using a PBE reactor could be further optimized.

1. Introduction

Hydrometallurgy is an important area of extractive metallurgy and accounted for 20–25% of global copper production in 2012, estimated at 17.0 million tons (USG Survey, 2013), using leach/solvent extraction/electrowinning technology (Cifuentes et al., 2005; Habashi, 2007; Hyvärinen and Hämäläinen, 2005; Panda and Das, 2001; Shakarji et al., 2011). In this process, flat plate electrodes are used for metal electrodeposition, which limits the applied current densities to values up to 450 A m^{-2}, although 300 A m^{-2} is commonly used in industrial processes. In all cases, large electrowinning tankhouses are required, which means that the space-time yield is low. Besides these constraints, there are other drawbacks, such as the need to harvest the electrodeposited metal from the substrate (cathode), which are often performed manually in small plants. Additionally, the acid mist released during the process can oxidize electrical contacts or affect the health of the operator (Evans et al., 2005; Jiricny et al., 2002; San Martin et al., 2005; Shakarji et al., 2011; Sigley et al., 2003; Wiechmann et al., 2010). Although PbO_2 anodes are generally used in electrowinning processes, these anodes are not stable and require the addition of chemical additives to the electrolyte in order to increase their working life (Lupi and Pilone, 1997; Moats et al., 2003; Muresan et al., 2000). However, the use of these additives does not prevent anode corrosion, and lead contamination of the electrodeposited metal must be strictly controlled (Lafront et al., 2010; Moats et al., 2003; Moskalyk et al., 1999).

Particulate electrodes have been studied as an alternative to overcome many of these drawbacks (Coeuret, 1980; Coeuret and Paulin, 1988; El-Shakre et al., 1994; Evans et al., 2005; Hadzismajlovic et al., 1996; Jiricny et al., 2002; Martins et al., 2012; Olive and Lacoste, 1979; Ruotolo and Gubulin, 2002). The main advantages of such electrodes are the very large increase in space-time yield, due to the smaller reactor volume required to produce the same amount of metal, as well as the higher currents that can be applied, which is made possible by the extended surface area provided by the particulate cathode (Evans et al., 2005; Jiricny et al., 2002; Martins et al., 2012; Salas-Morales et al., 1997). In the case of particulate bed electrodes, harvesting of the electrodeposited metal consists simply of collecting the particles at the end of a process cycle. Moreover, problems of acid mist can be easily eliminated by channeling it to the exit of the electrochemical reactor. The particles can be employed in the same way as granulated copper, in which case product preservation and prevention of surface oxidation are necessary, or the particles can be melted to produce ingots.

Another important advantage of using particulate electrodes is the possibility of replacing PbO_2 anodes by dimensionally stable anodes (DSA®), such as titanium–iridium or titanium–ruthenium oxide anodes. This can be economically viable because the use of three-dimensional cathodes can significantly reduce the necessity for large DSA® anodes. A further advantage is that replacement of PbO_2 by DSA® anodes can also eliminate the need for chemical additives (Lupi and Pilone, 1997; Muresan et al., 2000).

Among the particulate electrodes used for metal electrodeposition, the packed bed has been intensively studied, particularly for effluent treatment where the metal concentration is very low (Britto-Costa and Ruotolo, 2011; Hadzismajlovic et al., 1996; Olive and Lacoste, 1979; Pletcher et al., 1991; Ruotolo and Gubulin, 2002). The high

* Corresponding author. Tel.: +55 16 3351 8706; fax: +55 16 3351 8266.
E-mail address: pluis@ufscar.br (L.A.M. Ruotolo).

0304-386X/$ – see front matter © 2014 Elsevier B.V. All rights reserved.
http://dx.doi.org/10.1016/j.hydromet.2014.01.014

Abstract

This work concerns the electrowinning of copper from an acidic medium using a membraneless three-dimensional pulsed bed electrode (PBE). The effect of current density (i), packed bed time (t_p), and fluidized bed time (t_f) on current efficiency (CE), energy consumption (EC), and space-time yield (Y) was investigated using a fractional factorial design (FFD). The results showed that the most important variables affecting the electrodeposition process were i and t_p. Experiments using i greater than 3000 A m^{-2} and t_f lower than 2 s revealed that the process rapidly short circuited, mainly due to a non-uniform overpotential distribution inside the porous cathode. An important improvement of the reaction kinetics and EC was achieved by increasing t_p and decreasing t_f. The best values of CE (76.7%) and EC (2.5 kWh kg^{-1}) were obtained by applying 3000 A m^{-2}, with $t_f = 2$ s and $t_p = 60$ s. Although the CE value was lower than reported elsewhere, the EC value was within the range commonly found for industrial processes. The FFD results indicated ways by which copper electrowinning using a PBE reactor could be further optimized.

INTRODUCTION

Hydrometallurgy is an important area of extractive metallurgy and accounted for 20-25% of global copper production in 2012, estimated at 17.0 million tons (USG Survey, 2013), using leach/solvent extraction/electrowinning technology (Cifuentes *et al*., 2005; Habashi, 2007; Hyvärinen and Hämäläinen, 2005; Panda and Das, 2001; Shakarji *et al*., 2011). In this process, flat plate electrodes are used for metal electrodeposition, which limits the applied current densities to values up to 450 A m^{-2}, although 300 A m^{-2} is commonly used in industrial processes. In all cases, large electrowinning tankhouses are required, which means that the space-time yield is low. Besides these constraints, there are other drawbacks, such as the need to harvest the electrodeposited metal from the substrate (cathode), which are often performed manually in small plants. Additionally, the acid mist released during the process can oxidize electrical contacts or affect the health of the operator (Evans *et al*., 2005; Jiricny *et al*., 2002; San Martin *et al*., 2005; Shakarji *et al*., 2011; Sigley *et al*., 2003; Wiechmann *et al*., 2010). Although PbO_2 anodes are generally used in electrowinning processes, these anodes are not stable and require the addition of chemical additives to the electrolyte in order to increase their working life (Lupi and Pilone, 1997; Moats *et al*., 2003; Muresan *et al*., 2000). However, the

use of these additives does not prevent anode corrosion, and lead contamination of the electrodeposited metal must be strictly controlled (Lafront *et al*., 2010; Moats *et al*., 2003; Moskalyk *et al*., 1999).

Particulate electrodes have been studied as an alternative to overcome many of these drawbacks (Coeuret, 1980; Coeuret and Paulin, 1988; El-Shakre *et al*., 1994; Evans *et al*., 2005; Hadzismajlovic *et al*., 1996; Jiricny *et al*., 2002; Martins *et al*., 2012; Olive and Lacoste, 1979; Ruotolo and Gubulin, 2002). The main advantages of such electrodes are the very large increase in space-time yield, due to the smaller reactor volume required to produce the same amount of metal, as well as the higher currents that can be applied, which is made possible by the extended surface area provided by the particulate cathode (Evans *et al*., 2005; Jiricny *et al*., 2002; Martins *et al*., 2012; Salas-Morales *et al*., 1997). In the case of particulate bed electrodes, harvesting of the electrodeposited metal consists simply of collecting the particles at the end of a process cycle. Moreover, problems of acid mist can be easily eliminated by channeling it to the exit of the electrochemical reactor. The particles can be employed in the same way as granulated copper, in which case product preservation and prevention of surface oxidation are necessary, or the particles can be melted to produce ingots. Another important advantage of using particulate electrodes is the possibility of replacing PbO_2 anodes by dimensionally stable anodes (DSA®), such as titanium-iridium or titanium-ruthenium oxide anodes. This can be economically viable because the use of three-dimensional cathodes can significantly reduce the necessity for large DSA® anodes. A further advantage is that replacement of PbO_2 by DSA® anodes can also eliminate the need for chemical additives (Lupi and Pilone, 1997; Muresan *et al*., 2000).

Among the particulate electrodes used for metal electrodeposition, the packed bed has been intensively studied, particularly for effluent treatment where the metal concentration is very low (Britto-Costa and Ruotolo, 2011; Hadzismajlovic *et al*., 1996; Olive and Lacoste, 1979; Pletcher *et al*., 1991; Ruotolo and Gubulin, 2002). The high conductivity of the solid phase and high mass transfer coefficients enable the packed bed cathode to operate at high current efficiency (Britto-Costa and Ruotolo, 2011; Ruotolo and Gubulin, 2002).

Unfortunately, when the metal concentration is high (as in the electrowinning process), metal deposition results in very fast clogging of the electrode pores (Hadzismajlovic *et al*., 1996; Ruotolo and Gubulin, 2002). In order to overcome this problem, fluidized bed electrodes have been studied for metal electrodeposition, because clogging of the electrode can be avoided

by maintaining the conducting particles in a fluidized state using an upward electrolyte flow (Coeuret, 1980; Hadzismajlovic *et al*., 1996; Hutin and Coeuret, 1977; Kazdobin *et al*., 2000; Sabacky and Evans, 1979). However, for this type of electrode the reaction rate is very sensitive to the fluid dynamic conditions because the conductivity of the solid phase depends on the frequency of collisions between the particles, which is mainly determined by the bed expansion (Hadzismajlovic *et al*., 1996; Hutin and Coeuret, 1977). In some cases, when the local difference between the solid and liquid phase potentials is positive, metal dissolution zones inside the fluidized cathode can occur, especially in very acidic solutions (Coeuret, 1980; Hutin and Coeuret, 1977). For these reasons, the pulsed bed electrode (PBE) has emerged as an interesting alternative. This electrode benefits from the high current efficiency provided by the packed bed electrode, while avoiding electrode clogging during fluidization of the cathode (Argondizo, 2001; Coeuret and Paulin, 1988; Garfias-Vasquez *et al*., 2004). In this kind of electrode, the packed bed is periodically fluidized by applying regular flow rate pulses, which can be generated by mechanical or electrical devices (Argondizo, 2001; Garfias-Vasquez *et al*., 2004), as well as using special valve setups (Coeuret and Paulin, 1988). Another advantage of the PBE is the continuous particle mixing during the pulse, which enables the particles to grow uniformly.

In this study, a PBE electrochemical reactor for copper electrowinning from acidic electrolytes was investigated using typical concentrations found in industrial hydrometallurgical processes. The system was designed as a one compartment reactor, with no membrane separating the catholyte from the anolyte, which reduced the capital costs (Tonini *et al*., 2013). The flow rate pulses were generated by controlling the rotation of a centrifugal pump using a logic module and a frequency inverter. Considering the state of the art, there are only a few reports of the use of PBEs for metal electrodeposition; in all cases, the PBE was used to recover metals from dilute solutions, where the main objective was effluent treatment (Argondizo, 2001; Coeuret and Paulin, 1988). To the best of our knowledge, there are no reports in the literature concerning the use of PBEs in hydrometallurgy. Moreover, as far as we know, there are no papers reporting the use of membraneless PBEs or the pulsed flow rate technique proposed in this study. Here, the main operational variables that can affect copper electrowinning were studied using a fractional factorial design in order to determine the best conditions for optimal current efficiency, space-time yield, and energy consumption. In addition, the electrode overpotential distribution was measured experimentally and the electrochemical activity inside the porous electrode was investigated.

EXPERIMENTAL

Electrochemical reactor

Fig. 3.1(a) shows a schematic view of the pulsed bed electrochemical reactor used for copper electrowinning. The reactor consisted of three rectangular acrylic plates that were intercalated with silicone rubbers to avoid leaking and assembled using screws and nuts. The dimensions of the chamber containing the pulsed bed electrode were 3.4 cm (thickness) × 4.5 cm (width) × 35 cm (length). The external reactor dimensions were 7.4 cm (thickness) × 10.5 cm (width) × 37.5 cm (height). The electrolyte flowed upwards (6) and before reaching the three-dimensional electrode (2) it passed through a flow distributor made of polyethylene particles (3). Equilateral 1.0 mm cylindrical copper particles were used to form the porous cathode (2). Stainless steel 316 (1) and $Ti/Ti_{0.7}Ru_{0.3}O_2$ DSA® (DeNora, Brazil) (5) were used for the current feeder and the counter-electrode, respectively.

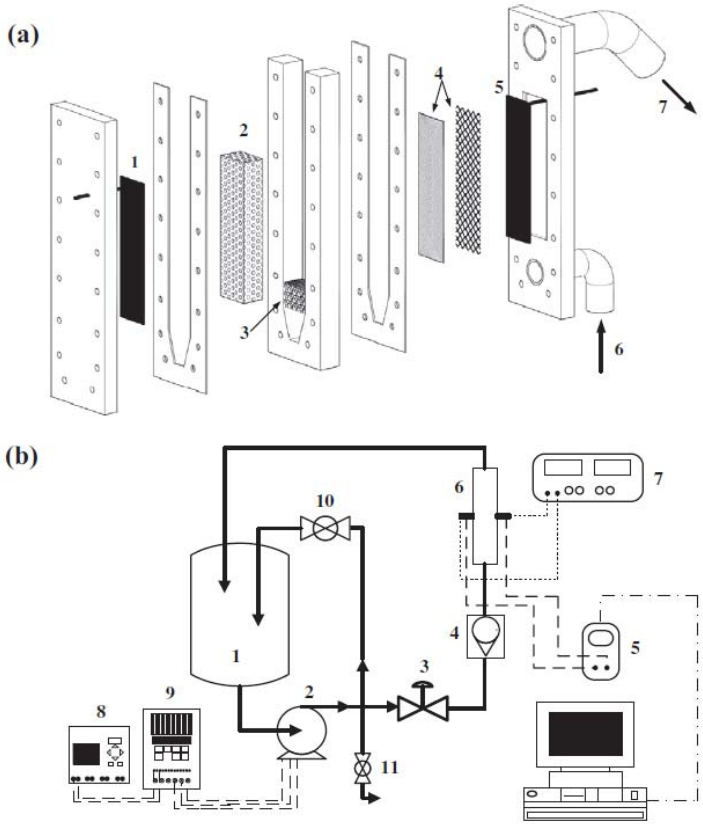

Fig. 3.1. (a) Schematic view of the electrochemical reactor: 1) current feeder, 2) porous cathode, 3) flow distributor, 4) separators, 5) counter-electrode, 6) electrolyte inlet, and 7) electrolyte exit; **(b)** Experimental setup: 1) electrolyte reservoir, 2) centrifugal pump, 3) rotameter, 4) diaphragm valve, 5) voltmeter, 6) electrochemical reactor, 7) current source, 8) logic module, 9) frequency inverter, 10) by-pass valve, and 11) drain valve.

Flow rate pulsation

Flow rate pulses were generated using a frequency inverter acting on the centrifugal pump rotation and, consequently, on the flow rate. The frequency inverter (MicroMaster MM55, Siemens) was controlled by a logic module (LOGO! 230RC, Siemens) that determined the time during which the bed remained in the packed (low frequency rotation) and fluidized (high frequency rotation) states.

Copper electrowinning

Fig. 3.1 (b) shows a schematic view of the experimental setup used for copper electrowinning. The process was carried out galvanostatically using a constant current source (Genesys™ 1500 W, Lambda). The cell potential (E_{cell}) was recorded every 2 s using a data acquisition system.

The electrolyte was prepared using deionized water and technical grade copper sulfate. The copper concentration varied from 35 to 40 g L^{-1} Cu^{2+}. Sulfuric acid was used as the supporting electrolyte, at a concentration of 150 g L^{-1}, which is a typical concentration employed in industrial processes. An electrolyte volume of 15 L was used in all experiments.

The copper concentration was determined colorimetrically by measuring the absorbance at 810 nm using an Ultrospec 2100 Pro UV-VIS spectrophotometer (Amersham Pharmacia). This technique was highly accurate for measurement of copper concentrations in the range used in this study, as also demonstrated by Silva-Martínez and Roy (2013). The calibration curve was linear, with an R^2 value of 0.9999.

The experimental procedure consisted of circulating the electrolyte between the reservoir and the reactor, and collecting samples for analysis of the copper concentration. The flow rates during the packed and fluidized bed conditions were maintained constant at 136 L h^{-1} and 625 L h^{-1}, respectively.

In some experiments, the potential profile in the interior of the porous cathode was measured throughout the thickness of the electrode. A complete description of the apparatus used for these measurements can be found elsewhere (Britto-Costa and Ruotolo, 2011).

Fractional experimental design (FFD)

Initially, a 2^{3-1} fractional factorial design with two replicates was used to evaluate the effects of current density (i), packed bed time (t_p), and fluidized bed time (t_f) on current efficiency (CE), energy consumption (EC), and space-time yield (Y). The coded values of the independent variables are given in Table 3.1, together with the fractional design.

Table 3.1
Actual and coded values of the variables studied using the 2^{3-1} fractional factorial design.

	Var1	**Var2**	**Var3**
Code	***i* / A m^{-2}**	**t_p / s**	**t_f / s**
-1	1500	10	3
+1	3000	30	5
Run	**Var1**	**Var2**	**Var3 = Var1 x Var2**
1	-1	-1	+1
2	+1	-1	-1
3	-1	+1	-1
4	+1	+1	+1
5*	+1	-1	-1
6**	-1	-1	+1

*Replicate of run 1; **Replicate of run 2

The values of CE, EC, and Y were calculated according to Eqs. (3.1), (3.2), and (3.3), respectively. In these equations, z is the number of electrons of the electrochemical reaction, F is the Faraday constant (96,496C mol^{-1}), M is the molar weight (g mol^{-1}), I is the applied current (A), V is the electrolyte volume (L), C is the copper mass concentration (g L^{-1}), t is the electrowinning time (s), E_{cell} is the cell potential (V), and V_R is the reactor volume (m^3). The constants 2.78×10^{-4} and 3.6 are conversion factors used to obtain EC in kWh kg^{-1} and Y in kg m^{-3}h^{-1}. The reaction rates (dC/dt) were determined from the concentration-time curves obtained experimentally.

$$CE = \frac{z \cdot F \cdot V}{M \cdot I} \cdot \frac{dC}{dt} \tag{3.1}$$

$$EC = \frac{z \cdot F \cdot E_{cell}}{CE \cdot M} \tag{3.2}$$

$$Y = \frac{V}{V_R} \cdot \frac{dC}{dt} \tag{3.3}$$

The current efficiency is related to reaction selectivity and process efficacy, both of which influence the operational and capital costs, while energy consumption affects the operational costs. It is therefore desirable to maximize CE and Y, and minimize EC.

RESULTS AND DISCUSSION

Fig. 3.2 shows the curves of copper concentration against time for the experimental conditions shown in Table 3.1. It can be observed that for Runs 2, 4, and 5 (those in which effective electrodeposition occurred), the copper concentration decreased linearly during the course of the electrolysis, indicating that the process was under activated control (Ruotolo and Gubulin, 2005, 2011). The zero-order kinetic constants were − 0.387, − 0.512, and − 0.335 g L^{-1} h^{-1} for Runs 2, 4, and 5, respectively, which were carried out applying 3000 A m^{-2}. When 1500 A m^{-2} was applied, there was an increase in the copper concentration due to dissolution of the copper particles. This could be attributed to the existence of positive overpotentials in the interior of the porous cathode, especially in this very acidic médium (Hutin and Coeuret, 1977), indicating that the applied current was not sufficiently high to guarantee the cathodic polarization of all particles of the porous cathode (Hadzismajlovic *et al*., 1996).

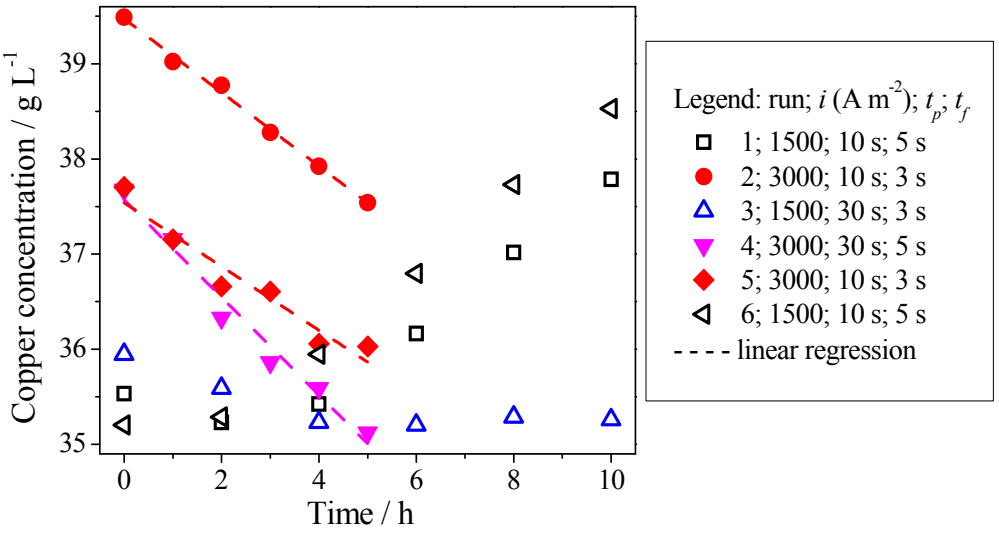

Fig. 3.2. Copper concentration as a function of time for Runs 1-6.

Comparison of Runs 1 and 3 showed that the time during which the particulate bed remained in the packed or fluidized state influenced the electrodeposition kinetics. For example, if the bed remained in the fluidized condition for 3 s (Run 3), the electrodeposition occurred for 4 h, after which a steady state was reached during which there was no change in the copper concentration, indicating that the processes of electrodeposition and dissolution occurred simultaneously at the same rate. In contrast, when t_f was increased and t_p was decreased (Run1), there was almost entirely dissolution, indicating that the electrodeposition rate was slower than the dissolution rate. Further evidence that electrodeposition and dissolution occurred

simultaneously was that copper electrodeposition on the current feeder was observed in all the experiments.

These results can be better understood considering that for three-dimensional electrodes, the electrochemical activity varies along the direction of the electric field, which can be caused by local differences between the liquid and solid phase potentials. Hence, the local overpotential (η) inside the PBE can be attributed to the ohmic drop in the liquid phase, which affects the potential of this phase and the conductivity of the solid phase. This is the main factor affecting the solid phase potential, especially when the solid phase is not continuous, as in the case of the fluidized bed (Coeuret, 1980).

Fig. 3.3 shows the overpotential profiles for the PBE, measured during the packed bed condition, for the two different current densities studied. As can be seen, the overpotentials were negative throughout the electrode thickness, indicating that the whole electrode was involved in the electrodeposition, despite the lower electrochemical activity observed close to the current feeder, where the overpotentials were less negative. It is also noteworthy that very negative overpotentials were concentrated in the region close to the separator and counter electrode. The metal electrodeposition rates in this region were therefore very high and could cause dendritic metal growth leading to particle agglomeration and short circuit, as observed in some experiments. The short circuit occurred when the dendritic metal deposit grew towards the counter electrode, passing through the separators and then contacting the anode. In this respect, another important advantage of the PBE is the particle homogenization during the flow rate pulse (fluidized state), which allows the use of high current densities without the risk of short circuit. It is also known that t_p plays an important role in avoidance of short circuit during metal electrodeposition using PBEs.

Although the overpotentials during the fluidized condition could not be measured in this work due to reactor design limitations, the literature contains many reports concerning the overpotential profiles inside fluidized bed electrodes. Zones of positive overpotential mainly occur in the middle of the fluidized cathode (Hutin and Coeuret, 1977; Ponte, 1998). In conclusion, dissolution was only obtained during the fluidization step; hence, t_f must be minimized as much as possible in order to avoid copper dissolution and improve the overall electrodeposition rate and the current efficiency.

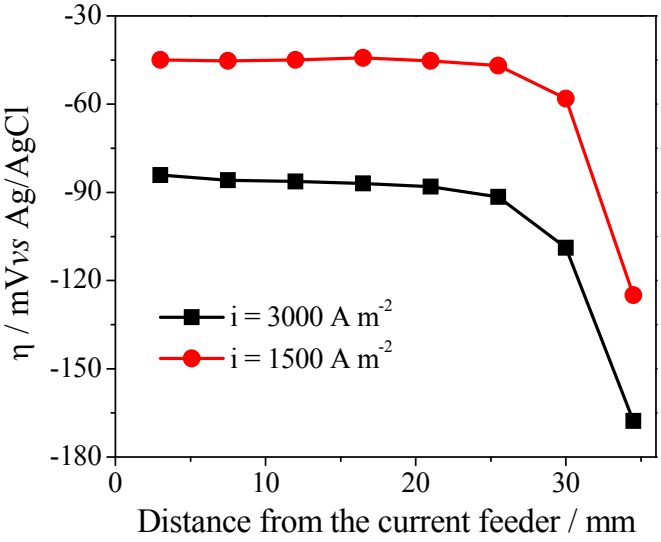

Fig. 3.3. Overpotential profiles for the packed bed electrode as a function of the distance from the current feeder. 35.9 g $L^{-1}Cu^{2+}$, 150 g L^{-1} H_2SO_4, flow rate = 136 L h^{-1}, T = 28 ºC, Equilibrium potential = 92.5 mV.

Fig. 3.4 (a) shows a typical profile of the cell potential during the electrolyses. In all cases, the cell potential followed the same trend shown in Fig. 3.4 (a), decreasing over time for both the packed and fluidized beds, although the decrease was greater for the fluidized bed than for the packed bed. For example, the difference between the initial and final cell potentials was approximately 1.0 V for the fluidized bed, while it was only 0.3 V for the packed bed (Fig. 3.4 (a)). This is an important finding because the decrease directly affects the average cell potential and, consequently, the energy consumption (EC).

The diminution of E_{cell} during the electrodeposition process was mainly due to the increase in the electrolyte temperature caused by the pumping operation, as shown in Fig. 3.4 (b). Comparison of the curve of temperature against time for Run 2 with the one obtained when no current was applied indicated that viscous dissipation was the main factor affecting the electrolyte temperature. Moreover, the highest temperature was observed for Run 1, where the fluidized state accounted for 33% of the total process time, with the high flow rate favoring viscous dissipation and an increase in temperature.

It was also observed that when the electrolyte temperature increase was greater, there was also a greater drop in E_{cell}, and that the times necessary to reach cell potential and temperature steady states almost coincided. This effect of temperature is very important because the value of E_{cell} must be minimized as much as possible in order to achieve low energy

consumption. In a hydrometallurgical process in which tons of metals are produced every day, any small reduction of E_{cell} will have a strong impact on the overall production cost.

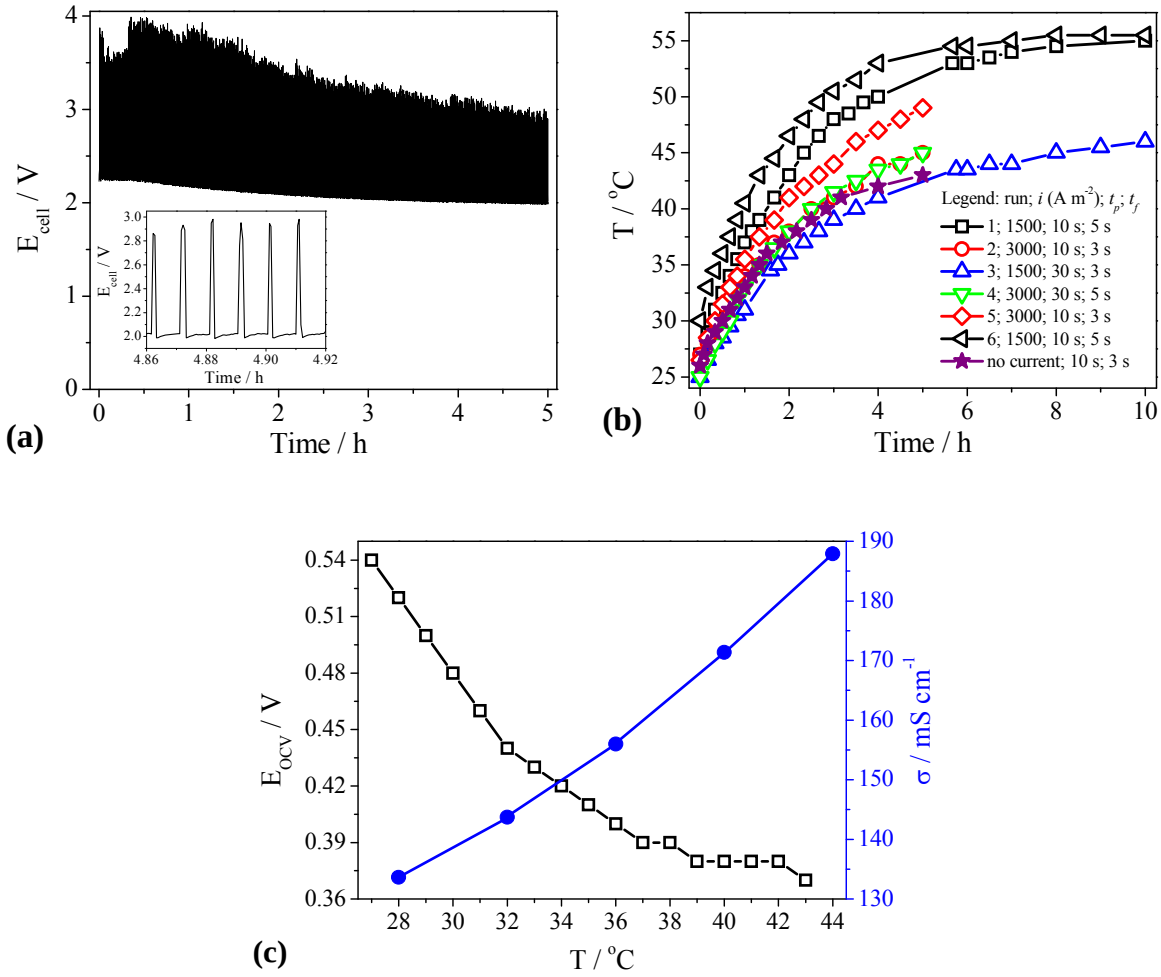

Fig. 3.4. **(a)** Cell potential against time (run 4). Inset: detailed view; **(b)** Electrolyte temperature against time, and **(c)** E_{cell} (open circuit) and conductivity against temperature for flow conditions of run 2.

The influence of temperature on E_{cell} could be attributed principally to the decrease in the ohmic resistance resulting from an increase in the electrolyte conductivity, as shown in Fig. 3.4 (c). The initial conductivity at 28 °C was 134 mS cm^{-1}, but when the electrolyte reached a temperature of 44 °C, the conductivity increased to 187 mS cm^{-1}. Consequently, the open circuit voltage (EOCV) decreased from 0.54 V to 0.37 V, so there was a reduction of 0.17 V due to temperature and conductivity enhancements of 17 °C and 56 mS cm^{-1}, respectively. When the electrolyte temperature reached 55 °C, the conductivity was 233 mS cm^{-1}, which was 78% higher than the conductivity observed at the beginning of the electrodeposition process. This confirmed the strong influence of temperature on the conductivity and E_{cell}.

Another contribution to the decrease of E_{cell} during the process was the reduction of the electrodeposition overpotential when the electrolyte temperature increased, as can be observed in the voltammograms obtained for an acidic copper solution (Fig. 3.5). In the galvanostatic process, a higher electrolyte temperature displaces the electrodeposition overpotentials to less negative values, which facilitates electron transfer. However, although the charge transfer overpotential can be reduced by increasing the temperature, according to Fig. 3.5 its contribution to the overall E_{cell} was very small, compared to the effect of the electrolyte conductivity. It is also worth noting that for Runs 2, 4, and 5 the electrodeposition rate remained almost constant, despite the temperature increase during the electrolysis, indicating that the copper deposition was not affected by temperature.

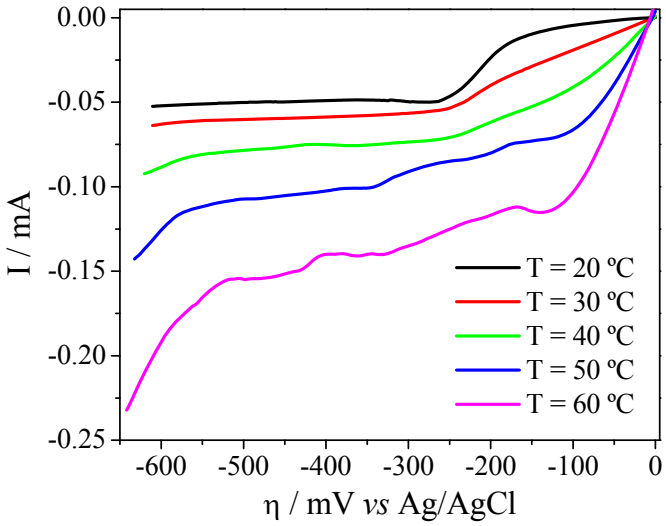

Fig. 3.5. Linear scan voltammetries for copper solution at different temperatures. 38.1 g L^{-1} Cu^{2+}, 150 g L^{-1} H_2SO_4. Scan rate = 10 mV s^{-1}.

It is also interesting to compare the overpotential values shown in Fig. 3.5 with those in Fig. 3.3. It can be seen that the absolute values of the overpotentials shown in Fig. 3.3 are very low, with the electrode potentials being very close to the equilibrium potential, indicating that during the packed bed state the process was totally controlled by activation (Pletcher and Walsh, 1990). The hydrogen evolution reaction (HER) only started at − 500 mV for a temperature of 60 °C (Fig. 3.5), and (in the worst case) the most negative overpotential observed for the packed bed was − 170 mV (Fig. 3.3). From this, it can be concluded that no hydrogen was formed and that copper dissolution was the only factor contributing to the low value of CE observed for the PBE (Table 3.2). During the electrodeposition, the values of E_{cell} observed during the fluidized

and packed bed states were very different (see inset in Fig. 3.4 (a)), as a result of which their contributions to the overall E_{cell} were dependent on t_p and t_f. Hence, energy consumption (Wiechmann *et al*., 2010) was calculated using the average cell potential ($E_{cell,av.}$) determined by integration of the E_{cell}-time curve. The current efficiency (CE) and space-time yield (Y) were calculated using the slopes obtained from the concentration-time curves shown in Fig. 3.2. When the slope was positive, indicating that dissolution was greater than electrodeposition (corresponding to an increase in the copper concentration), a negative value of CE was obtained. The more negative the value of CE, the greater the amount of copper that was dissolved. In these cases, Y and EC were not calculated.

Table 3.2 shows the values of CE, $E_{cell, av.}$, EC, Y, and m_{cf} for the different experimental conditions. It is important to take into account the amount of copper deposited onto the current feeder (m_{cf}), because it is desirable to deposit copper only onto particles in order to avoid hydrodynamic disturbances that could facilitate localized electrodeposition and short circuit. Moreover, it would be more difficult to remove the electrodeposited copper from the current feeder.

Table 3.2
Current efficiency, average cell potential, energy consumption, space-time yield, and mass of copper electrodeposited on the current feeder for the runs shown in Fig. 3.2.

run	i	t_p	t_f	CE / %	$E_{cell, av.}$ / V	EC / kWh kg^{-1}	Y / kg m^{-3} h^{-1}	m_{cf} / g
1	-1	-1	1	-52.8	1.87	-	-	2.9
2	1	-1	-1	45.3	2.16	4.0	35.8	5.7
3	-1	1	-1	16.1	1.83	9.6	6.3	0.9
4	1	1	1	60.0	2.27	3.2	47.4	1.4
5	1	-1	-1	39.3	2.29	4.9	31.0	3.8
6	-1	-1	1	-77.9	1.83	-	-	3.3

The values of CE shown in Table 3.2 are much lower than observed for industrial processes using flat plate electrodes for copper electrowinning (82-92%). On the other hand, the values of E_{cell} are in the same range commonly found in industry (1.9-2.3 V), which suggests that low CE was the main factor responsible for the high EC observed. It is therefore essential to optimize the operational variables in order to increase the current efficiency.

The values of CE were lower than expected for copper electrodeposition from highly concentrated solutions, especially when 1500 A m^{-2} and high t_f were used (Table 3.2). As discussed previously, these low values of CE could be attributed to copper dissolution during the fluidization pulse. It is important to note that electrodeposition still occurred at very negative CE, as confirmed by the values of m_{cf}.

Concerning the space-time yield, the values obtained using the PBE were higher than reported for flat plate electrodes (Gallone, 1977; Pletcher and Walsh, 1990). This was expected because the amount of electrodeposited copper per unit of reactor volume is greatly increased using three-dimensional electrodes. Despite the high values of Y, the energy consumption remained very high, mainly due to the low values of CE, and would need to be significantly reduced in order to make the PBE reactor competitive for application in large-scale processes. The present data show that the main parameter to be optimized is CE, since the values of E_{cell} were within the range found in hydrometallurgical processes used for copper production (Wiechmann *et al*., 2010).

The data shown in Table 3.2 were analyzed statistically in order to identify a strategy to improve CE. The results are shown in the contrast diagram of Fig. 3.6, where it can be seen that the most important variable affecting CE was the current density (i), followed by t_p and t_f. Higher values of CE could be obtained by increasing the current density and t_p, or by decreasing t_f. All these strategies were explored. Firstly, current densities greater than 3000 A m^{-2} were applied, but the electrodeposition stopped after a few minutes of electrolysis due to the short circuit caused by dendritic copper deposition close to the counter electrode. This finding was in agreement with the results illustrated in Fig. 3.3, with highly negative overpotentials and high electrodeposition rates in the region close to the counter electrode. It could be concluded that use of current densities higher than 3000 A m^{-2} was unable to avoid short circuit.

Fig. 3.7 shows the concentration-time curves obtained varying t_p and t_f. Runs 7 and 8 revealed that when t_f was reduced from 3 s to 2 s, there was an important enhancement of the electrodeposition kinetics. Attempts were made to use t_f times shorter than 2 s, but these fluidization times were not sufficiently long to ensure good particle homogenization, with particle agglomeration and short circuit occurring after only a few minutes of electrolysis. An enhancement of CE was obtained by increasing t_p from 30 s to 60 s. Values of t_p greater than 60 s were also tested, but were not useful due to particle agglomeration close to the counter electrode, which resulted in short circuit limitations.

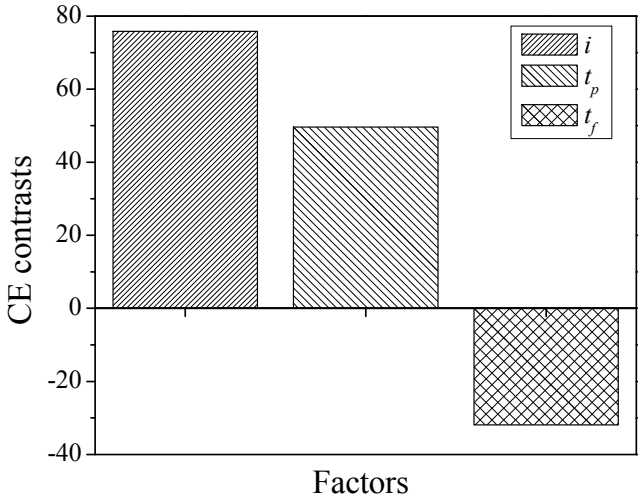

Fig. 3.6. Contrast analysis for current efficiency.

It can be seen from Fig. 3.7 that the process was again controlled by electron transfer, with zero-order kinetic constant values of − 0.499, − 0.596, and − 0.654 g L^{-1} h^{-1} for Runs 7, 8, and 9, respectively. Comparison of these kinetic constants with those obtained in the previous experiments showed that faster kinetics were achieved by increasing t_p and decreasing t_f, in agreement with the FFD results. The temperatures at the end of the electrolyses in Runs 7, 8, and 9 were in the range 38-44 °C, and the temperature-time curves were quite similar to the curves obtained in the previous experiments.

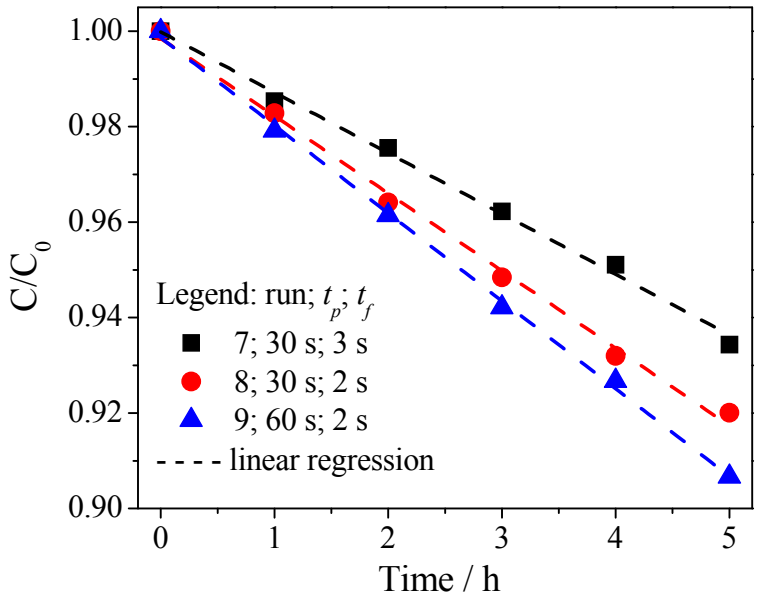

Fig. 3.7. Normalized copper concentration against time for runs 7 to 9. C_0 = 37.2 g L^{-1} Cu^{2+}, 150 g L^{-1} H_2SO_4, i = 3000 A m^{-2}.

The values of CE, Y, $E_{cell,av.}$, EC, and m_{cf} obtained for Runs 7, 8, and 9 are provided in Table 3.3. It is notable that the values of m_{cf} were significantly reduced and that in Run 9 no appreciable amount of copper was deposited on the current feeder. A significant reduction of $E_{cell,av.}$ was observed, compared with the values shown in Table 3.2, when 3000 A m^{-2} was used. Compared to the previous values, a very large increase of CE was obtained when the value of t_f was reduced from 3 s to 2 s. The highest CE value (~ 77%) was obtained when t_p was increased to 60 s, but this was still lower than commonly found in industry (82-92%) (Wiechmann *et al*., 2010). Despite the low CE values, the value of EC for Run 9 was in the same range found for large-scale processes.

Table 3.3
CE, $E_{cell,av.}$, EC, Y, and m_{cf} for the runs shown in Fig. 7.

Run	i / A m^{-2}	t_p /s	t_f /s	CE / %	$E_{cell, av.}$/ V	EC / kWh kg^{-1}	Y / kg m^{-3} h^{-1}	m_{cf} / g
7	3000	30	3	58.5	2.27	3.3	46.2	1.0
8	3000	30	2	69.9	2.23	2.7	55.2	0.5
9	3000	60	2	76.7	2.30	2.5	60.6	-
Industry*	250- 320	-	-	82-92	1.9-2.3	1.7-2.5	~ 5	-

*Based on references (BEUKES e BADENHORST, 2009, WIECHMANN; MORALES e AQUEVEQUE, 2010)

Finally, the electrodeposits obtained using the acidic copper sulfate solution described in the experimental section (without any organic additive) were investigated using scanning electron microscopy (SEM) and energy-dispersive X-ray (EDX) analysis. Electrodeposition was also performed using a flat plate electrode, with application of the current density commonly employed in industrial processes (300 A m^{-2}), in order to compare the electrodeposit with that obtained using the copper particles and application of 3000 A m^{-2}. It should be noted that the current density of 3000 A m^{-2} considered the area of the current feeder (4.5 cm × 8.0 cm), and that the current density would be lower than 100 A m^{-2} if the area of the particle surface was used instead. Analysis of the composition of the electrodeposits showed that in both cases only metallic copper was deposited. Copper oxides were not formed, as indicated by an almost complete absence of oxygen in the EDX analyses. However, the morphologies of the electrodeposits were quite different. At low magnification, the electrodeposit obtained on the flat plate was rough, while on the copper particles it was quite smooth. At higher magnification,

the electrodeposit was comparable with those produced on a flat plate electrolyzer operated at a current density of 250 A m^{-2} in the presence of organic additives (thiourea and animal glue) (Muresan *et al*., 2000).

CONCLUSIONS

The PBE electrode can be used for copper electrowinning with low energy consumption. The maximum current density that can be applied is 3000 A m^{-2}, which is approximately 10 times higher than employed using flat plate electrodes. The packed bed duration must be as long as possible in order to achieve the highest current efficiency; however, limitations imposed by metal clogging and short circuit restricts this time to a maximum of 60 s. Conversely, the fluidized bed duration must be as short as possible in order to avoid the metal dissolution responsible for low current efficiencies. In the present case, the minimum t_f value was 2 s. Although the maximum current efficiency was ~ 77%, the energy consumption (2.5 kWh kg^{-1}) was in the range commonly found for hydrometallurgical processes.

Acknowledgments

The authors are grateful to FAPESP (Fundação de Amparo à Pesquisa do Estado de São Paulo) for financial support, and CNPq (Coordenação de Aperfeiçoamento de Pessoal de Nível Superior) for a PhD fellowship.

References

Argondizo, A., 2001. Remoção de íons cobre de soluções aquosas diluídas em eletrodo de leito pulsante. (PhD Thesis) Federal University of São Carlos, São Carlos, Brazil (131 pp.).

Beukes, N.T., Badenhorst, J., 2009. Copper electrowinning: theoretical and practical design. J. S. Afr. I. Min. Metall. 109, 343-356.

Britto-Costa, P.H., Ruotolo, L.A.M., 2011. Electrochemical removal of copper ions from aqueous solutions using a modulated current method. Sep. Sci. Technol. 46, 1205-1211.

Cifuentes, L., Ortiz, R., Casas, J.M., 2005. Electrowinning of copper in a lab-scale squirrel-cage cell with anion membrane. AIChE J 51, 2273-2284.

Coeuret, F., 1980. The fluidized bed electrode for the continuous recovery of metals. J. Appl. Electrochem. 10, 687-696.

Coeuret, F., Paulin, M., 1988. Experiments on copper recovery in a pulsed granular fixed bed electrode. J. Appl. Electrochem. 18, 162-165.

El-Shakre, M.E., Saleh, M.M., El-Anadouli, B.E., Ateya, B.G., 1994. Applications of porous flow-through electrodes. J. Electrochem. Soc. 141, 441-447.

Evans, J.W., Ding, R., Doyle, F.M., Jiricny, V., 2005. Copper electrodeposition onto extended urface area electrodes and the treatment of copper containing waste streams. Scand. J. Metall. 34, 363-368.

Gallone, P., 1977. Achievements and tasks of electrochemical engineering. Electrochim. Acta 22, 913-920.

Garfias-Vasquez, F.J., Duverneuil, P., Lacoste, G., 2004. Behaviour, modelling and simulation of a pulsed three-dimensional radial electrode with continuous solid flow: Part I. J. Appl. Electrochem. 34, 417-426.

Habashi, F., 2007. Copper metallurgy at the crossroads. J. Min. Met. 43 B, 1-19. Hadzismajlovic, D.Z.E., Popov, K.I., Pavlovic, M.G., 1996. The visualization of the electrochemical behavior of metal particles in spouted, fluidized and packed beds. Powder Technol. 86, 145-148.

Hutin, D., Coeuret, F., 1977. Experimental study of copper deposition in a fluidized bed electrode. J. Appl. Electrochem. 7, 463-471.

Hyvärinen, O., Hämäläinen, M., 2005. HydroCopper™ a new technology producing copper directly from concentrate. Hydrometallurgy 77, 61-65.

Jiricny, V., Roy, A., Evans, J.W., 2002. Copper electrowinning using spouted-bed electrodes: part I. Experiments with oxygen evolution or matte oxidation at the anode. Metall. Mater. Trans. B 33, 669-676.

Kazdobin, K., Shvab, N., Tsapakh, S., 2000. Scaling-up fluidized-bed electrochemical reactors. Chem. Eng. J. 79, 203-209.

Lafront, A.M., Zhang, W., Ghali, E., Houlachi, G., 2010. Electrochemical noise studies of the corrosion behavior of lead anodes during zinc electrowinning maintenance. Electrochim. Acta 55, 6665-6675.

Lupi, C., Pilone, D., 1997. New lead alloy anodes and organic depolarizer utilization in zinc electrowinning. Hydrometallurgy 44, 347-358.

Martins, R., Britto-Costa, P.H., Ruotolo, L.A.M., 2012. Removal of toxic metals from aqueous

effluents by electrodeposition in a spouted bed electrochemical reactor. Environ. Technol. 33, 1123-1131.

Moats, M., Hardee, K., Brown, C., 2003. Mesh-on-lead anodes for copper electrowinning. JOM 55, 46-48.

Moskalyk, R.R., Alfantazi, A., Tombalakian, A.S., Valic, D., 1999. Anodes effect in electrowinning. Miner. Eng. 12, 65-73.

Muresan, L., Varvara, S., Maurin, G., Dorneanu, S., 2000. The effect of some organic additives upon copper electrowinning from sulphate electrolytes. Hydrometallurgy 54, 161-169.

Olive, H., Lacoste, G., 1979. Application of volumetric electrodes to the recuperation of metals in industrial effluents-I. Mass transfer in fixed beds of spherical conductive particles. Electrochim. Acta 24, 1109-1114.

Panda, B., Das, S.C., 2001. Electrowinning of copper from sulfate electrolyte in presence of sulfurous acid. Hydrometallurgy 59, 55-67.

Pletcher, D., Walsh, F.C., 1990. Industrial Electrochemistry. Chapman and Hall, Cambridge. Pletcher, D., White, I., Walsh, F.C., Millington, J.P., 1991. Reticulated vitreous carbon cathodes for metal ion removal from process streams Part II: Removal of copper(II) from acid sulphate media. J. Appl. Electrochem. 21, 667-671.

Ponte, M.J.J.S., 1998. Study of copper ion removal from aqueous solutions using particulate electrodes. (PhD Thesis) Federal University of São Carlos, São Carlos, Brazil (215 pp.).

Ruotolo, L.A.M., Gubulin, J.C., 2002. Electrodeposition of copper ions on fixed bed electrodes: kinetic and hydrodynamic study. Braz. J. Chem. Eng. 19 (1), 105-118.

Ruotolo, L.A.M., Gubulin, J.C., 2005. A factorial-design study of the variables affecting the electrochemical reduction of Cr(VI) at polyaniline-modified electrodes. Chem. Eng. J. 110 (1-3), 113-121.

Ruotolo, L.A.M., Gubulin, J.C., 2011. A mathematical model to predict the electrode potential profile inside a polyaniline-modified reticulated vitreous carbon electrode operating in the potentiostatic reduction of Cr(VI). Chem. Eng. J. 171 (3), 1170-1177.

Sabacky, B.J., Evans, J.W., 1979. Electrodeposition of metals in fluidized bed electrodes. J. Electrochem. Soc. 126, 1176-1187.

Salas-Morales, J.C., Evans, J.W., Newman, O.M.G., Adcock, P.A., 1997. Spouted bed electrowinning of zinc: Part I. Laboratory-scale electrowinning experiments. Metall. Mater.

Trans. B 28B, 59-68.

San Martin, R.M., Otero, A.F., Cruz, A., 2005. Use of quillaja saponins (Quillaja saponaria Molina) to control acid mist in copper electrowinning processes Part 2: pilot plant and industrial scale evaluation. Hydrometallurgy 77, 171-181.

Shakarji, R.A., He, Y., Gregory, S., 2011. Statistical analysis of the effect of operating parameters on acid mist generation in copper electrowinning. Hydrometallurgy 106, 113-118.

Sigley, J.L., Johnson, P.C., Beaudoin, S.P., 2003. Use of nonionic surfactant to reduce sulfuric acid mist in the copper electrowinning process. Hydrometallurgy 70, 1-8.

Silva-Martínez, S., Roy, S., 2013. Copper recovery from tin stripping solution: galvanostatic deposition in a batch-recycle system. Sep. Purif. Technol. 118, 6-12.

Tonini, G.A., Farinos, R.M., Prado, P.F.A., Ruotolo, L.A.M., 2013. Box-Behnken factorial design study of the variables affecting metal electrodeposition in membraneless fluidized bed electrodes. J. Chem. Technol. Biotechnol. 88, 800-807.

USG Survey, 2013. Mineral Commodity Summaries. U.S. Geological Survey, Reston.

Wiechmann, E.P., Morales, A.S., Aqueveque, P., 2010. Improving productivity and energy efficiency in copper electrowinning plants. IEEE Trans. Ind. Appl. 46, 1264-1269.

3.3 Conclusões

Os resultados apresentados neste capítulo mostraram que o eletrodo de leito pulsante pode ser utilizado no processo de eletrorrecuperação de cobre apresentando baixo consumo energético. A densidade de corrente elétrica máxima que pode ser aplicada ao reator é de 3000 A m^{-2}, sem que haja problemas de curto-circuito, que corresponde a, aproximadamente, uma densidade 10 vezes maior que a utilizada em eletrodos industriais convencionais. A duração do leito fixo deve ser estendida ao máximo possível (60 segundos neste caso), sem que haja aglomeração das partículas ou curto-circuito, para que valores ótimos de eficiência de corrente sejam obtidos. Opostamente, a duração do leito fluidizado deve ser reduzida ao mínimo para evitar a dissolução de cobre devido a potenciais anódicos que surgem durante a fluidização e que são responsáveis pelos baixos valores de *EC* obtidos. O valor mínimo do tempo de leito fluidizado determinado para o reator utilizado foi de 2 segundos. Embora a *EC* máxima obtida tenha sido de ~77%, o consumo energético foi de 2,5 kWh kg^{-1}, que é um valor próximo àqueles usualmente encontrados nos processos hidrometalúrgicos industriais.

4 ESTUDO PARAMÉTRICO DA ELETRORRECUPERAÇÃO DE COBRE UTILIZANDO ELETRODO DE LEITO PULSANTE

4.1 Introdução

A hidrometalurgia é um importante segmento da metalurgia extrativa na produção mundial de cobre. Geralmente são empregados nesta atividade eletrodos planos, os quais não apresentam valores de rendimento espaço-tempo baixos devido à pequena área dos eletrodos que limitam o valor de corrente a ser aplicado. Além disso, outras desvantagens são inerentes a esse tipo de eletrodo como a necessidade de recolher o material depositado, os vapores ácidos gerados durante o processo que podem oxidar contatos elétricos, além de gerar um ambiente insalubre e finalmente a necessidade de utilizar aditivos químicos a fim de aumentar a vida útil dos ânodos de PbO_2. Na tentativa de superar tais deficiências, buscou-se neste estudo, obter bons resultados de *EC*, *CE*, *Y* e qualidade de depósito na eletrorrecuperação de cobre utilizando ELP. Adicionalmente, este reator possibilita o uso de ânodos dimensionalmente estáveis, uma vez que apresenta considerável aumento de produtividade, quando comparado ao reator convencional e, consequentemente, utiliza menor quantidade de ânodos.

Neste capítulo investigou-se a aplicação de um reator eletroquímico de ELP para a eletrorrecuperação de cobre, onde foram abordados os efeitos da concentração do ácido sulfúrico, densidade de corrente elétrica, e o tempo de leito fixo, empregando para isso as concentrações de cobre típicas encontradas na indústria hidrometalúrgica. O reator ELP utilizado foi projetado como sendo de um compartimento, ou seja, sem membrana para separar o catolito do anolito, o que diminui seus custos. Neste capítulo realizou-se um estudo estatístico, através de um planejamento fatorial completo, como ferramenta para se entender o efeito das variáveis densidade de corrente elétrica (i), tempo de leito fixo (t_p) e concentração de ácido sulfúrico (C_s) no processo de eletrorrecuperação de cobre.

Observou-se uma diminuição linear da concentração de cobre durante a eletrólise, característica da cinética de ordem zero. Tal comportamento é típico de processos controlados por transferência de elétrons, portanto, esperado para uma concentração elevada de cobre e de uma corrente aplicada muito inferior à corrente limite. Com a utilização do ELP, com apenas 10,6% do volume de um reator convencional, foi possível recuperar a mesma quantidade de cobre, que permite ainda a possibilidade de operação contínua. Todos os efeitos próximos de

zero, usando uma abordagem linear, foram atribuídas à variabilidade aleatória normal, e podendo, portanto, serem excluídos do planejamento por não serem estatisticamente significativos. A concentração do ácido por si só não promoveu efeito estatisticamente significativo sobre a *EC*, o que pode ser explicado pelo fato da concentração do ácido apresentar dois efeitos opostos e que se sobrepõem a *EC*. Finalmente, dois experimentos foram realizados utilizando um eletrodo de placa plana, sem aditivos químicos, a fim de comparar a qualidade dos depósitos obtidos, através de microscopia de varredura eletrônica (MEV), empregando o ELP e o eletrodo plano convencional.

4.2 Desenvolvimento

O desenvolvimento detalhado do Capítulo 4 é apresentado a seguir, no artigo intitulado *Parametric study of copper electrowinning using a pulsed-bed electrode*, aceito para publicação no periódico *Journal of Chemical Technology and Biotechnology*.

Research Article

Received: 12 March 2014 Revised: 10 June 2014 Accepted article published: 26 June 2014 Published online in Wiley Online Library:

(wileyonlinelibrary.com) DOI 10.1002/jctb.4472

Parametric study of copper electrowinning using a pulsed-bed electrode reactor

Pedro H. Britto-Costa and Luís A. M. Ruotolo*

Abstract

BACKGROUND: The pulsed bed electrode (PBE) has been used successfully for copper electrodeposition from highly concentrated acidic electrolytes. Advantages of this electrode include high space-time yield (*Y*) and simple operation and maintenance. In this work, the effects of operational conditions were investigated in an attempt to achieve current efficiencies (*CE*) higher than 76.7%, which was the maximum value obtained in a previous study.

RESULTS: The results showed that use of a high current density and low acid concentration provided the best operational conditions for maximizing *CE* and *Y*, and minimizing the energy consumption (*EC*). Nonetheless, the highest current density was limited to 3000 A cm^{-2} and the lowest acid concentration was limited to 110 g L^{-1}, due to limitations such as metal dissolution, dendrite growth, and short circuiting. The highest *CE* achieved was 77.7%, using 2838 A m^{-2}. According to a statistical model, the maximum *CE* value that could be achieved is 82.4%, with application of 3000 A cm^{-2}. This suggests that further improvement of *CE* would lead to values of *EC* lower than those found in electrowinning plants.

CONCLUSIONS: Electrowinning using a pulsed-bed electrode is an excellent method for copper production, but additional improvements are required to increase *CE*.

Keywords: pulsed bed; porous electrodes; electrowinning; flow rate pulses

INTRODUCTION

Hydrometallurgy is an important area of extractive metallurgy and accounted for 20–25% of global copper production in 2012, estimated at 17.0 million tons,[1] using the leach–solvent–extraction electrowinning technology.[2–6] In this process, flat plate electrodes are used for metal electrodeposition, typically applying current densities of around 300 A m^{-2}, which requires large electrowinning tankhouses, so that the space-time yield is low. Besides these constraints, there are other drawbacks, such as the need to harvest the electrodeposited metal from the substrate (cathode), which is often performed manually in small plants. Additionally, the acid mist released during the process can oxidize electrical contacts or affect the health of the operator.[6–11] Although PbO_2 anodes are generally used in electrowinning, these anodes are not stable and require the addition of chemical additives to the electrolyte to increase their working life.[12–14] However, the use of these additives does not prevent anode corrosion, and lead contamination of the electrodeposited metal must be strictly controlled.[13,15,16]

Particulate electrodes have been studied as an alternative to overcome many of these drawbacks.[7,8,17–23] The main advantages of such electrodes are the very large increase in space-time yield, due to the smaller reactor volume required to produce the same amount of metal, as well as the higher currents that can be applied, which is made possible by the extended surface area provided by the particulate cathode.[7,8,21,24] In the case of particulate bed electrodes, harvesting of the electrodeposited metal consists simply of collecting the particles at the end of a process cycle. Moreover, problems of acid mist can be easily eliminated by channeling it at the exit of the electrochemical reactor. Another important advantage of using particulate electrodes is the possibility of replacing the PbO_2 anodes by dimensionally stable anodes (DSA®), such as titanium–iridium or titanium–ruthenium oxide anodes. This can be economically viable because the use of three-dimensional cathodes can alleviate the need for large DSA® anodes. A further advantage is that replacement of PbO_2 by DSA® anodes could eliminate the need for chemical additives.[12,14]

Among the particulate electrodes used for metal electrodeposition, packed beds have been widely studied, particularly for effluent treatment, where the metal concentration is very low.[20,22–26] The high conductivity of the solid phase and high mass transfer coefficients enable the packed bed cathode to operate at high current efficiency.[23,25]

Unfortunately, when the metal concentration is high (as in the case of electrowinning processes), metal deposition results in very fast clogging of the electrode pores.[20–23] In order to overcome this problem, fluidized bed electrodes have been studied for metal electrodeposition, because clogging of the electrode can be avoided by maintaining the conducting particles in a fluidized state using an upward electrolyte flow.[17,20,27–29] However, for this type of electrode, the reaction rate is very sensitive to the

* *Correspondence to: L.A.M. Ruotolo, Department of Chemical Engineering, Federal University of São Carlos, P.O. Box 676, 13565-905 São Carlos – SP, Brazil. E-mail: pluis@ufscar.br*

Department of Chemical Engineering, Federal University of São Carlos, P.O. Box 676, 13565-905, São Carlos, SP, Brazil

Abstract

BACKGROUND: The pulsed bed electrode (PBE) has been used successfully for copper electrodeposition from highly concentrated acidic electrolytes. Advantages of this electrode include high space-time yield (Y) and simple operation and maintenance. However, there is still a need to improve current efficiency (CE) in order to reduce energy consumption (EC) and make the PBE competitive with traditional flat plate electrodes. In this work, the effects of acid concentration, current density, and packed bed time were investigated in an attempt to achieve current densities higher than 76.7%, which was the maximum value obtained in a previous study.

RESULTS: The results showed that use of a high current density and low acid concentration provided the best operational conditions for maximizing CE and Y, and minimizing EC. Nonetheless, the highest current density was limited to 3000 A cm^{-2} and the lowest acid concentration was limited to 110 g L^{-1}, due to limitations such as metal dissolution, dendrite growth, and short circuit. The highest CE achieved was 77.7%, using 2838 A m^{-2}. According to a statistical model, the maximum CE value that could be achieved is 82.4%, with application of 3000 A cm^{-2}. This suggests that further improvement of CE would lead to values of EC lower than those found in real electrowinning processes. The electrodeposit was smooth, and comparable with the deposit produced on a flat plate electrolyzer.

CONCLUSIONS: Electrowinning using a pulsed-bed electrode is an excellent method for copper production, but additional improvements must be done in order to increase CE.

INTRODUCTION

Hydrometallurgy is an important area of extractive metallurgy and accounted for 20-25% of global copper world's production in 2012, estimated at 17.0 million tons,[1] using the leach-solvent-extraction electrowinning technology.[2-6] In this process, flat plate electrodes are used for metal electrodeposition, typically applying current densities of around 300 A m^{-2}, which requires large electrowinning tankhouses, so that the space-time yield is low. Besides these constraints, there are other drawbacks, such as the need to harvest the electrodeposited metal from the substrate (cathode), which is often performed manually in small plants. Additionally, the acid mist released during the process can oxidize electrical contacts or affect the health of the operator.[6-11] Although PbO_2 anodes are generally used in electrowinning processes, these anodes are not stable and require the addition of chemical additives to the electrolyte in order to increase their working life.[12-14] However, the use of these additives does not prevent anode corrosion, and lead contamination of the electrodeposited metal must be strictly controlled.[13,15,16]

Particulate electrodes have been studied as an alternative to overcome many of these drawbacks.[7,8,17-23] The main advantages of such electrodes are the very large increase in space-time yield, due to the smaller reactor volume required to produce the same amount of metal, as well as the higher currents that can be applied, which is made possible by the extended surface area provided by the particulate cathode.[7,8,21,24] In the case of particulate bed electrodes, harvesting of the electrodeposited metal consists simply of collecting the particles at the end of a process cycle. Moreover, problems of acid mist can be easily eliminated by channeling it at the exit of the electrochemical reactor. Another important advantage of using particulate electrodes is the possibility of replacing the PbO_2 anodes by dimensionally stable anodes (DSA®), such as titanium-iridium or titanium-ruthenium oxide anodes. This can be economically viable because the use of three-dimensional cathodes can alleviate the need for large DSA® anodes. A further advantage is that replacement of PbO_2 by DSA® anodes could eliminate the need for chemical additives.[12,14]

Among the particulate electrodes used for metal electrodeposition, packed beds have been widely studied, particularly for effluent treatment, where the metal concentration is very low.[20,22-26] The high conductivity of the solid phase and high mass transfer coefficients enable the packed bed cathode to operate at high current efficiency.[23,25]

Unfortunately, when the metal concentration is high (as in the case of electrowinning processes), metal deposition results in very fast clogging of the electrode pores.[20-23] In order to overcome this problem, fluidized bed electrodes have been studied for metal electrodeposition, because clogging of the electrode can be avoided by maintaining the conducting particles in a fluidized state using an upward electrolyte flow.[17,20,27-29] However, for this type of electrode, the reaction rate is very sensitive to the fluid dynamic conditions because the conductivity of the solid phase depends on the frequency of collisions between the particles, which is mainly determined by the bed dimensions.[20,27] In some cases, when the local difference between the solid and liquid phase potentials is positive, zones of metal dissolution inside the fluidized cathode can occur.[17,27] For these reasons, the pulsed bed electrode (PBE) has emerged as an interesting alternative. This electrode benefits from the high current efficiency provided by the packed bed electrode, while avoiding clogging by fluidization.[18,30,31] In this kind of electrode, the packed bed is periodically fluidized by applying regular flow rate pulses, which can be generated by mechanical or electrical devices,[30,31] as well as using special valve setups.18 Another advantage regarding use of the PBE is the continuous particle mixing during the pulse, which enables the particles to grow uniformly.

In this study, a PBE electrochemical reactor for copper electrowinning was investigated in terms of acid concentration, current density, and packed bed time, using typical copper concentrations found in industrial hydrometallurgical processes. The PBE was designed as a one compartment reactor, with no membrane separating the catholyte from the anolyte, which reduced the capital costs.[32] The flow rate pulses were generated by controlling the rotation of a centrifugal pump using a logic module and a frequency inverter. Considering the state of the art, there are only a few works reporting the use of PBE's for metal electrodeposition. In most cases, PBEs were used to recover metals from dilute solutions, where the main objective was effluent treatment.[18,30] Moreover, as far as we know, there are no papers reporting the use of membraneless PBEs or the pulsed flow rate technique proposed in this study.

In a previous study, Britto-Costa et al.[33] investigated the effect of variables such as packed bed and fluidized bed times, temperature, and current density on the process efficiency. After all these variables had been optimized, the maximum current efficiency and energy consumption obtained were 76.7% and 2.5 kWh kg^{-1}, respectively. This energy consumption is comparable to those found in industrial processes that use flat plate electrodes. However, there remains the possibility of improving the current efficiency and, consequently, reducing the energy consumption. As a strategy to increase the current efficiency, this work considers the influence of the acid concentration, current density, and packed bed time on current efficiency (CE), energy consumption (EC), and space-time yield (Y). The acid concentration of the supporting electrolyte influences the local particle-solution potential within the three-dimensional cathode, and therefore influences the local kinetics. The parameters packed bed time and current density were chosen because they could have strong interaction effects with the acid concentration, hence influencing current penetration and metal dissolution. Throughout the experiments, the fluidized bed time was maintained constant at the previously optimized value.[33] The morphology of the electrodeposited copper was analyzed by scanning electron microscopy (SEM).

EXPERIMENTAL

Electrochemical reactor

Figure 4.1(a) shows a schematic view of the pulsed bed electrochemical reactor used for copper electrowinning. The reactor consisted of three rectangular acrylic plates that were intercalated with silicone rubbers to avoid leaking and assembled using screws and nuts. The dimensions of

the chamber containing the pulsed bed electrode were 3.4 cm (thickness) x 4.5 cm (width) x 35 cm (length). The external reactor dimensions were 7.4 cm (thickness) x 10.5 (width) x 37.5 (height). The electrolyte flowed upwards (6), and before reaching the three-dimensional electrode (2) it passed through a flow distributor made of polyethylene particles (3). Equilateral 1.0 mm cylindrical copper particles were used to form the porous cathode (2). Stainless steel 316 (1) and $Ti/Ti_{0.7}Ru_{0.3}O_2$ DSA® (DeNora, Brazil) (5) were used for the current feeder and counter-electrode, respectively.

An important characteristic distinguishing this reactor from many others used for metal electrodeposition is that it did not have two compartments with a membrane separating catholyte and anolyte (it was a membraneless reactor). There was only one separator (4) composed of a polyethylene mesh covered with a polyamide fabric. This separator was placed between the porous cathode and the counter-electrode in order to avoid short circuit. This reactor configuration has some advantages over the membrane reactor, such as low cell potential, low energy consumption, simple maintenance, and low capital costs because the use of expensive membranes is eliminated.

Flow rate pulsation

Flow rate pulses were generated using a frequency inverter acting on the centrifugal pump rotation and, consequently, on the flow rate. The frequency inverter (MicroMaster MM55, Siemens) was controlled by a logic module (LOGO! 230RC, Siemens) that determined the time during which the bed remained in the packed (low frequency rotation) and fluidized (high frequency rotation) states.

Copper electrowinning

Figure 4.1(b) shows a schematic view of the experimental setup used for copper electrowinning. The process was carried out galvanostatically using a constant current source (GenesysTM 1500W, Lambda). The cell potential (E_{cell}) was recorded every 2 s using a data acquisition system.

The electrolyte was prepared using deionized water, technical grade copper sulfate, and sulfuric acid. The copper concentration varied from 35 to 40 g L^{-1} Cu^{2+}, and the acid concentration varied from 100 to 180 g L^{-1}. The porous cathode was composed of 580 g of copper particles. These copper and acid concentrations are typical of those found in the copper electrowinning industry. An electrolyte volume of 15 L was used in all experiments.

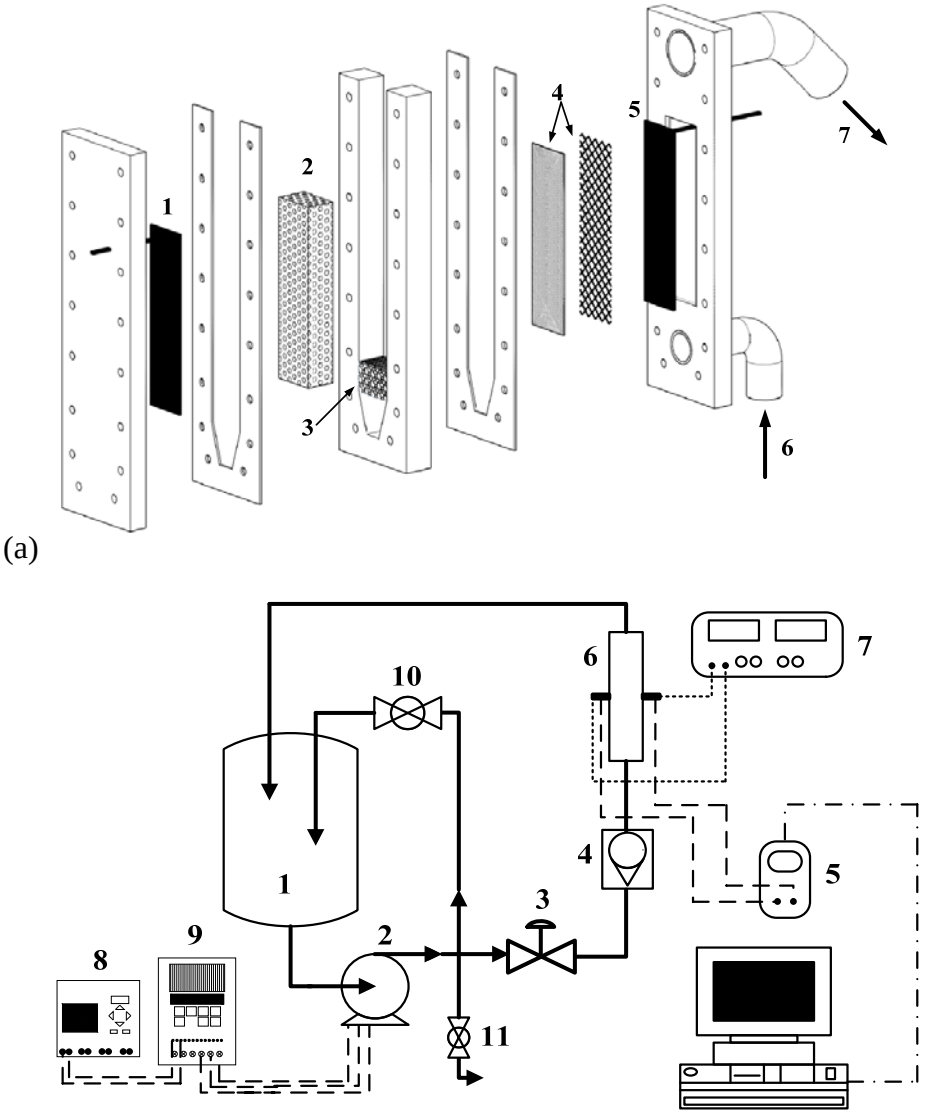

Figure 4.1. (a) Schematic view of the electrochemical reactor: 1) current feeder; 2) porous cathode; 3) flow distributor; 4) separators; 5) counter-electrode; 6) electrolyte inlet; and 7) electrolyte exit; (b) Experimental setup: 1) electrolyte reservoir; 2) centrifugal pump; 3) rotameter; 4) diaphragm valve; 5) voltmeter; 6) electrochemical reactor; 7) current source; 8) logic module; 9) frequency inverter; 10) by-pass valve; and 11) drain valve.

The experimental procedure consisted of circulating the electrolyte between the reservoir and the reactor, and collecting samples for analysis of the copper concentration. The flow rates during the packed and fluidized bed conditions were maintained constant at 136 L h^{-1} and 625 L h^{-1}, respectively. The variables current density, packed bed time, and fluidized bed time were previously studied by Britto-Costa et al.[33]. It was concluded that anodic zones can occur during the fluidized state, indicating that this variable should be reduced to the minimum possible value, which was found to be 2 s. For shorter fluidized bed times, short circuit or

electrode clogging could occur. From these results, the value of t_f used in the present work was 2 s.

The copper concentration was determined colorimetrically by measuring the absorbance at 810 nm using an Ultrospec 2100Pro UV-VIS spectrophotometer (Amersham Pharmacia). This technique was highly accurate for measurement of copper concentrations in the range used in this study.

The electrowinning process was evaluated in terms of current efficiency (CE), energy consumption (EC), and space-time yield (Y), as a function of acid concentration and the operational variables current density and packed bed time. The values of CE, EC, and Y were calculated according to Equations (4.1), (4.2), and (4.3), respectively. In these equations, z is the number of electrons of the electrochemical reaction, F is the Faraday constant (96,496 C mol^{-1}), M is the molar weight (g mol^{-1}), I is the applied current (A), V is the electrolyte volume (L), C is the copper mass concentration (g L^{-1}), t is the electrowinning time (s), E_{cell} is the cell potential (V), and VR is the reactor volume (m^3). The constants 2.78 x 10^{-4} and 3.6 are conversion factors used to obtain EC in kWh kg^{-1} and Y in kg m^{-3} h^{-1}. The reaction rates (dC/dt) were determined from the concentration-time curves obtained experimentally.

$$CE = \frac{zFV}{MI}\frac{dC}{dt} \tag{4.1}$$

$$EC = \frac{2.78\ x\ 10{-}4zFE_{cell}}{MCE} \tag{4.2}$$

$$Y = 3.6\frac{V}{V_R}\frac{dC}{dt} \tag{4.3}$$

Design of experiments (DoE)

Design of experiments is a powerful technique that can be used for the statistical analysis of processes influenced by several independent variables.[34] In this study, different DoEs were used to evaluate the effects of the applied current density (i), packed bed time (t_p), and acid concentration ($C_{ac.}$) on CE, EC, and Y. Response surface methodology (RSM) was employed to determine the best operational conditions that maximized CE and Y, and minimized EC.

The coded values of the independent variables were calculated using the equation:

$$x_j = \frac{(\xi_j - \xi_0)}{(\xi_1 - \xi_0)} \tag{4.4}$$

where x_i is the dimensionless coded value of the independent variable j, ξ_j is the uncoded value of j, ξ_0 is the uncoded value of the variable at the center point, and ξ_1 is the uncoded value of the variable at the highest level. Two DoE's were used to investigate the effects of the independent variables. In a first attempt, a 2^3 central composite rotatable design (CCRD) was carried out, but this factorial design was found to be unsuitable. A 2^3 full factorial design (FFD) was then successfully used to describe the effects of the independent variables and to optimize the process.

In Tables 4.1 and 4.2 the levels ±1.68 represent the axial points of the CCRD. The FFD was performed considering only the levels -1 and +1, with three central points (level 0). As mentioned before, the levels of the variables i and t_p were established based on our previous work.[33] Preliminary experiments were carried out to establish the acid concentration levels. It was found that acid concentrations below 100 g L^{-1} resulted in short circuit, for reasons that will be discussed later. On the other hand, acid concentrations higher than 180 g L^{-1} caused high rates of copper dissolution during the fluidization step.

Table 4.1. Actual and coded values of the independent variables.

	Var1	Var2	Var3
Code	i / A m^{-2}	t_p / s	$C_{ac.}$ / g L^{-1}
-1.68	2200	30	100
-1	2362	36	116
0	2600	45	140
+1	2838	54	164
+1.68	3000	60	180

Table 4.2. Central composite rotatable design (CCRD) and full factorial design (FFD).

Design		Run	i / A m^{-2}	t_p / s	$C_{ac.}$ / g L^{-1}
CCRD	FFD	1	-1	-1	-1
		2	+1	-1	-1
		3	-1	+1	-1
		4	+1	+1	-1
		5	-1	-1	+1
		6	+1	-1	+1
		7	-1	+1	+1
		8	+1	+1	+1
		9	-1.68	0	0
		10	+1.68	0	0
		11	0	-1.68	0
		12	0	+1.68	0
		13	0	0	-1.68
		14	0	0	+1.68
Central Points		15	0	0	0
		16	0	0	0
		17	0	0	0

RESULTS AND DISCUSSION

Copper electrowinning

Figure 4.2(a) shows the normalized copper concentration against time for Runs 1 to 8. There was a linear decrease of the copper concentration during the electrolysis, indicative of the zero order kinetics that is typical of processes controlled by electron transfer, as expected for a very high copper concentration and an applied current far below the limiting current. The temperature varied from 25 ºC to 40 ºC from the beginning to the end of the experiments, but this temperature shift did not affect the reaction rate, since the zero order kinetics did not change during the experiments. The effect of temperature on the electrowinning process was discussed in detail previously,[33] where it was found that the main effect of temperature was on the electrolyte conductivity and E_{cell}. According to Fig. 4.2(b), which shows a typical E_{cell}-time curve, the effect of temperature on E_{cell} was more significant when the electrode was in the fluidized bed state. During the packed bed state, E_{cell} remained almost constant at ~2.5 V. The increase of E_{cell} during the fluidization step was due to the poor conductivity of the solid phase, which depends on the probability of collision between particles. For the fluidized bed, the reduction of E_{cell} during the electrolysis could be explained by enhancement of electrolyte conductivity due to the increase in temperature. In this case, the difference of electrode potential

between the solid and liquid phases becomes smaller, and E_{cell} therefore decreases.[35,36] Although the use of fluidization pulses seems to be contrary to the notion of low energy consumption, due to the high E_{cell} values, the pulses are essential in order to avoid electrode clogging. Nonetheless, considering that the fluidization pulse lasted only 2 s (see inset of Fig. 4.2(b)), its contribution to the overall E_{cell} was only approximately 0.2 V and could be even lower if the electrolyte was maintained at a high temperature.

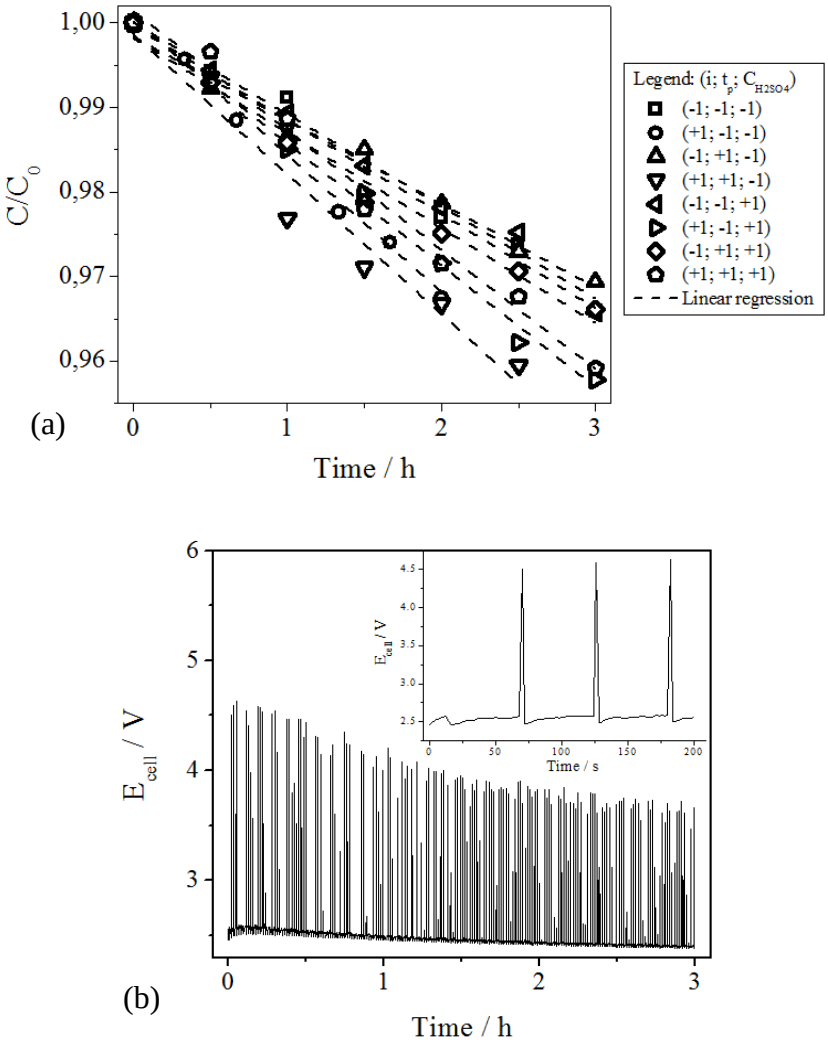

Figure 4.2. (a) Normalized copper concentration against time; (b) E_{cell} against time for Run 4.

The slopes of the copper concentration-time curves were determined by linear regression (lines in Fig. 4.2(a)) and corresponded to the zero order constants or reaction rates (dC/dt). With few exceptions, the values of the squared correlation coefficient (R^2) were high. CE and Y were calculated using Equations (4.1) and (4.3) and the values of dC/dt. The average cell potentials ($E_{cell,av}$) were determined from the plots of E_{cell} against time, by integration of

the curves. EC was calculated using Equation (4.2) and $E_{cell,av}$. The values of the response variables are provided in Table 4.3, together with the dC/dt, R^2, and $E_{cell,av}$ values.

Statistical analyses

In previous work,[33] we studied the effect of current density, packed bed time, and fluidized bed time on CE, EC, and Y. It was found that the fluidized bed time should be kept to a minimum in order to avoid anodic zones and maximize CE. The optimum fluidized bed time was 2 s, with shorter times resulting in particle agglomeration close to the counter-electrode, causing short circuit of the system after a few minutes of electrolysis. The packed bed time was also optimized, with its value depending on the applied current. After optimization, the maximum CE was 76.7%, which is lower than found in electrowinning plants (82-92%, for current densities in the range 250-320 A m^{-2}). However, despite this value of CE, the EC was 2.5 kWh kg^{-1}, which is comparable to typical industry values (1.7-2.5 kWh kg^{-1}). Hence, the PBE reactor appears to hold considerable promise, once the current efficiency is improved. In an attempt to increase the CE, and consequently decrease the EC, investigation was made of the effect of the supporting electrolyte (in this case sulfuric acid) on the copper electrodeposition. Previous work using three-dimensional electrodes for the electroreduction of metal in dilute solutions, for wastewater treatment,[30,37] has shown that the acid concentration plays an important role in the electrodeposition process. This is due to the change in the difference between the electrode potentials of the solid and liquid phases, when the electrolyte conductivity is increased. A difficulty is that a higher acid concentration can favor zones of metal dissolution within the three-dimensional electrode. In order to avoid or minimize metal dissolution, simultaneous investigation of the effects of acid concentration and current density is essential. This work therefore evaluated the effects of packed bed time, acid concentration, and current density, in an attempt to improve the electrodeposition process and obtain CE higher than 76.7% and EC lower than 2.5 kWh kg^{-1}. The first experiments were performed using a CCRD factorial design, and the results are shown in Table 4.3.

The best CE and EC values were obtained for Runs 4 and 2, respectively, but were only slightly better than obtained in the previous work. In the case of Y, the values were much higher than found for conventional electrowinning cells (~5 kg m^{-3} h^{-1}), with use of the PBE requiring only 10.6% of the conventional reactor volume to produce the same amount of copper, while also enabling the possibility of continuous operation. Although improved values of CE and EC were not obtained, statistical analysis could provide a means of indicating ways in which these parameters might be improved.

Table 4.3. CCRD codes, dC/dt, $E_{cell,av.}$, CE, EC, and Y.

Run	i	t_p	$C_{ac.}$	dC/dt / g L^{-1} h^{-1}	R^2	$E_{cell,av.}$ / V	CE / %	EC / kWh kg^{-1}	Y / kg $m^{-3}h^{-1}$
1	-1	-1	-1	6.11	96.8	2.36	57.6	3.47	29.2
2	1	-1	-1	9.27	97.7	2.42	76.7	2.66	46.6
3	-1	1	-1	5.71	98.0	2.27	56.7	3.38	28.7
4	1	1	-1	9.39	94.7	2.50	77.7	2.72	47.2
5	-1	-1	1	6.01	98.7	2.19	59.7	3.10	30.2
6	1	-1	1	6.97	99.4	2.27	57.7	3.33	35.1
7	-1	1	1	6.41	98.0	2.22	63.6	2.95	32.2
8	1	1	1	7.16	98.4	2.30	59.2	3.28	36.0
9	-1.68	0	0	4.79	96.6	2.10	51.1	3.47	24.1
10	1.68	0	0	8.14	99.7	2.19	63.6	2.91	40.9
11	0	-1.68	0	5.01	95.0	2.25	44.9	4.23	25.2
12	0	1.68	0	6.52	99.4	2.29	58.5	3.30	32.8
13	0	0	-1.68	7.26	98.5	2.46	60.6	3.30	34.0
14	0	0	1.68	7.20	96.6	2.27	64.6	2.97	36.2
15	0	0	0	6.89	97.9	2.25	61.8	3.07	34.6
16	0	0	0	6.25	98.2	2.12	56.1	3.19	31.4
17	0	0	0	6.11	98.5	2.25	54.9	3.46	30.7

Table 4 shows the analysis of variance (ANOVA) for the three responses. The models failed the F-test, since the F-values calculated for CE and EC were lower than the tabulated value, at a significance level of 95%.[34] The F-value obtained for Y was higher than the F-distribution, but not sufficiently high to guarantee statistical significance.

The poor fit responsible for the lack of statistical significance was attributed to the axial points (±1.68), where the values of the variables could lead to anomalous results. The CCRD was therefore abandoned and only the full factorial design (FFD) was used, considering only experiments 1-8 and the central points (Table 4.2).

The ANOVA for the FFD is shown in Table 4.5. In this case, high F-values were obtained for CE, EC, and Y, confirming that the axial points were responsible for the lack of fit observed using the CCRD. Given that statistical significance was achieved with the FFD, the analysis of effects was then performed in order to determine the main variables affecting the electrochemical process.

Table 4.4. CCDR ANOVA for each dependent variable.

Current Efficiency R^2=0.73	SS	DF	MS	F-value	F-distribution (95%)
Model	741	9	82.4	2.11	3.68
Residual Errors	273	7	39.1		
Pure Error	27.7	2	13.8	3.55	19.3
Lack of Fit	246	5	49.1		
Energy Consumption R^2=0.72	**SS**	**DF**	**MS**	**F-value**	**F-distribution (95%)**
Model	1.50	9	0.167	2.01	3.68
Residual Errors	0.584	7	0.0834		
Pure Error	0.0807	2	0.0403	2.49	19.3
Lack of Fit	0.503	5	0.101		
Space-time Yield R^2=0.86	**SS**	**DF**	**MS**	**F-value**	**F-distribution (95%)**
Model	565	9	62.8	4.97	3.68
Residual Errors	88.4	7	12.6		
Pure Error	8.70	2	4.35	3.67	19.3
Lack of Fit	79.7	5	15.9		

Table 4.5. FFD ANOVA for each dependent variable.

Current Efficiency R^2=0.89	SS	DF	MS	F-value	F-distribution (95%)
Model	256	3	85.2	19.7	3.68
Residual Errors	30.3	7	4.32		
Pure Error	27.2	6	4.53	0.680	19.3
Lack of Fit	3.08	1	3.08		
Energy Consumption R^2=0.92	**SS**	**DF**	**MS**	**F-value**	**F-distribution (95%)**
Model	0.303	3	0.101	28.5	3.68
Residual Errors	0.0248	7	0.00354		
Pure Error	0.0798	6	0.0133	4.14	19.3
Lack of Fit	0.0550	1	0.0550		
Space-time Yield R^2=0.95	**SS**	**DF**	**MS**	**F-value**	**F-distribution (95%)**
Model	192	3	64.0	48.7	3.68
Residual Errors	9.19	7	1.31		
Pure Error	8.65	6	1.44	0.377	19.3

Analysis of effects

The effects of the independent variables and their interactions on the response variables were investigated by plotting the normal probability Z-values as a function of the effects, ordered

from small to large values (Fig. 4.3). All effects close to zero, using a linear approach, were attributed to the normal random variability, and could therefore be excluded from the design because they were not statistically significant. These effects are shown in the dashed circle (Fig. 4.3). According to Fig. 4.3, the packed bed time and its interaction effects had no significant effect on any response variable.

Exclusion of the t_p variable from the FFD (Table 2) resulted in a 2^2 factorial design (FD) with three central points (Table 6). Here, Runs 1, 2, 5, and 6 became replicate 1 (Rep1), and Runs 3, 4, 7, and 8 became replicate 2 (Rep2). The central points (Runs 15, 16, and 17) became Rep1, Rep2, and Rep3, respectively. It is noteworthy that exclusion of t_p resulted in very similar values of Rep1 and Rep 2, confirming that t_p had no statistical significance. In Table 4.6, the variable Var corresponds to the variation, calculated as the difference between the maximum and minimum values of the replicates. These values were used for comparison with the residual errors of the statistical model.

Table 4.6. 2^2 FD for CE, EC, and Y, with replicates.

I	**Cac.**	**CE / %**				**EC / kWh kg-1**				**Y / kg m-3 h-1**			
		Rep1	**Rep2**	**Rep3**	**Var**	**Rep1**	**Rep2**	**Rep3**	**Var**	**Rep1**	**Rep2**	**Rep3**	**Var**
-1	-1	57.6	56.7	-	0.90	3.47	3.38	-	0.090	29.2	28.7	-	0.50
1	-1	76.7	77.7	-	1.0	2.66	2.72	-	0.060	46.6	47.2	-	0.60
-1	1	59.7	63.6	-	3.9	3.10	2.95	-	0.15	30.2	32.2	-	2.0
1	1	57.7	59.2	-	1.5	3.33	3.28	-	0.050	35.1	36.0	-	0.90
0	0	61.8	56.1	54.9	6.9	3.07	3.19	3.46	0.39	34.6	31.4	30.7	3.9

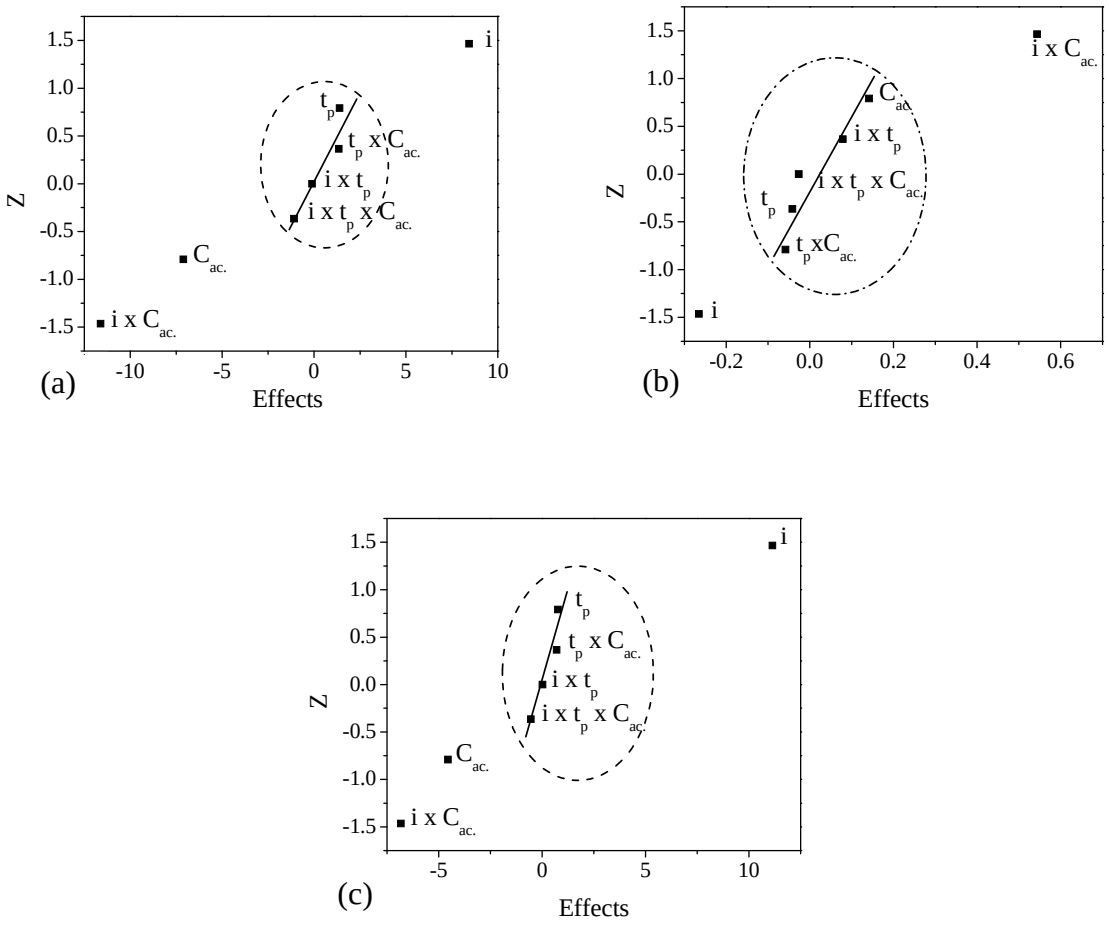

Figure 4.3. Normal probability plot of effects for CE (a), EC (b), and Y (c).

Table 4.6. 2^2 FD for CE, EC, and Y, with replicates.

I	$C_{ac.}$	CE / %				EC / kWh kg^{-1}				Y / kg m^{-3} h^{-1}			
		Rep1	**Rep2**	**Rep3**	**Var**	**Rep1**	**Rep2**	**Rep3**	**Var**	**Rep1**	**Rep2**	**Rep3**	**Var**
-1	-1	57.6	56.7	-	0.90	3.47	3.38	-	0.090	29.2	28.7	-	0.50
1	-1	76.7	77.7	-	1.0	2.66	2.72	-	0.060	46.6	47.2	-	0.60
-1	1	59.7	63.6	-	3.9	3.10	2.95	-	0.15	30.2	32.2	-	2.0
1	1	57.7	59.2	-	1.5	3.33	3.28	-	0.050	35.1	36.0	-	0.90
0	0	61.8	56.1	54.9	6.9	3.07	3.19	3.46	0.39	34.6	31.4	30.7	3.9

The effects of each independent variable were evaluated using the mean values of the replicates. Figure 4.4 shows Pareto charts of the absolute effects for CE, EC, and Y. The critical values of the Student's t-test were calculated using the standard deviation of all replicates, for each response (shown by the dashed line). Values lower than the critical value indicated that the effect had no statistical significance, and did not need to be considered in the statistical model.

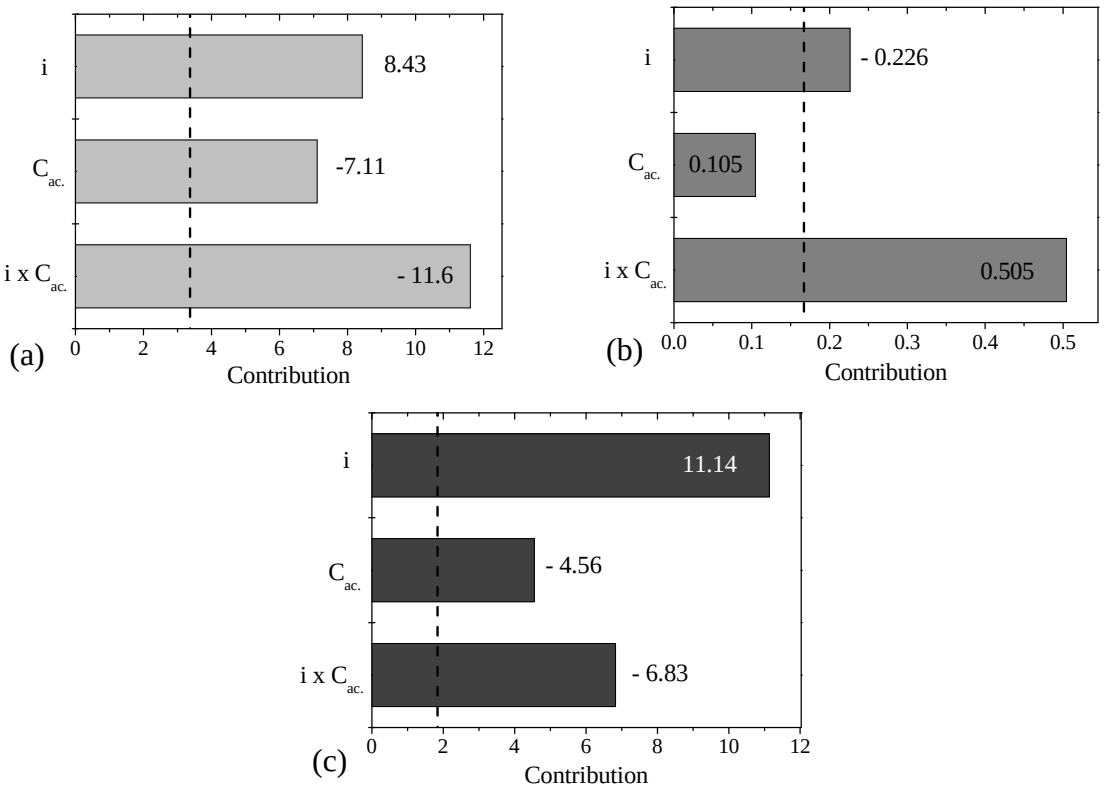

Figure 4.4. Pareto chart of absolute effects for CE (a), EC (b), and Y (c).

It can be seen from Fig. 4.4 that interaction effects made the most significant contributions to CE and EC. The acid concentration alone had no statistically significant effect on EC (as also shown in Fig. 4.3(b)). This can be explained by the fact that the acid concentration has two opposite and overlapping effects on EC. The higher the acid concentration, the lower is E_{cell}, due to the increase of electrolyte conductivity, which acts to diminish EC. On the other hand, when the current density is maintained at a constant value and the acid concentration is increased, CE will decrease due to metal dissolution, and EC will increase.[23] This explains the importance of the interaction effect of i and Cac. in determining the best operational conditions for optimization of CE and EC.

Statistical models and response surface analysisEquations (4.5), (4.6), and (4.7) are the statistical models for CE, EC, and Y, respectively, considering only the significant effects.

$$CE = 62.0 + 4.22i - 3.55C_{ac.} - 5.81iC_{ac.} \quad (4.5)$$

$$EC = 3.15 - 0.113i + 0.252iC_{ac.} \quad (4.6)$$

$$Y = 34.7 + 5.57i - 2.28C_{ac.} - 3.41iC_{ac.} \quad (4.7)$$

Table 4.7 shows the experimental mean values, the predicted values, and the residual errors (the difference between experimental mean and predicted values). In order to check the accuracy of these models, the residual values were compared to the experimental variation (Var) shown in Table 4.6. It was found that the differences between Res and Var were very small, confirming that the models for CE, EC, and Y could accurately predict the experimental responses, since the errors (residues) cannot be lower than the intrinsic experimental variation.

Table 4.7. Mean values of the dependent variables (Exp. Mean), predicted values (Pred), and residual errors (Res).

i	**$C_{ac.}$**	**CE**			**EC**			**Y**		
		Exp. mean	**Pred**	**Res**	**Exp. mean**	**Pred**	**Res**	**Exp. mean**	**Pred**	**Res**
-1	-1	57.1	55.5	1.6	3.42	3.51	-0.090	29.0	28.0	1.0
1	-1	77.2	75.5	1.7	2.69	2.78	-0.090	46.9	46.0	0.90
-1	1	61.6	60.0	1.6	3.02	3.01	0.010	31.2	30.3	0.90
1	1	58.5	56.8	1.7	3.30	3.28	0.020	35.5	34.6	0.90
0	0	57.6	62.0	-4.4	3.24	3.15	0.090	32.3	34.7	-2.4

Figure 4.5 shows the contour plots for the dependent variables. As shown in Fig. 4.5(a), the best CE was achieved using the highest *i* and the lowest C_{ac} values. There is a wide region in this graph (blue region) where the values of CE are very low (<62%). This region corresponds to the application of low current densities, regardless of the acid concentration or the region in which high current densities were applied, which were not sufficiently high to avoid or minimize metal dissolution at high acid concentrations (upper right corner of Fig. 4.5(a)).

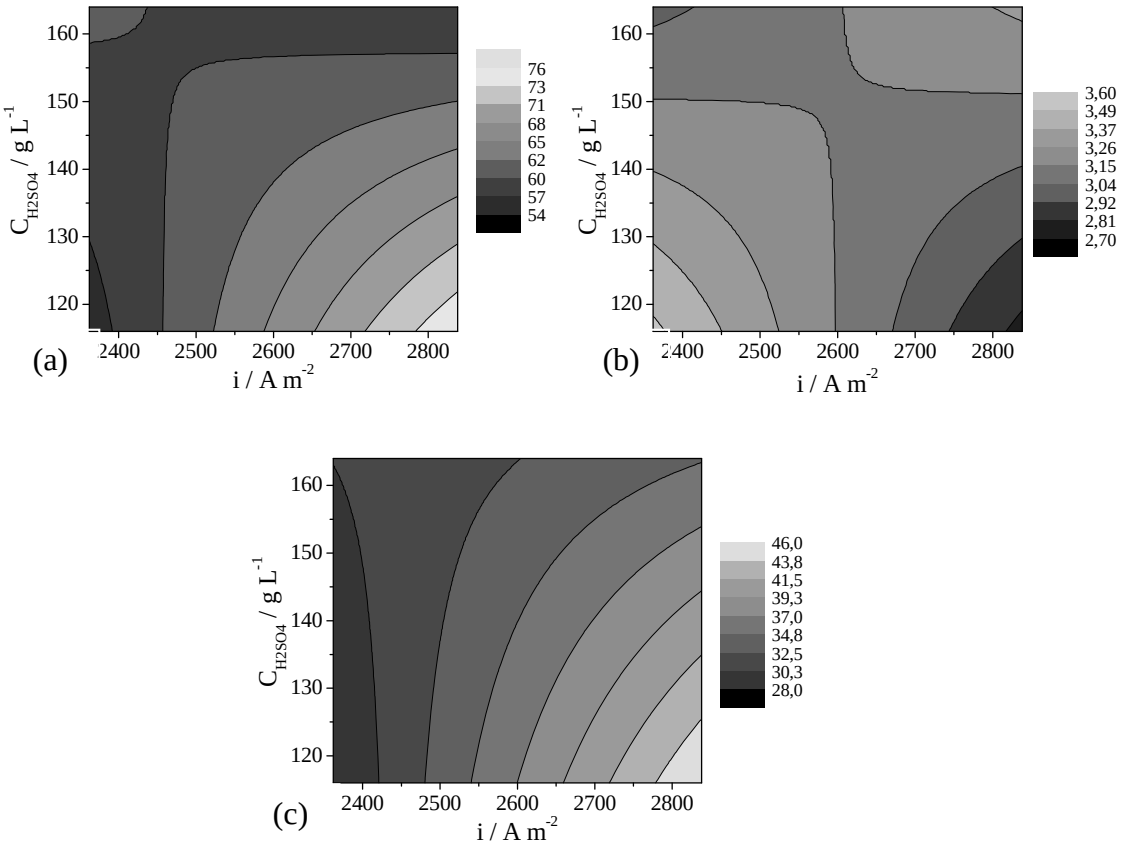

Figure 4.5. Contour surface plots for CE (a), EC (b), and Y (c).

The phenomena occurring inside three-dimensional electrodes are very complex due to the non-uniform current and overpotential distributions in the direction of the electric field, resulting in zones with different reaction rates inside the porous matrix.[38,39] During the fluidized state in very acidic medium, anodic zones cause the metal dissolution rate to predominate over the electrodeposition rate, leading to low CE values. On the other hand, at low acid concentrations, the current distribution within the porous electrode is less uniform, resulting in dendritic growth of the electrodeposited copper in zones very close to the anode, leading to short circuit. A higher acid concentration was used in an attempt to improve current penetration during the fluidized bed state, since the local overpotential (and, consequently, the local current) depends on the difference between the potentials of the solid phase (particles) and the liquid phase (electrolyte). Increasing the conductivity of the liquid phase by increasing the acid concentration makes the overpotential profile within the three dimensional electrode more uniform, and dissolution zones can be avoided with the application of high current densities. This effect has been observed for metal removal from wastewater using fluidized bed cathodes, but in this case, metal electrodeposition was not so intense and short circuit was not a limiting

factor.[38] It was also found that increasing the current density caused an increase in current penetration, by making the particles cathodically polarized, and decreased the effect of metal dissolution during fluidization. From Fig. 4.5(a), it would be expected that CE could be improved by increasing the current density to values greater than 2838 A m^{-2}. However, in the previous work, it was found that the maximum current density that could be applied in order to avoid particle agglomeration and short circuit was 3000 A m^{-2}. Unfortunately, this current density was not sufficient to avoid metal dissolution and improve CE at high acid concentration, and could not provide uniform potential profiles while at the same time eliminating anodic zones.

Another strategy to improve CE could be to use acid concentrations lower than 100 g L^{-1}, but it was observed previously that this was not viable due to the formation of dendritic deposits in the region close to the counter-electrode, causing short circuit of the electrochemical system.

In Figure 4.5(b), a saddle-like shape can be observed and the best EC was achieved at i = +1, $C_{ac.}$= -1, in agreement with Figure 4.5(a). Considering that E_{cell} has a minor influence on EC compared to CE, the best values of EC were obtained under exactly the same conditions that provided higher values of CE. The value of Y (Fig. 4.5(c)) depended mainly on the electric current, which is the limiting factor in processes controlled by electron transfer, but also depended on dC/dt, which is related to CE. The best values of Y were also obtained at i = +1, $C_{ac.}$= -1.

Finally, the three plots of Fig. 4.5 show that the best conditions for optimization of the three variables at the same time were a maximum current and a minimum acid concentration. However, the maximum CE and minimum EC for the experimental system employed in this work were below the values found in real electrowinning plants. As discussed previously, it was not possible to improve CE and EC by increasing the current density to values greater than 3000 A m^{-2} or decreasing the acid concentration to values lower than 110 g L^{-1}, due to electrochemical limitations. However, improvement of CE is essential in order to make the PBE an economically viable alternative for use in metal electrowinning. A high CE is necessary to avoid or minimize metal dissolution during the fluidization step, and to achieve this, it is necessary to improve the overpotential and current distributions in order to avoid anodic zones. In the present work, the influence of acid concentration and current density were investigated in an attempt to improve the performance of the PBE, but the CE values remained low. In future

work, a reduction of the porous cathode width will be studied as a possible strategy to increase CE, as the overpotential distribution can be made more uniform by using thin electrodes.

Deposit quality

Two experiments were carried out using a flat plate electrode, without chemical additives, in order to compare the electrodeposits obtained using the three-dimensional electrode with those produced in conventional processes. These experiments were performed with the same electrolyte used in the PBE experiments. The deposit morphologies were compared using scanning electron microscopy (SEM). Figure 4.6(a) and 4.6(b) show SEM images of the flat plate electrode after 30 min of electrodeposition, applying 300 A m^{-2}, which is the current density commonly used in electrowinning plants. It can be seen that the electrodeposit was very uniform, compact, and rough. The electrodeposit obtained using the PBE operated at 3000 A m^{-2} (Figs. 4.6(c)-(e)) was smooth and more compact. At high magnification, the electrodeposit was comparable with that produced on a flat plate electrolyzer operated at a current density of 250 A m^{-2} in the presence of organic additives (thiourea and animal glue).[14]

A contributing factor to the better deposit quality obtained using the PBE was the low current density when the particle surface area was taken into account. Furthermore, the low dissolution during the fluidization step due to the existence of anodic zones, as discussed previously,[33] acts mainly on the crystal edges and therefore tends to smooth the electrodeposit.[40] This effect is very interesting because it simulates the situation in which the current supply is stopped for a few seconds in order to cause metal dissolution and improve the electrodeposit.[41] Finally, collisions between the particles during fluidization also contribute to the uniformity and compactness of the electrodeposit.

The images for the flat plate and the copper particles revealed a substantial difference in terms of the amounts of grains. It is possible that HSO_4^- and SO_4^{2-} were strongly adsorbed onto the particle surface in the anodic zones inside the fluidized bed, forcing the creation of new nuclei rather than the growth of existing particles.[42] In terms of composition, EDS analysis (Fig. 4.6(f)) showed that the electrodeposits consisted almost entirely of metallic copper. Small amounts of oxygen could be attributed to surface oxides formed during exposure to air.

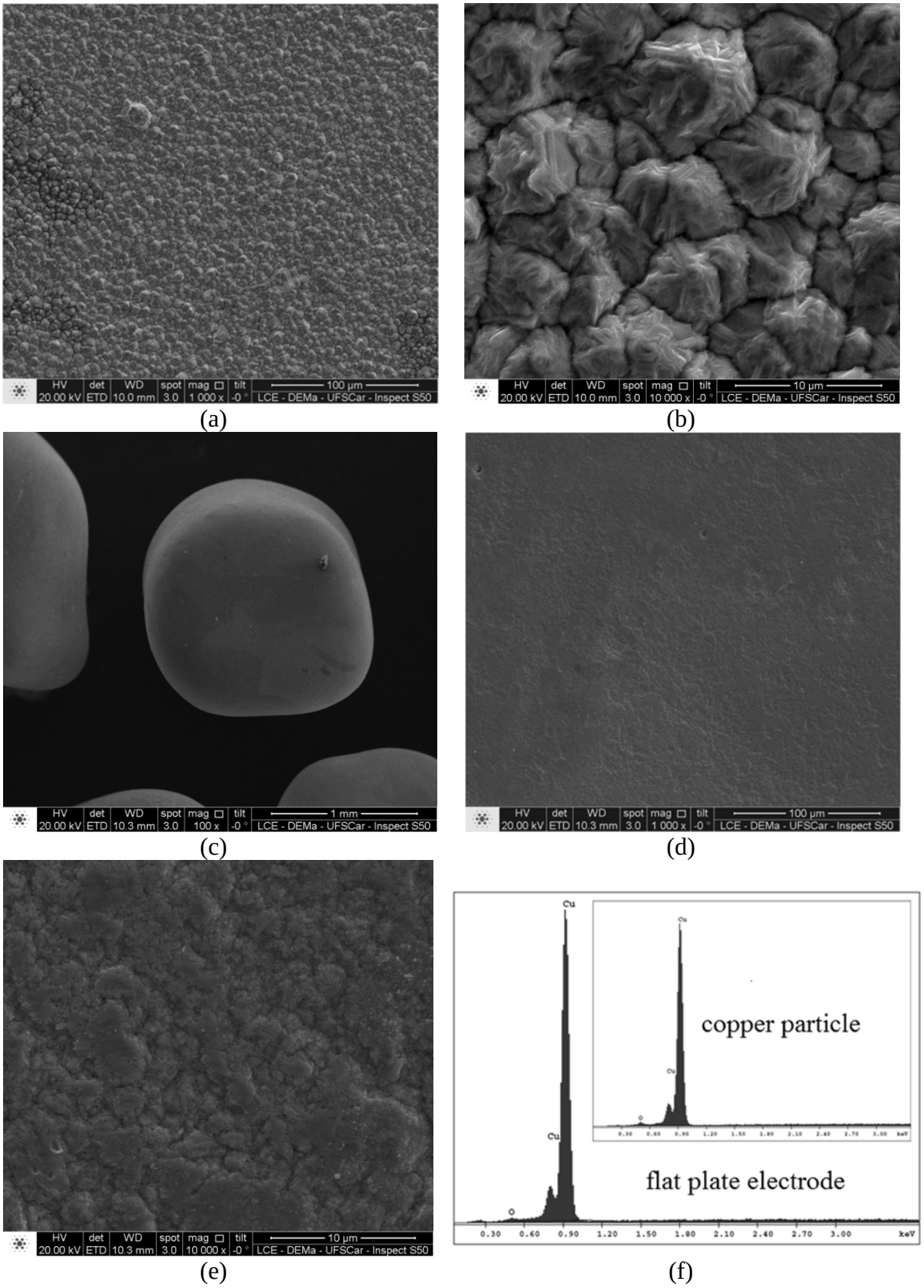

Figure 4.6. SEM/EDS analysis. (a)-(b) SEM images of flat plate copper electrode at magnifications of x1,000 and x10,000, respectively. (c)-(e) SEM images of copper particle at magnifications of x100, x1,000, and x10,000, respectively. (f) EDS spectra of the copper electrodeposits. Conditions: 1) flat plate electrode: 300 A m^{-2}; 2) particulate electrode: 2838 A m^{-2}.

CONCLUSIONS

The PBE can be used for copper electrodeposition with low EC (2.72 kWh kg^{-1}), despite the low CE. The maximum CE (77.7%) was achieved using 2838 A m^{-2} and 110 g L^{-1} H_2SO_4. According to the statistical model (Equation (4.5)), the CE could be improved to 82.4% by applying 3000 A m^{-2}, although this is still a low value, indicating that further improvements should be possible using new operational or design strategies. In previous work, it was found that 2 s was the ideal fluidized bed time, while in the present case it was found that the packed bed time was not a limiting factor, because no statistically significant effect on the response variable was observed, enabling a time of 54 s to be used. The analysis of effects showed that increasing the current density and decreasing the acid concentration is a good strategy to obtain high values of CE, although the values of these variables are limited to 3000 A m^{-2} (as found in the previous work) and 110 g L^{-1}, because higher values of i or lower values of $C_{ac.}$ lead to high metal dissolution rates, dendritic growth, and short circuit. A reduction of the electrode thickness is suggested as a new strategy to improve CE, as the improved current and potential distributions within thin electrodes can reduce metal dissolution, due to the cathodic polarization of all particles during the fluidization step. In all cases, the electrodeposits were very smooth, despite the absence of any organic additive, and were similar to those obtained using flat plate electrodes in the presence of organic additives.

Acknowledgments

The authors are grateful to FAPESP (Fundação de Amparo à Pesquisa do Estado de São Paulo) for financial support, and CNPq (Conselho Nacional de Desenvolvimento Científico e Tecnológico) for a PhD fellowship.

References

1 U.S.G. Survey, Mineral Commodity Summaries. U.S. Geological Survey, Reston (2013).

2 Cifuentes L, Ortiz R, Casa JM, Electrowinning of copper in a lab-scale squirrel-cage cell with anion membrane. *AIChE J.* **51**:2273-2284 (2005).

3 Habashi F, Copper metallurgy at the crossroads. *J Min Met* **43B**:1-19 (2007).

4 Hyvärinen O, Hämäläinen M, HydroCopper™ a new technology producing copper directly from concentrate. *Hydrometallurgy* **77**:61-65 (2005).

5 Panda B, Das SC, Electrowinning of copper from sulfate electrolyte in presence of sulfurous acid. *Hydrometallurgy* **59**:55-67 (2001).

6 Shakarji RA, He Y, Gregory S, Statistical analysis of the effect of operating parameters on acid mist generation in copper electrowinning. *Hydrometallurgy* **106**:113-118 (2011).

7 Evans JW, Ding R, Doyle FM, Jiricny V, Copper electrodeposition onto extended surface area electrodes and the treatment of copper containing waste streams. *Scand J Metall* **34**:363-368 (2005).

8 Jiricny V, Roy A, Evans JW, Copper electrowinning using spouted-bed electrodes: part I. Experiments with oxygen evolution or matte oxidation at the anode. *Metall Mater Trans B* **33**:669-676 (2002).

9 San Martin RM, Otero AF, Cruz A, Use of quillaja saponins (Quillaja saponaria Molina) to control acid mist in copper electrowinning processes Part 2: pilot plant and industrial scale evaluation. *Hydrometallurgy* **77**:171-181 (2005).

10 Sigley JL, Johnson PC, Beaudoin SP, Use os nonionic surfactant to reduce sulfuric acid mist in the copper electrowinning process. *Hydrometallurgy* **70**:1-8 (2003).

11 Wiechmann EP, Morales AS, Aqueveque P, Improving productivity and energy efficiency in copper electrowinning plants. *IEEE Trans Ind Appl* **46**:1264-1269 (2010).

12 Lupi C, Pilone D, New lead alloy anodes and organic depolarizer utilization in zinc electrowinning. *Hydrometallurgy* **44**:347-358 (1997).

13 Moats M., Hardee K, Brown C, Mesh-on-Lead Anodes for Copper Electrowinning. *JOM* **55**: 46-48 (2003).

14 Muresan L, Varvara S, Maurin G, Dorneanu S, The effect of some organic additives upon copper electrowinning from sulphate electrolytes. *Hydrometallurgy* **54**:161-169 (2000).

15 Lafront AM, Zhang W, Ghali E, Houlachi G, Electrochemical noise studies of the corrosion behavior of lead anodes during zinc electrowinning maintenance. *Electrochim Acta* **55**:6665-6675 (2010).

16 Moskalyk RR, Alfantazi A, Tombalakian AS, Valic D, Anodes effect in electrowinning. *Miner Eng* **12**:65-73 (1999).

17 Coeuret F, The fluidized bed electrode for the continuous recovery of metals. *J Appl Electrochem* **10**:687-696 (1980).

18 Coeuret F, Paulin M, Experiments on copper recovery in a pulsed granular fixed bed electrode. *J Appl Electrochem* **18**:162-165 (1988).

19 El-Shakre ME, Saleh MM, El-Anadouli BE, Ateya BG, Applications of porous flow-through electrodes. *J Electrochem Soc* **141**:441-447 (1994).

20 Hadzismajlovic DZE, Popov KI, Pavlovic MG, The visualization of the electrochemical behavior of metal particles in spouted, fluidized and packed beds. *Powder Technol* **86**:145-148 (1996).

21 Martins R, Britto-Costa PH, Ruotolo LAM, Removal of toxic metals from aqueous effluents by electrodeposition in a spouted bed electrochemical reactor. *Environ Technol* **33**:1123-1131 (2012).

22 Olive H, Lacoste G, Application of volumetric electrodes to the recuperation of metals in industrial effluents-I. Mass transfer in fixed beds of spherical conductive particles. *Electrochim Acta* **24**:1109-1114 (1979).

23 Ruotolo LAM, Gubulin JC, Electrodeposition of copper ions on fixed bed electrodes: kinetic and hydrodynamic study. *Braz J Chem Eng* **19**:105-118 (2002).

24 Salas-Morales JC, Evans JW, Newman OMG, Adcock PA, Spouted bed electrowinning of zinc: Part I. Laboratory-scale electrowinning experiments. *Metall Mater Trans B* **28B**:59-68 (1997).

25 Britto-Costa PH, Ruotolo LAM, Electrochemical removal of copper ions from aqueous solutions using a modulated current method. *Sep Sci Technol* **46**:1205-1211 (2011).

26 Pletcher D, White I, Walsh FC, Millington JP, Reticulated vitreous carbon cathodes for metal ion removal from process streams Part II: Removal of copper(II) from acid sulphate media. *J Appl Electrochem* **21**:667-671 (1991).

27 Hutin D, Coeuret F, Experimental study of copper deposition in a fluidized bed electrode. *J Appl Electrochem* **7**:463-471 (1977).

28 Kazdobin K, Shvab N, Tsapakh S, Scaling-up fluidized-bed electrochemical reactors. Chem Eng J 79: 203-209 (2000).

29 Sabacky BJ, Evans JW, Electrodeposition of metals in fluidized bed electrodes. *J Electrochem Soc* **126**:1176-1187 (1979).

30 Argondizo A, Copper ions removal from aqueous solutions on pulsed bed electrode. Dissertation, Federal University of São Carlos (1996).

31 Garfias-Vasquez FJ, Duverneuil P, Lacoste G, Behaviour, modelling and simulation of a pulsed three-dimensional radial electrode with continuous solid flow: Part I. *J Appl Electrochem* **34**:417-426 (2004).

32 Tonini GA, Farinos RM, Prado PFA, Ruotolo LAM, Box-Behnken factorial design study of the variables affecting metal electrodeposition in membraneless fluidized bed electrodes. *J Chem Technol Biotechnol* **88**:800-807 (2013).

33 Britto-Costa PH, Pereira-Filho ER, Ruotolo LAM, Copper electrowinning using a three-dimensional electrode. *Hydrometallurgy* **144-145**:15-22 (2014).

34 Montgomery DC, Design and Analysis of Experiments, John Wiley and Sons, New York (1991).

35 Beenackers AACC, Van Swaaij WPM, Mechanism of charge transfer in the discontinuous metal phase of a fluidized bed electrode. *Electrochim Acta* **22**:1277-1281 (1977).

36 Volkman Y, Optimization of the effectiveness of a three-dimensional electrode with respect to its ohmic variables. *Electrochim Acta* **24**:1145-1149 (1979).

37 Ruotolo LAM, Gubulin JC, Chromium(VI) reduction using conducting polymer films. *React Funct Polym* **62**:141-151 (2005).

38 Bareau JY, Coeuret F, The anodic dissolution of copper in a fluidized bed electrode. *J Appl Electrochem* **9**:737-743 (1979).

39 Ruotolo LAM, Gubulin JC, A mathematical model to predict the electrode potential profile inside a polyaniline-modified reticulate vitreous carbon electrode operating in the potentiostatic reduction of Cr(VI). *Chem Eng J* **171**:1170-1177 (2011).

40 Yao QX, The effects of duty cycle and frequency on the crystal size of pulse-plated gold. *Plat Surf Finish* **76**:52-53 (1989).

41 Saba AE, Elsherief AE, Afifi SE, Effect of pulsating current and periodic current reversal on electrorefining of copper. *Trans Inst Min Metall C* **101**:91-98 (1992).

42 Saba AE, Elsherief AE, Continuous electrowinning of zinc. *Hydrometallurgy* **54**:91-106 (2000).

4.3 Conclusões

O eletrodo de leito pulsante pode ser empregado para a eletrorrecuperação de cobre com baixo consumo energético, porém a eficiência de corrente ainda foi baixa, indicando que ainda há possibilidade de uma melhoria do processo. A eficiência de corrente máxima obtida foi de aproximadamente 78%, aplicando-se 2838 A m^{-2} e 110 g L^{-1} de H_2SO_4. De acordo com o modelo estatístico obtido, a *EC* poderia ser melhorada para 82,4% aplicando-se 3000 A m^{-2}, embora este valor ainda seja considerado baixo, indicando que melhorias futuras são possíveis por meio de mudanças operacionais ou do projeto do reator. Anteriormente, determinou-se que um tempo de fluidização de 2 s era ideal. Neste estudo verificou-se que o tempo de leito fixo não foi o fator limitante, uma vez que não apresentou nenhum efeito estatisticamente significativo nas variáveis resposta, permitindo a utilização de 54 s para esta variável. A análise dos efeitos mostrou que aumentar a densidade de corrente e diminuir a concentração do ácido seria uma boa estratégia para se obter altos valores de *EC*, entretanto os valores destas variáveis estão limitados a 3000 A m^{-2} de *i* e 110 g L^{-1} de ácido, uma vez que maiores valores maiores acarretam em eletrodepósito dendrítico que leva ao curto-circuito do eletrodo. A análise de MEV revelou que em todos os casos o eletrodepósito era bastante uniforme e similares aos obtidos em eletrodos planos na presença de aditivos.

5 OTIMIZAÇÃO DA ELETRORRECUPERAÇÃO DE COBRE UTILIZANDO ELETRODO DE LEITO PULSANTE

5.1 Introdução

Nos dias atuais, o estudo sobre a produção de metais utilizando métodos eletrolíticos é muito importante devido à preservação do meio ambiente, uma vez que processos pirometalúrgicos poluidores devem ser evitados.

Este trabalho conclui uma série de estudos sobre a utilização de eletrodo de leito pulsante no processo de eletrorrecuperação de cobre presente em eletrólito ácido utilizando concentrações típicas daquelas encontradas na indústria hidrometalúrgica. Nos capítulos anteriores, foram identificados os principais parâmetros que afetam a eficiência de corrente, o consumo energético e o rendimento espaço-tempo.

Diante do que foi exposto, neste trabalho foram estudadas as principais variáveis que afetam a eletrorrecuperação de cobre empregando um reator eletroquímico com espessura aproximadamente 30% menor do que o utilizado nos capítulos 3 e 4. A redução da espessura do eletrodo de 3,4 centímetros para 2,4 centímetros foi feita com o intuito de tornar mais uniforme a distribuição do sobrepotencial de eletrodo no interior da matriz porosa e reduzir o efeito da zona anódica durante a fluidização do leito. Os efeitos das variáveis independentes concentração de ácido sulfúrico, densidade de corrente elétrica e tempo de leito fixo foram analisados nas variáveis resposta *CE*, *EC*, e *Y* através de um planejamento composto central rotacional com o intuito de se otimizar o processo de eletrorrecuperação de cobre. O tempo de leito fluidizado foi mantido constante ao longo dos experimentos com o valor previamente estabelecido (2 s). Finalmente, a morfologia do ânodo antes e após os processos de eletrodeposição foram analisadas por microscopia eletrônica de varredura (MEV), uma vez que neste tipo de reator, a densidade de corrente elétrica no ânodo é muito alta, podendo causar danos à sua estrutura.

5.2 Desenvolvimento

O desenvolvimento detalhado do Capítulo 5 é apresentado a seguir, no artigo intitulado Optimization of copper electrowinning from synthetic copper sulfate solution using a pulsed bed electrode, aceito para publicação no periódico *Hydrometallurgy*.

Hydrometallurgy 150 (2014) 52–60

Contents lists available at ScienceDirect

Hydrometallurgy

journal homepage: www.elsevier.com/locate/hydromet

Optimization of copper electrowinning from synthetic copper sulfate solution using a pulsed bed electrode

Pedro H. Britto-Costa, Luís A.M. Ruotolo *

Department of Chemical Engineering, Federal University of São Carlos, P.O. Box 676, 13565-905 São Carlos, SP, Brazil

ARTICLE INFO

Article history:
Received 21 June 2014
Received in revised form 15 September 2014
Accepted 23 September 2014
Available online 5 October 2014

Keywords:
Pulsed bed
Three-dimensional electrode
Electrowinning
Flow rate pulses
Optimization

ABSTRACT

This paper concludes a series of investigations concerning the use of pulsed bed electrodes (PBEs) for copper electrowinning. In previous papers, the main operational parameters affecting the current efficiency (*CE*), space–time yield (*Y*), and energy consumption (*EC*) were identified and their effects on the performance of the process were analyzed. In light of the results, the fluidized bed time was set at 2 s and it was found that the electrode thickness should be reduced in order to achieve values of *CE* and *EC* lower than those obtained in conventional industrial processes using flat plate electrodes. In this work, the electrode thickness was reduced from 3.4 to 2.4 cm and the process was optimized using factorial experimental design and the Derringer desirability method to obtain current density (i), acid concentration (C_{ac}), and pulsed bed time (t_p) values that maximized *CE* and *Y* and minimized *EC*. The best C_{ac} value was 100 mg L^{-1} (a low level), while the optimum i and t_p values were 2600 A m^{-2} and 60 s, respectively (high levels). Use of these values avoided short circuit and minimized copper dissolution during fluidization. The overpotential distribution within the porous cathode was improved using the 2.4 cm electrode, and values of 100% (*CE*), 102 kg m^{-3} h^{-1} (*Y*), and 1.7 kWh kg^{-1} (*EC*) were achieved under the optimized conditions. These values are better than those found for flat plate electrodes.

1. Introduction

Three-dimensional (3-D) electrodes offer a promising alternative for metal electrodeposition from very dilute solutions, due to their extended surface areas and higher rates of mass transfer (Coeuret, 1980; Coeuret and Paulin, 1988; El-Shakre et al., 1994; Evans et al., 2005; Hadzismajlovic et al., 1996; Jiricny et al., 2002; Martins et al., 2012; Olive and Lacoste, 1979; Ruotolo and Gubulin, 2002). However, little attention has been paid to metal electrowinning from concentrated solutions in hydrometallurgical processes. Although mass transfer is not a process limitation for concentrated electrolytes, the high surface area provided by 3-D electrodes leads to an improved space–time yield (*Y*). This means that the large electrowinning tankhouses usually found in industrial processes that employ flat plate electrodes could be replaced by a few 3-D reactors, hence decreasing the reactor volume needed to produce the same amount of metal (Evans et al., 2005; Jiricny et al., 2002; Martins et al., 2012; Salas-Morales et al., 1997). The current densities that can be applied for copper electrodeposition using flat plate electrodes typically vary from 250 to 300 A m^{-2}, which therefore requires many plates in order to achieve the desired level of copper production. On the other hand, the extended surface area provided by the 3-D cathode enables the application of current densities up to 3000 A m^{-2} in 3-D reactors (Britto-Costa et al., 2014). Another advantage is that it is not necessary to remove the electrodeposited metal from the substrate, which is often performed manually in small plants. In the case of particulate bed cathodes, harvesting the electrodeposited metal simply consists of collecting the particles at the end of a process cycle.

Another important issue in electrowinning plants is the release of acid mists that can oxidize electrical contacts, creating additional resistances, or affect the health of the operators (Evans et al., 2005; Jiricny et al., 2002; San Martin et al., 2005; Shakarji et al., 2011; Sigley et al., 2003; Wiechmann et al., 2010). The use of 3-D electrodes enables the acid mist to be easily channeled and expelled outside the process.

Three-dimensional cathodes also permit the use of fewer anode plates, compared to processes carried out using flat plate electrodes. For example, a porous particulate cathode had an estimated surface area of 920 cm^2, while the counter-electrode had a surface area of 90 cm^2 (Britto-Costa et al., 2014). In conventional electrowinning processes, the most commonly used anode is composed of PbO_2, which has the disadvantage of being unstable and therefore requires the addition of chemical additives to the electrolyte in order to increase its operational lifetime (Lupi and Pilone, 1997; Moats et al., 2003; Muresan et al., 2000). However, the use of additives does not prevent anode corrosion and care must be taken to prevent lead contamination of the electrodeposited metal (Lafront et al., 2010; Moats et al., 2003; Moskalyk et al., 1999). Since the use of 3-D cathodes can avoid the need for large anodes, the replacement of PbO_2 by dimensionally stable anodes (DSA®) based on titanium–iridium or titanium–ruthenium

* Corresponding author. Tel.: +55 16 3351 8706; fax: +55 16 3351 8266.
E-mail address: pluis@ufscar.br (L.A.M. Ruotolo).

http://dx.doi.org/10.1016/j.hydromet.2014.09.014
0304-386X/

Abstract

This paper concludes a series of investigations concerning the use of pulsed bed electrodes (PBE's) for copper electrowinning. In previous papers, the main operational parameters affecting the current efficiency (CE), space-time yield (Y), and energy consumption (EC) were identified and their effects on the performance of the process were analyzed. In light of the results, the fluidized bed time was set at 2 s and it was found that the electrode thickness should be reduced in order to achieve values of CE and EC lower than obtained in conventional industrial processes using flat plate electrodes. In this work, the electrode thickness was reduced from 3.4 to 2.4 cm and the process was optimized using factorial experimental design and the Derringer desirability method to obtain current density (i), acid concentration (C_{ac}), and pulsed bed time (t_p) values that maximized CE and Y and minimized EC. The best C_{ac} value was 100 mg L^{-1} (a low level), while the optimum i and t_p values were 2600 A m^{-2} and 60 s, respectively (high levels). Use of these values avoided short circuit and minimized copper dissolution during fluidization. The overpotential distribution within the porous cathode was improved using the 2.4 cm electrode, and values of 100% (CE), 102 kg m^{-3} h^{-1} (Y), and 1.7 kWh kg^{-1} (EC) were achieved under the optimized conditions. These values are better than those found for flat plate electrodes.

INTRODUCTION

Three-dimensional (3-D) electrodes offer a promising alternative for metal electrodeposition from very dilute solutions, due to their extended surface areas and higher rates of mass transfer (Coeuret, 1980; Coeuret and Paulin, 1988; El-Shakre et al., 1994; Evans et al., 2005; Hadzismajlovic et al., 1996; Jiricny et al., 2002; Martins et al., 2012; Olive and Lacoste, 1979; Ruotolo and Gubulin, 2002). However, little attention has been paid to metal electrowinning from concentrated solutions in hydrometallurgical processes. Although mass transfer is not a process limitation for concentrated electrolytes, the high surface area provided by 3-D electrodes leads to an improved space-time yield (Y). This means that the large electrowinning tankhouses usually found in industrial processes that employ flat plate electrodes could be replaced by a few 3-D reactors, hence decreasing the reactor volume needed to produce the same amount of metal (Evans et al., 2005; Jiricny et al., 2002; Martins et al., 2012; Salas-Morales et al., 1997). The current

densities that can be applied for copper electrodeposition using flat plate electrodes typically vary from 250 to 300 A m^{-2}, which therefore requires many plates in order to achieve the desired level of copper production. On the other hand, the extended surface area provided by the 3-D cathode enables the application of current densities up to 3000 A m^{-2} in 3-D reactors (SILVA-MARTÍNEZ e ROY, 2013). Another advantage is that it is not necessary to remove the electrodeposited metal from the substrate, which is often performed manually in small plants. In the case of particulate bed cathodes, harvesting of the electrodeposited metal simply consists of collecting the particles at the end of a process cycle.

Another important issue in electrowinning plants is the release of acid mists that can oxidize electrical contacts, creating additional resistances, or affect the health of the operators (Evans et al., 2005; Jiricny et al., 2002; San Martin et al., 2005; Shakarji et al., 2011; Sigley et al., 2003; Wiechmann et al., 2010). The use of 3-D electrodes enables the acid mist to be easily channeled and expelled outside the process.

Three-dimensional cathodes also permit the use of fewer anode plates, compared to processes carried out using flat plate electrodes. For example, a porous particulate cathode had an estimated surface area of 920 cm^2, while the counter-electrode had a surface area of 90 cm^2 (Britto-Costa et al., 2014). In conventional electrowinning processes, the most commonly used anode is composed of PbO_2, which has the disadvantage of being unstable and therefore requires the addition of chemical additives to the electrolyte in order to increase its operational lifetime (Lupi and Pilone, 1997; Moats et al., 2003; Muresan et al., 2000). However, the use of additives does not prevent anode corrosion and care must be taken to prevent lead contamination of the electrodeposited metal (Lafront et al., 2010; Moats et al., 2003; Moskalyk et al., 1999). Since the use of 3-D cathodes can avoid the need for large anodes, the replacement of PbO_2 by dimensionally stable anodes (DSA®) based on titanium-iridium or titanium-ruthenium oxides, or platinized titanium, could become economically viable. A further advantage is that the replacement of PbO_2 by DSA® anodes eliminates the need for chemical additives (Lupi and Pilone, 1997; Muresan et al., 2000).

Particulate 3-D electrodes have been used previously for metal electrodeposition in applications involving the treatment of effluents in which metal concentrations are very low (Britto-Costa and Ruotolo, 2011; Hadzismajlovic et al., 1996; Olive and Lacoste,

1979; Pletcher et al., 1991; Ruotolo and Gubulin, 2002). The high conductivity of the solid phase, together with high mass transfer coefficients, enable packed bed cathodes to operate at high current efficiency (Britto-Costa and Ruotolo, 2011; Ruotolo and Gubulin, 2002). Unfortunately, when the metal concentration is high (as in the case of electrowinning processes), metal deposition results in very fast clogging of the electrode pores (Hadzismajlovic et al., 1996; Ruotolo and Gubulin, 2002). The use of fluidized bed electrodes for metal electrodeposition offers a way of overcoming this problem, because clogging of the electrode can be avoided by maintaining the conducting particles in a fluidized state using an upward flow of electrolyte (Coeuret, 1980; Hadzismajlovic et al., 1996; Hutin and Coeuret, 1977; Kazdobin et al., 2000; Sabacky and Evans, 1979). However, for this type of electrode, the reaction rate is very sensitive to the fluid dynamic conditions because the conductivity of the solid phase depends on the frequency of collisions between the particles, which is mainly determined by the bed expansion (Hadzismajlovic et al., 1996; Hutin and Coeuret, 1977). In some cases, when the local difference between the solid and liquid phase potentials is positive, zones of metal dissolution can occur inside the fluidized cathode (Coeuret, 1980; Hutin and Coeuret, 1977). For these reasons, the pulsed bed electrode (PBE) has emerged as a promising alternative. This electrode benefits from the high current efficiency provided by the packed bed electrode, while avoiding electrode clogging by fluidization of the cathode (Argondizo, 2001; Coeuret and Paulin, 1988; Garfias-Vasquez et al., 2004). In this type of electrode, the packed bed is periodically fluidized by applying regular flow rate pulses generated by mechanical or electrical devices (Argondizo, 2001; Garfias-Vasquez et al., 2004), or by using special valve setups (Coeuret and Paulin, 1988). Another advantage of the use of PBEs is the continuous mixing of particles during the pulse, which enables the particles to grow uniformly.

This study describes a PBE electrochemical reactor for copper electrowinning using copper concentrations typically found in industrial hydrometallurgical processes. The operational parameters considered were the acid concentration, current density, and packed bed time. The system was designed as a single compartment reactor, with no membrane separating the catholyte from the anolyte, which minimizes capital expenditure (Tonini et al., 2013). The flow rate pulses were generated by controlling the rotation of a centrifugal pump using a logic module and a frequency inverter. Considering the state of the art, there have only been a few reports on the use of PBEs for metal

electrodeposition, most of which concern the recovery of metals from dilute solutions during the treatment of effluents (Argondizo, 2001; Coeuret and Paulin, 1988). There has only been one study of the use of the PBE in hydrometallurgy (Coeuret and Paulin, 1988), but the system used for pulse generation was very different to that used in the present work. As far as we know, there have been no papers published concerning the use of membraneless PBEs or the pulsed flow rate technique proposed here.

In a previous study, Britto-Costa et al. (2014) investigated the effects of variables such as packed bed and fluidized bed times, temperature, current density, and acid concentration on the process efficiency. After all these variables had been optimized, the best current efficiency (CE) and energy consumption (EC) values obtained were 76.7% and 2.5 kWh kg^{-1}, respectively. Although the energy consumption was comparable to values found in industrial processes using flat plate electrodes, it should be possible to make further improvements using strategies to increase the current efficiency and reduce the energy consumption. The present work therefore investigates the main variables affecting copper electrowinnning, using an electrode with a thickness ~30% lower than that used in the previous work. The electrode thickness was reduced from 3.4 to 2.4 cm in an attempt to improve current penetration within the porous cathode and avoid anodic zones. The effects of acid concentration, current density, and packed bed time on CE, EC, and Y were studied using a central composite rotatable design (CCRD). Optimization of the parameters was performed using the desirability method in order to maximize CE and Y, while minimizing EC. The operational variables investigated were selected because the acid concentration influences the local particle-solution potential within the three-dimensional cathode, and therefore affects the local kinetics, while the packed bed time and current density have strong interaction effects with the acid concentration, influencing current penetration and determining whether metal dissolution will occur. In all the experiments, the fluidized bed time was maintained constant at the previously optimized value (Britto-Costa et. al., 2014). Scanning electron microscopy (SEM) was used to analyze the morphology of the anode, before and after the electrowinning processes, as well as the electrodeposited copper.

EXPERIMENTAL

The pulsed bed electrochemical reactor used for copper electrowinning has been described in detail elsewhere (Britto-Costa et al., 2014). Briefly, the reactor consisted of three rectangular acrylic plates assembled using bolts and nuts. The dimensions of the particulate cathode were 2.4 cm (thickness) and 4.5 cm (width). The same electrode was used in the previous work (Britto-Costa and Ruotolo, 2014), but with a thickness of 3.4 cm. The bed heights were 8 and 12.5 cm during the packed and fluidized states, respectively. Equilateral 1.0 mm cylindrical copper particles were used to form the porous cathode. Stainless steel 316 and a $Ti/Ti_{0.7}Ru_{0.3}O_2$ DSA® (DeNora, Brazil) were used as the current feeder and counter-electrode, respectively.

An important characteristic distinguishing this reactor from many others used for metal electrodeposition is that it did not have two compartments with a membrane separating the catholyte from the anolyte (it was a membraneless reactor). There was only one separator, composed of a polyethylene mesh covered with a polyamide fabric, which was placed between the porous cathode and the counter-electrode to prevent short circuit. Advantages of this reactor configuration, compared to membrane reactors, include low cell potential, low energy consumption, ease of maintenance, and low capital expenditure because the use of expensive membranes is avoided.

The flow rate pulses were generated using a frequency inverter acting on the centrifugal pump rotation and, consequently, on the flow rate. The frequency inverter (MicroMaster MM55, Siemens) was controlled by a logic module (LOGO! 230RC, Siemens) that determined the time during which the bed remained in the packed (low frequency rotation) and fluidized (high frequency rotation) states.

Copper electrowinning

The copper electrowinning was carried out galvanostatically using a constant current source (Genesys™ 1500W, Lambda). The cell potential (E_{cell}) was recorded every 2 s using a data acquisition system. A complete description of the experimental setup used for copper electrowinning has been provided previously (Britto-Costa et al., 2014).

The electrolyte was prepared using deionized water, technical grade copper sulfate, and sulfuric acid. The copper concentration ranged from 35 to 40 g L^{-1} (Cu^{2+}) and the

acid concentration ranged from 100 to 180 g L^{-1}, in line with the concentrations typically used in the copper electrowinning industry. The porous cathode consisted of 410 g of copper particles. An electrolyte volume of 15 L was used in all the experiments.

The experimental procedure consisted of circulating the electrolyte between the reservoir and the reactor and collecting samples for determination of the copper concentration. The flow rates during the packed and fluidized bed conditions were maintained constant at 136 and 568 L h^{-1}, respectively. The variables current density, packed bed time, and fluidized bed time (t_f) were studied previously by Britto-Costa et al. (2014). It was concluded that anodic zones could occur during the fluidized state, which should therefore be maintained for as short a period as possible (2 s). For shorter fluidized bed times, short circuit or electrode clogging could occur. Given these results, the value of t_f used in this work was 2 s.

The copper concentration was determined colorimetrically by measuring the absorbance at 810 nm using an Ultrospec 2100Pro UV-VIS spectrophotometer (Amersham Pharmacia). This technique was highly accurate for the measurement of copper concentrations in the selected range.

The electrowinning process was evaluated in terms of current efficiency (CE), energy consumption (EC), and space-time yield (Y), as a function of the acid concentration, current density, and packed bed time. The values of CE, EC, and Y were calculated using Eqs. (5.1), (5.2), and (5.3), respectively. In these equations, z is the number of electrons involved in the electrochemical reaction, F is the Faraday constant (96,496 C mol^{-1}), M is the molar weight (g mol^{-1}), I is the applied current (A), V is the electrolyte volume (L), C is the copper concentration (g L^{-1}), t is the electrowinning time (s), E_{cell} is the cell potential (V), and V_R is the reactor volume (m^3). The constants 2.78 x 10^{-4} and 3.6 are conversion factors used to obtain EC in kWh kg^{-1} and Y in kg m^{-3} h^{-1}, respectively. The reaction rates (dC/dt) were determined from the concentration-time curves obtained experimentally.

$$CE = \frac{zFV}{MI}\frac{dC}{dt} \tag{5.1}$$

$$EC = \frac{2.78\ x\ 10^{-4} zFE_{cell}}{MCE} \tag{5.2}$$

$$Y = 3.6\frac{V}{V_R}\frac{dC}{dt} \tag{5.3}$$

Design of Experiments (DoE)

Design of experiments (DoE) is a powerful technique that can be used for the statistical analysis of processes influenced by several independent variables (Montgomery, 1991). In this study, a 2^3 central composite rotatable design (CCRD), together with response surface methodology (RSM), were used to evaluate the effects of the applied current density (i), packed bed time (t_p), and acid concentration (C_{ac}) on CE, EC, and Y.

The coded values of the independent variables were calculated using Eq. (5.4):

$$x_j = \frac{(\xi_j - \xi_0)}{(\xi_1 - \xi_0)} \tag{5.4}$$

where x_j is the dimensionless coded value of the independent variable j, ξ_j is the uncoded value of j, ξ_0 is the uncoded value of the variable at the center point, and ξ_1 is the uncoded value of the variable at the highest level.

Table 5.1 shows the coded variables. The CCRD codification is shown in Table 5.2. The levels ±1.68 represent the axial points. As mentioned before, the levels of the variables i and t_p were established based on our previous work (Britto-Costa et al., 2014). Preliminary experiments were carried out in order to establish the acid concentration levels. It was found that acid concentrations below 100 g L^{-1} could result in short circuit, even at low t_p, while concentrations higher than 180 g L^{-1} favored copper dissolution during the fluidization step.

Table 5.1
Actual and coded values of the independent variables.

	Var1	Var2	Var3
Code	i / A m^{-2}	t_p / s	$C_{ac.}$ / g L^{-1}
-1.68	1900	30	100
-1	2042	36	116
0	2250	45	140
+1	2458	54	164
+1.68	2600	60	180

Optimization

The use of multiple response experiments has become increasingly popular over the past few decades (Del Castillo et al., 1996), with optimization techniques including response

surface overlaying or nonlinear programming methods. A simple procedure for multiple response optimization is the desirability method proposed by Derringer and Suich (1980). This technique is based on the concept of transforming the response variables into numbers between 0 and 1, according to their desirability. The most undesirable value of each response variable is assigned a value of 0, or close to 0, and the most desirable value is assigned 1. In this procedure, all the response variables can be analyzed together and then be grouped into a single response, known as the global desirability (GD), which is the geometric mean of the desirable variables. The optimal conditions of the DoE can then be easily found. Eqs. (5.5) and (5.6) are used to maximize and minimize the desirability, respectively:

$$d_j = \begin{cases} 0 & y < L \\ \left(\frac{y-L}{T-L}\right)^w & L \leq y \leq T \\ 1 & y > T \end{cases} \tag{5.5}$$

$$d_j = \begin{cases} 1 & y < T \\ \left(\frac{U-y}{U-T}\right)^w & T \leq y \leq U \\ 0 & y > U \end{cases} \tag{5.6}$$

where d_j is the desirable response of variable j; y is the response; L is the lower acceptable value; U is the upper acceptable value; T is the target; and w is the weighting. The weighting must be specified by the user, considering three possibilities: 1) if $w = 1$, the desirability grows constantly with the response; 2) if $w > 1$, all the values close to the target will be highly desirable; and 3) if $w < 1$, desirability rapidly increases with the response even for values far from the target, which diminishes the contribution of that response to the global desirability. The global desirability is described by the equation:

$$GD = \left(\prod_{r=1}^{R} d_r\right)^{1/R} \tag{5.7}$$

where R is the number of responses.

RESULTS

Copper electrowinning

Fig. 5.1(a) shows plots of the normalized concentration against time (the dashed lines represent the linear regression). The best and worst electrodeposition curves for the 2.4 cm cathode were compared to those obtained for the 3.4 cm cathode under similar operational conditions (Britto-Costa and Ruotolo, 2014). It is important to note that the current density applied to the 2.4 cm electrode was ~13% lower than that applied to the 3.4 cm electrode. This reduction was necessary because of the new overpotential distribution in the 2.4 cm cathode. Application of 2838 A m^{-2} resulted in very fast dendrite growth and short circuit. According to Fig. 5.1(b), the reduction in the electrode thickness caused a decrease of E_{cell}, especially in the fluidized bed state. However, when $E_{cell,av.}$ was considered, this reduction was only ~3.7%, confirming the earlier finding (Britto-Costa et al., 2014) that the contribution of E_{cell} to $E_{cell,av.}$ during the fluidized bed state was minimal due to the very fast fluidization pulse.

Considering the best results in terms of electrodeposition kinetics (Run 4 for both electrode thicknesses), it was evident that when the electrode thickness was reduced from 3.4 to 2.4 cm, the electrodeposition rate (dC/dt) reached its maximum, corresponding to 100% CE (Table 5.2). Despite the low current density applied to the 2.4 cm cathode, the space-time yield obtained for Run 4 using this thickness (76.1 kg m^{-3} h^{-1}) was much higher than that obtained using a thickness of 3.4 cm (47.2 kg m^{-3} h^{-1}). This improvement in Y can be attributed to two factors, namely the better current efficiency and the small reactor volume.

The 100% CE obtained for Run 4 indicates that metal dissolution during the fluidized bed step could be avoided using these operational conditions, suggesting that current penetration was more effective for the 2.4 cm cathode, despite application of a lower current density. On the other hand, for the worst electrodeposition kinetics, this situation was inverted and zones of anodic dissolution (positive overpotentials) could be observed for the fluidized bed, as shown in Fig. 5.1(c). The procedure used to measure the electrode overpotentials has been described in detail elsewhere (Ruotolo and Gubulin, 2005, 2011). It can be seen from Fig. 5.1(c) that the packed bed electrode was more electroactive than the fluidized bed, because the packed bed showed overpotentials that

were more negative. In both cases, the most cathodic zone was always observed in the region close to the counter-electrode, which was the main reason for rapid short circuit when high current densities were applied (hence limiting the current density that could be used). This also explains why t_p must be maintained at a high level (short circuit is the limitation for t_p) and t_f should be maintained at a low level (2 s), because the electrodeposition rate was maximized under these conditions.

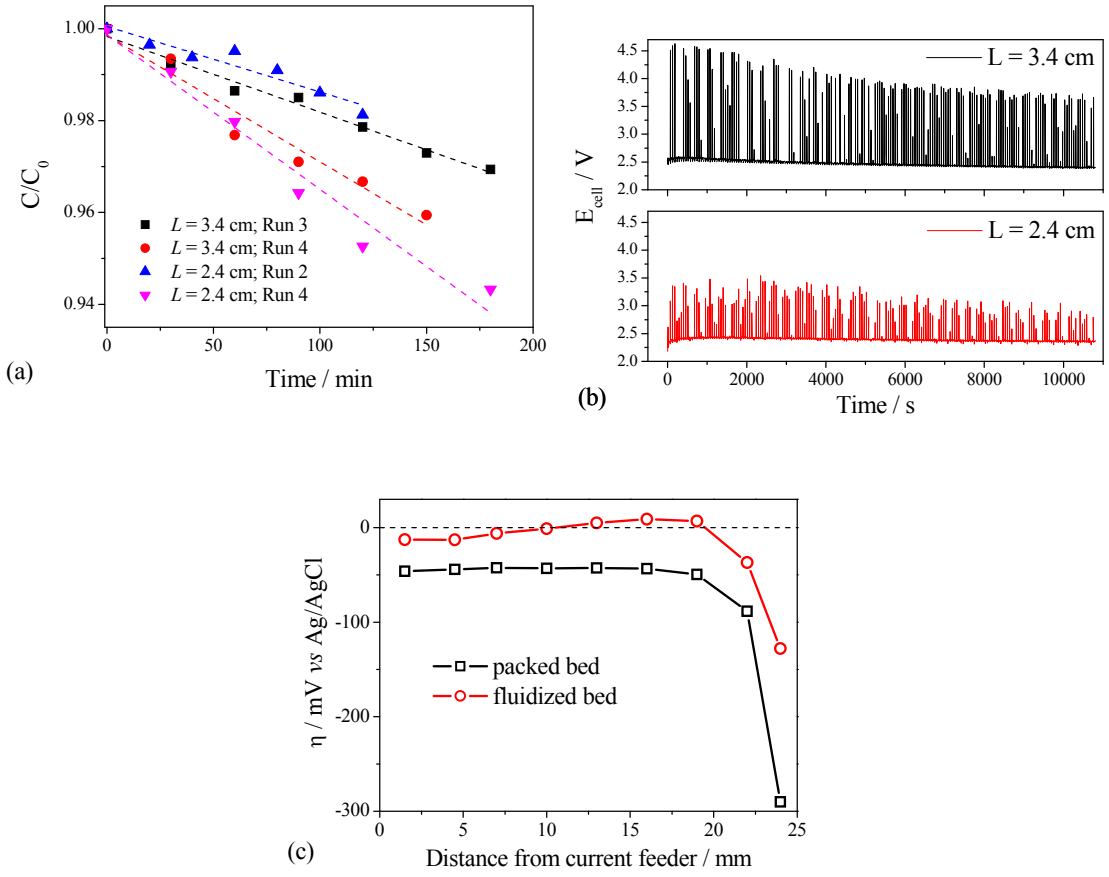

Fig. 5.1. Normalized copper concentration (a) and cell potential (b) against time. Run 3 (3.4 cm): 2362 A m^{-2}, 54 s, and 116 g L^{-1} acid; Run 4 (3.4 cm): 2838 A m^{-2}, 54 s, and 116 g L^{-1} acid; Run 2 (2.4 cm): 2458 A m^{-2}, 36 s, and 116 g L^{-1} acid; Run 4 (2.4 cm): 2458 A m^{-2}, 54 s, and 116 g L^{-1} acid. (c) Overpotential profiles, Run 15 (L = 2.4 cm).

Statistical analysis

The slopes of the copper concentration-time curves were determined by linear regression (dashed lines in Fig. 5.1(a)) and corresponded to the zero order constants or reaction rates (dC/dt). With few exceptions, the values of the squared correlation coefficient (R^2) were high. CE and Y were calculated using Eqs. (5.1) and (5.3) and the values of dC/dt. The

average cell potentials ($E_{cell,av}$) were determined by integrating the E_{cell}-time curves. EC was calculated using Eq. (5.2) and $E_{cell,av}$. The values of the response variables for the CCRD are provided in Table 5.2, together with the dC/dt, R^2, $E_{cell,av}$, and GD values.

Table 5.2
Results for dC/dt, $E_{cell,av.}$, CE, EC, Y, and GD.

Run	i*	t_p*	C_{ac}*	dC/dt (g L^{-1} h^{-1})	R^2	$E_{cell,av.}$ (V)	CE (%)	EC (kWh kg^{-1})	Y (kg $m^{-3}h^{-1}$)	GD
1	-1	-1	-1	0.382	93.9	2.22	65.3	2.87	40.8	0.329
2	1	-1	-1	0.339	89.9	2.59	48.7	4.50	36.2	0.001
3	-1	1	-1	0.466	96.1	2.27	79.7	2.41	49.8	0.579
4	1	1	-1	0.713	95.7	2.41	102	2.03	76.1	1.000
5	-1	-1	1	0.373	97.9	2.43	63.7	3.22	39.8	0.278
6	1	-1	1	0.453	99.7	2.23	65.1	2.89	48.4	0.416
7	-1	1	1	0.316	99.1	2.11	54.1	3.29	33.8	0.016
8	1	1	1	0.462	98.4	2.16	66.4	2.75	49.4	0.449
9	-1.68	0	0	0.353	97.1	2.13	65.7	2.74	37.7	0.280
10	1.68	0	0	0.519	99.1	2.29	69.8	2.77	55.4	0.529
11	0	-1.68	0	0.388	98.6	2.24	60.6	3.12	41.4	0.287
12	0	1.68	0	0.429	99.5	2.31	67.0	2.91	45.8	0.403
13	0	0	-1.68	0.491	98.7	2.33	76.8	2.56	52.5	0.575
14	0	0	1.68	0.353	97.7	2.10	55.1	3.21	37.7	0.182
15	0	0	0	0.467	95.4	2.38	72.9	2.76	49.9	0.503
16	0	0	0	0.447	99.5	2.28	69.8	2.76	47.8	0.458
17	0	0	0	0.422	97.7	2.17	65.9	2.78	45.1	0.397
						L or U	48.7	4.50	33.8	
						T	100	2.03	76.1	

*Refers to the variables in their coded value; L: lower value, U: upper value, T: target.

In previous work (Britto-Costa and Ruotolo, 2014), the effects of current density, packed bed time, and acid concentration on CE, EC, and Y were studied for a cathode with a thickness of 3.4 cm. The fluidized bed time had been previously optimized (Britto-Costa et al., 2014) and was maintained at 2 s, since shorter times resulted in particle agglomeration close to the counter-electrode, causing short circuit of the system after a few minutes of electrolysis. The packed bed time was also optimized for the 3.4 cm cathode, but its value depended on the applied current. After optimization, the maximum CE achieved was 77.7%, using a low acid concentration and a high current density, but this value was still lower than found in electrowinning plants (82-92% for current densities in the range 250-320 A m^{-2}). However, despite this value of CE, the EC was 2.72 kWh kg^{-1}, which is slightly higher than the typical values found in industry (2.5 kWh kg^{-1}). Therefore, the PBE reactor appears to hold considerable promise, once the current efficiency is improved.

Using the results of the experimental designs, attempts to increase CE by manipulating the operational conditions were unsuccessful, because other operational problems (such as short circuit) occurred outside the experimental domain identified previously (Britto-Costa et al., 2014; Britto-Costa and Ruotolo, 2014). According to the findings of Britto-Costa et al. (2014), the overpotential was not constant across the electrical field, as a result of which the electrodeposition rates were very different in regions such as close to the counter-electrode or the current feeder. This overpotential could also cause dissolution zones inside the fluidized bed (Fig. 5.1(c)), leading to low values of CE. For these reasons, and considering that a reduced electrode thickness could provide better overpotential distribution and current penetration, in the present work it was decided to use a lower electrode thickness in an attempt to increase the value of CE and consequently decrease the value of EC. Table 5.2 shows the results obtained using the CCRD factorial design.

The best CE and EC values were obtained for Runs 4 and 3, respectively. For both runs, the value of EC was lower than found in industry, while the maximum CE value was only obtained for Run 4, indicating that further improvement could only be achieved by reducing E_{cell} in order to obtain a lower EC. In the case of Y, the values were much higher than found for conventional electrowinning cells (~5 kg m^{-3} h^{-1}), with use of the PBE requiring only 7% of the volume of a conventional reactor in order to produce the same amount of copper, while also enabling the possibility of continuous operation. Although improved values of CE and EC were obtained, statistical analysis could provide a means of indicating ways in which EC and Y might be improved.

Table 5.3 shows analysis of variance (ANOVA) results for the three responses. The model for EC failed the F-test, since the calculated F-values were lower than the tabulated value, at a significance level of 95% (Montgomery, 1991). In contrast, the F-values obtained for CE and Y were higher than the F-distribution, indicating the statistical significance of the models for these responses. An analysis of effects was then performed in order to determine the main variables affecting the electrochemical process.

Table 5.3
ANOVA for CE, EC, Y, and GD.

Current Efficiency					
R^2=0.89	SS	DF	MS	F-value	F-distribution*
Model	1875	9	208.3	6.53	3.68
Residual Errors	223.2	7	31.89		
Pure Error	24.63	2	12.31	3.23	19.3
Lack of Fit	198.6	5	39.72		
Energy Consumption					
R^2=0.80	SS	DF	MS	F-value	F-distribution*
Model	3.34	9	0.372	3.09	3.68
Residual Errors	0.842	7	0.120		
Pure Error	3.94E-04	2	1.97E-04	8.55	19.3
Lack of Fit	0.842	5	0.168		
Space-Time Yield					
R^2=0.90	SS	DF	MS	F-value	F-distribution*
Model	1401.9	9	155.8	7.12	3.68
Residual Errors	153.2	7	21.9		
Pure Error	11.5	2	5.8	4.92	19.3
Lack of Fit	141.7	5	28.3		
Global Desirability					
R^2=0.93	SS	DF	MS	F-value	F-distribution*
Model	0.794	9	0.0882	9.87	3.68
Residual Errors	0.0626	7	0.00894		
Pure Error	0.00563	2	0.00282	4.04	19.3
Lack of Fit	0.0569	5	0.0114		

SS: sum of squares; DF: degrees of freedom; MS: mean square; *t-Student (95%, 6 DF)

Analysis of effects

Pareto charts of the contributions of the different effects to CE and Y are shown in Fig.**Error! Reference source not found.** 5.2. The critical values of the Student's t-test were calculated using the standard deviation of all replicates, for each response (not shown). These values were used to determine the significant effects (indicated by the blue bars). Values lower than the critical value indicated that the effect was not statistically significant (orange bars) and did not need to be considered in the model. In contrast to the 3.4 cm thickness cathode, for which t_p had no statistically significant effect (Britto-Costa and Ruotolo, 2014), in this case CE and Y were influenced by the three independent variables, as well as by their interactions.

It can be seen from Fig. 5.2 that the principal effect on CE and Y was the factor corresponding to interaction between t_p and C_{ac}. The interaction between i and t_p was the

second most important effect for CE and the third main effect for Y (after *i*). The effect of *i* on Y was expected, because the electrical current is the basis of the electrochemical reaction, so that a higher value of *i* results in a faster reaction rate, despite the loss in CE. This was confirmed by the positive value obtained for the effect (+11.09).

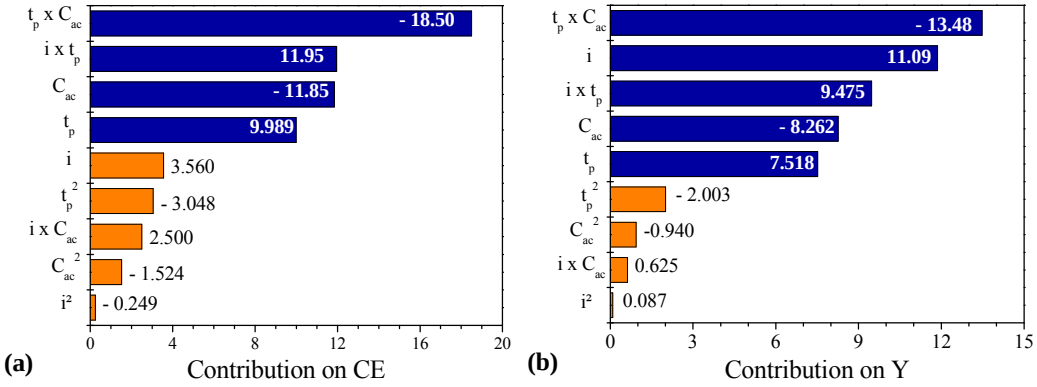

Fig. 5.2. Pareto chart of effects for CE (a) and Y (b).

Both CE and Y were also influenced by C_{ac} and t_p individually. Improvements in CE and Y could be obtained by decreasing $C_{ac.}$ (effect values of -11.85 and -8.262 for CE and Y, respectively) and increasing t_p (effect values of +9.989 and +7.518 for CE and Y, respectively). From analysis of the individual effects separately, it would be expected that a lower acid concentration and a longer packed bed time would contribute to better CE and Y values, because metal dissolution during the fluidized bed step (in the anodic zones shown in Fig. 5.1(c)) would be minimized. However, the existence of the interaction effects makes the process much more complex, as can be observed in the contour graphs of Fig. 5.3.

Statistical models and response surface analysis

The statistical models for CE and Y are described by Eqs. (5.8) and (5.9), respectively, considering only the significant effects.

$$CE = 69.4 + 5.0t_p - 5.9C_{ac} + 6.0it_p - 9.3t_pC_{ac} \quad (5.8)$$

$$Y = 47.5 + 5.5i + 3.8t_p - 4.1C_{ac} + 4.7it_p - 6.7t_pC_{ac} \quad (5.9)$$

Eqs. (5.8) and (5.9) are represented by the contour plots shown in Figs. 5.3 and 5.4, respectively, maintaining the value of the third variable at its central level (0). In both cases, the regions of maximum CE and Y coincided, and corresponded to a low acid concentration and high values of t_p and i. The values of CE greater than 100% (Fig. 5.3(a)) occurred because the plots were constructed using Eq. (5.8), although the maximum possible value of CE is 100%. In all the cases illustrated in Figs. 5.3 and 5.4, t_p played a role in maximizing CE and Y. The use of a high value of t_p is a necessary condition to obtain the best values of CE and Y. However, the acid concentration must be maintained at a low level while applying a high current density, in order to avoid the electrochemical process operating at very low CE and Y. The worst performance, observed at low values of t_p, was mainly due to the overall contribution of the fluidization time to the electrodeposition process. When t_p is decreased, there are increases in both the pulse frequency and the number of fluidization pulses. Hence, given that metal dissolution occurs during the fluidization step, due to the presence of anodic zones (see Fig. 5.1(c)), the net electrodeposition rate decreases. This problem was exacerbated at high acid concentrations, because anodic potentials (more positive overpotentials) are favored under these conditions (Huttin and Coeuret, 1977; Ruotolo and Gubulin, 2002). Therefore, it is necessary to increase t_p and decrease C_{ac} in order to minimize the deleterious effects of metal dissolution during fluidization. Unfortunately, values of t_p higher than 60 s were prohibitive due to the short circuit caused by the penetration and contact of the dendritic deposit formed in the region close to the counter-electrode, where the electrochemical activity is greatest due to the high cathodic overpotentials (Fig. 5.1(c)). Moreover, the current density must also be optimized in order to obtain the best values of CE and Y.

In Fig. 5.3(b) there is a wide region (represented by the green and blue colors) where the values of CE are very low (<75%). This region corresponds either to the application of low current densities, regardless of the packed bed time, or to the application of high current densities, with t_p being so fast that the effect of metal dissolution in the fluidized state prevailed. Hence, it is important to ensure low C_{ac}, high t_p, and high I when optimizing CE and Y. An attempt was made to increase i to values greater than 2600 A m^{-2}, but the combination of a high current and, consequently, a high electrodeposition rate concentrated in the region close to the anode resulted in short circuit of the electrodes after a few minutes of operation.

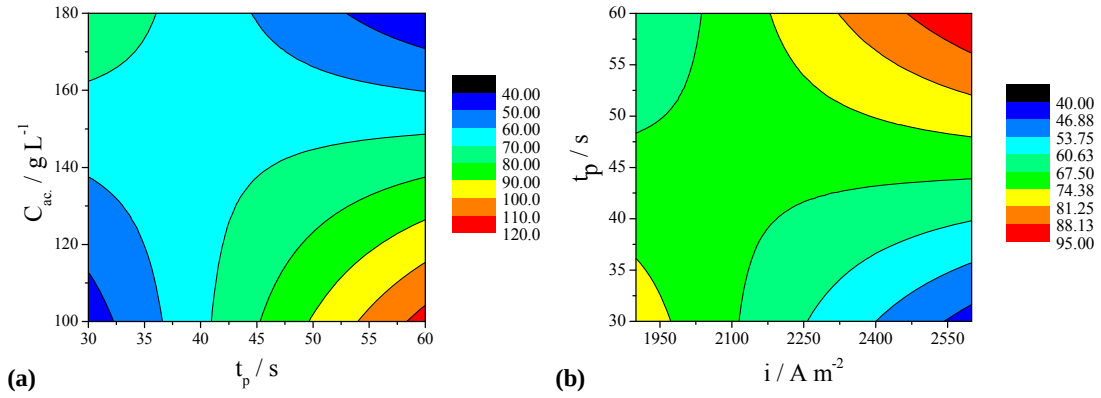

Fig. 5.3. Contour plots for CE: (a) C_{ac} against i; (b) t_p against i.

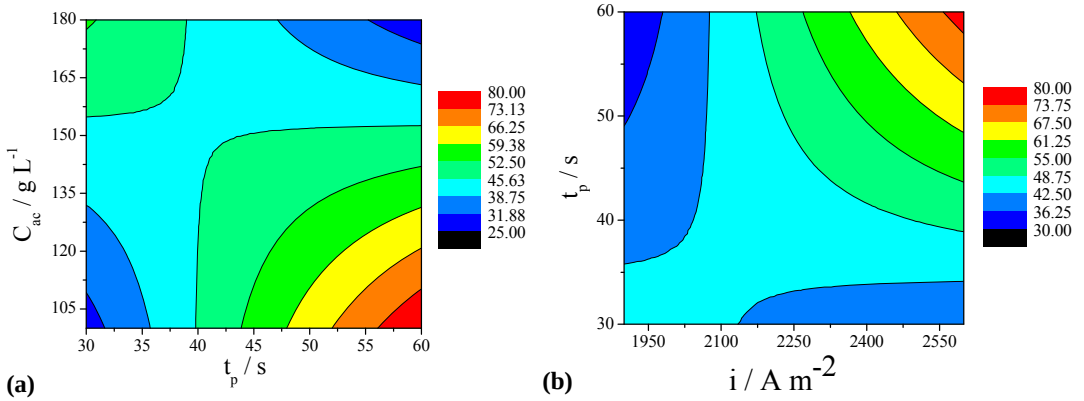

Fig. 5.4. Contour plots for Y: (a) C_{ac} against i; (b) t_p against i.

Global optimizationAlthough process optimization could be performed for CE and Y, no information about EC has been considered up to now because the statistical model showed a lack of fit for this response variable. However, EC is the main variable taken into account in industry in order to determine the feasibility of a process, so it is imperative to consider energy consumption during the optimization procedure. Despite the absence of a statistical model for EC, the global desirability (GD) method could be used for simultaneous optimization of all response variables, including EC.

Eqs. (5.5) and (5.6) were employed to calculate the individual desirability values (d_j) for CE, Y, and EC (not shown), using the upper (U), lower (L), and target (T) values shown in Table 5.2. In the case of CE and Y, the L-value was used because maximization was desired. In contrast, the U-value was used for EC because minimization was required.

The best experimental values of each response variable were taken to be the target values, but the weighting (W) attributed to Y was lower than that attributed to CE and EC, since it was more desirable to obtain high CE and low EC, rather than high Y. In other words, maximization of Y was not a priority because even the low value of Y obtained using the pulsed bed (~33.8 kg m^{-3} h^{-1}) was many times higher than that obtained using a flat plate electrode (~5 kg m^{-3} h^{-1}). The use of Eq. (5.7) and the values of d_j enabled calculation of the global desirability. The values are shown in the last column of Table 5.2.

The results of statistical analysis of the GD values are shown in Table 5.3. The F-value was almost 3 times the value of the F-distribution, confirming the effect of the independent variables on GD. The value of R^2 was also high, indicating that 93% of the experimental data could be predicted by the model. Therefore, identification of the values of the independent variables that maximized GD provided a means of simultaneously optimizing CE, Y, and EC.

According to the Pareto chart shown in Fig. 5.5(a), all the individual effects of the variables exerted an influence on GD, but once again, the interaction effects of t_p x C_{ac} and i x t_p were responsible for the greatest impact of the variables on the process responses. Eq. (5.10) represents the GD model, considering only the significant effects.

$$GD = 0.46 + 0.16i + 0.18t_p - 0.21C_{ac} + 0.26it_p - 0.37t_pC_{ac} \quad (5.10)$$

The contour plots shown in Figs. 5.5(b), 5.5(c), and 5.5(d) were constructed using Eq. (5.1). It can be seen that the contour plots in Figs. 5.5(b) and 5.5(c) are quite similar to those obtained for CE and Y (Figs. 3 and 4, respectively), indicating that higher values of GD approximately coincided with higher values of CE and Y. Hence, the operational conditions that optimized CE and Y also optimized EC. Fig. 5.5(d) shows that high current density must be applied with low C_{ac} in order to optimize the process. Despite the high conductivity of very acidic electrolytes, which would decrease E_{cell} and minimize EC, the effects of the other variables (C_{ac} and t_p) were more important for CE, which is the main response variable affecting the optimization of this process.

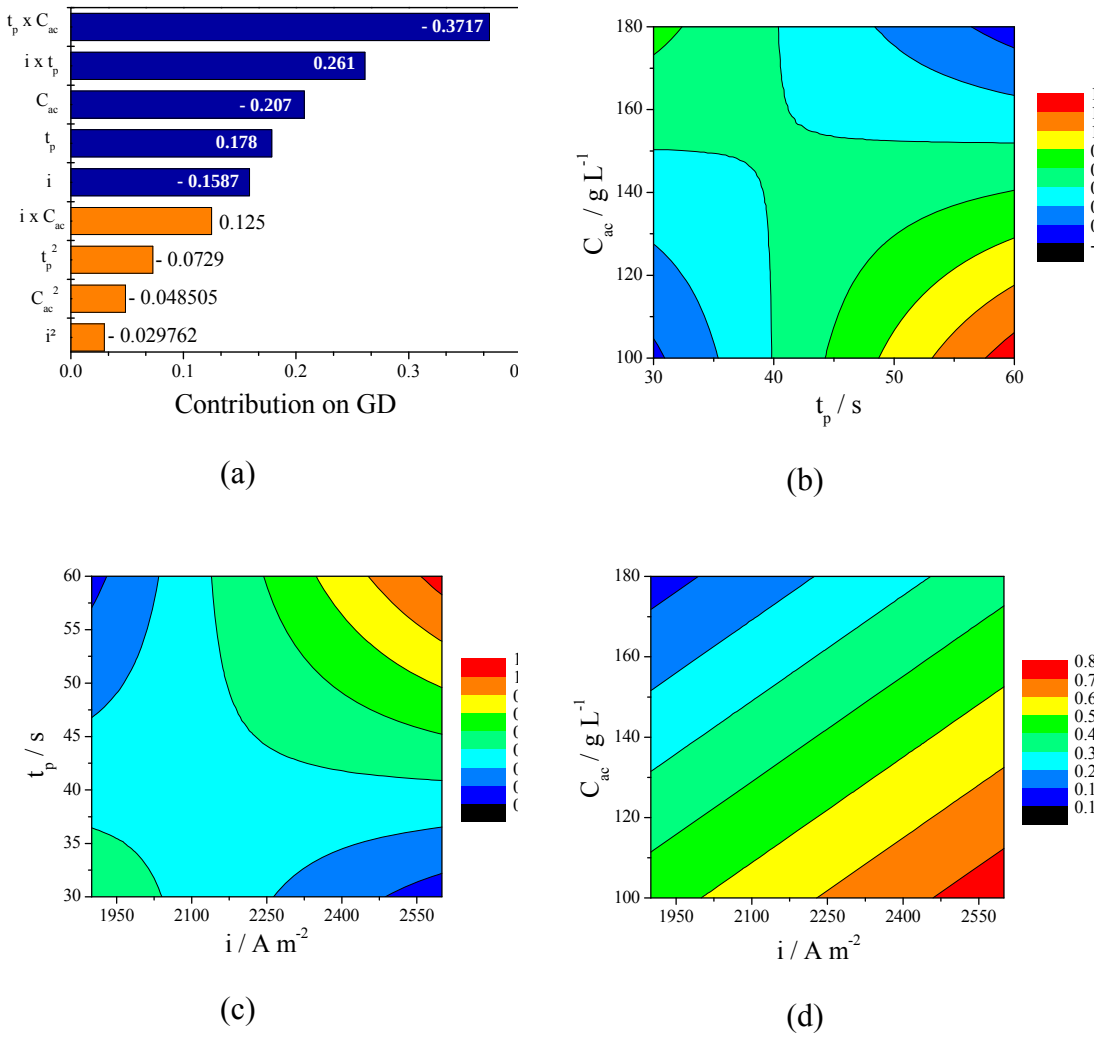

Fig. 5.5. (a) Pareto chart for GD. Contour plots for GD: (b) C_{ac} against t_p; (c) t_p against i; (d) C_{ac} against i.

Anode analysis

Another possible advantage of using PBE cathodes is that a smaller anode area can be used to achieve the same metal production. However, the high current densities obtained in the counter-electrode could lead to degradation and deactivation of the anode. In this study, a DSA® anode composed of $Ti/Ti_{0.7}Ru_{0.3}O_2$ was used for many hours during the performance of the experiments. After approximately 50 h of electrolysis, there was an increase of E_{cell} to values (6-8 V) much higher than measured in the initial experiments, suggesting the existence of an additional electrical resistance. In order to investigate the reason for the E_{cell} enhancement, scanning electron microscopy (SEM) was performed using a brand new anode and the deactivated anode. The SEM images are shown in Fig. 5.6. The new anode (Fig. 5.6(a)) presented the typical morphology of cracked clay, which

formed an adhesive and uniform film on the titanium plate, while the used DSA® showed an uneven oxide film (Fig. 5.6(b)). It can be seen from the inset of Fig. 5.6(b) that the oxide film was becoming detached, revealing a large portion of the uncovered substrate. This anode deactivation was also confirmed by linear sweep voltammetry, Fig. 5.6(c), in which the current densities observed for the used DSA® anode were lower than for the brand new anode. It can be concluded that the increase of E_{cell} was due to the destruction of the RuO_2 film, exposing the titanium substrate to oxidation and forming a very resistive passivating film of TiO_2.

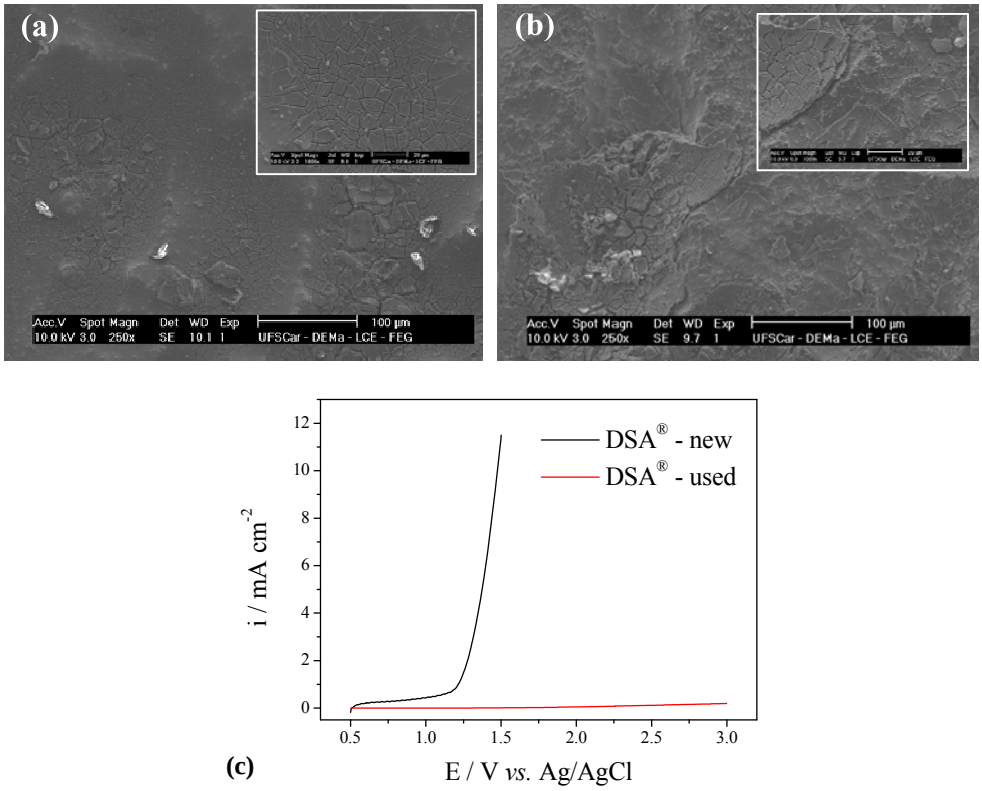

Fig. 5.6. SEM images of the DSA® before (a) and after electrolysis (b). (c) Linear sweep voltammetry for the new and used DSA® in H_2SO_4 150 g L^{-1} (scan rate = 10 mV s^{-1}).

In this case, oxide anodes were not the best choice for use in the PBE reactor, due to deactivation. Platinized titanium, for example, would be a better choice since it would not only be more stable, but would also offer another advantage in the high overpotential for the oxygen evolution reaction. This could provide a further reduction of E_{cell} and, consequently, a decrease of EC (Kötz et al., 1991).

CONCLUSIONS

This work concludes a series of studies concerning the use of a PBE reactor for metal electrowinning. The results showed that copper electrodeposition could be performed in this reactor with high current efficiency, high space-time yield, and low energy consumption. However, it was first necessary to optimize the thickness of the three-dimensional electrode. In the present case, the best cathode thickness was 2.4 cm. Thicknesses greater than 2.4 cm resulted in poor process performance, while thicknesses smaller than 2.4 cm could lead to hydrodynamic difficulties and low space-time yield (although a better overpotential distribution could be expected). In terms of the operational variables, it was found that higher *i* resulted in higher CE and Y, although there were restrictions related to E_{cell} and short circuit. The best value of *i* for copper electrowinning using the PBE was 2600 A m^{-2}. It was necessary to keep the fluidization time as short as possible (2 s) in order to avoid electrode clogging and short circuit. A low acid concentration (100 g L^{-1}) was required in order to avoid short circuit and to reduce the risk of anodic overpotentials during the fluidization step. Using these experimental conditions and statistical models, values of 100% (CE), 102 kg m^{-3} h^{-1} (Y), and 1.7 kWh kg^{-1} (EC) could be achieved. In conventional electrowinning plants for copper production, typical values of CE, Y, and EC are 82-92%, 5 kg m^{-3} h^{-1}, and 2.5 kWh kg^{-1}, respectively. The PBE reactor therefore offers a promising alternative to the use of flat plate electrodes.

Acknowledgments

The authors are grateful to FAPESP (Fundação de Amparo à Pesquisa do Estado de São Paulo) for financial support, and CNPq (Conselho Nacional de Desenvolvimento Científico e Tecnológico) for a PhD fellowship.

References

Argondizo, A., 2001. Remoção de íons cobre de soluções aquosas diluídas em eletrodo de leito pulsante. PhD Thesis, Federal University of São Carlos, São Carlos, Brazil, 131 pp.

Britto-Costa, P.H. and Ruotolo, L.A.M., 2011. Electrochemical removal of copper ions from aqueous solutions using a modulated current method. Sep. Sci. Technol. 46, 1205-1211.

Britto-Costa, P.H., Pereira-Filho, E.R. and Ruotolo, L.A.M., 2014. Copper electrowinning using a pulsed bed three-dimensional electrode. Hydrometallurgy 144-145, 15-22.

Britto-Costa, P.H. and Ruotolo L.A.M., 2014. Parametric study of copper electrowinning using a pulsed-bed electrode. J. Chem. Biochem. Technol.

Coeuret, F., 1980. The fluidized bed electrode for the continuous recovery of metals. J. Appl. Electrochem. 10, 687-696.

Coeuret, F. and Paulin, M., 1988. Experiments on copper recovery in a pulsed granular fixed bed electrode. J. Appl. Electrochem. 18, 162-165.

Del Castillo, E., Montgomery, D.C. and MacCarville, D.R., 1996. Modified desirability functions for multiple response optimization. J. Qual. Technol. 28, 337-345.

Derringer, G. and Suich, R., 1980. Simultaneous optimization of several response variables. J. Qual. Technol. 12, 214-219.

El-Shakre, M.E., Saleh, M.M., El-Anadouli, B.E. and Ateya, B.G., 1994. Applications of porous flow-through electrodes. J. Electrochem. Soc. 141, 441-447.

Evans, J.W., Ding, R., Doyle, F.M. and Jiricny, V., 2005. Copper electrodeposition onto extended surface area electrodes and the treatment of copper containing waste streams. Scand. J. Metall. 34, 363-368.

Garfias-Vasquez, F.J., Duverneuil, P. and Lacoste, G., 2004. Behaviour, modelling and simulation of a pulsed three-dimensional radial electrode with continuous solid flow: Part I. J. Appl. Electrochem. 34, 417-426.

Hadzismajlovic, D.Z.E., Popov, K.I. and Pavlovic, M.G., 1996. The visualization of the electrochemical behavior of metal particles in spouted, fluidized and packed beds. Powder Technol. 86, 145-148.

Hutin, D. and Coeuret, F., 1977. Experimental study of copper deposition in a fluidized bed electrode. J. Appl. Electrochem. 7, 463-471.

Jiricny, V., Roy, A. and Evans, J.W., 2002. Copper electrowinning using spouted-bed electrodes: part I. Experiments with oxygen evolution or matte oxidation at the anode. Metall. Mater. Trans. B 33, 669-676.

Kazdobin, K., Shvab, N. and Tsapakh, S., 2000. Scaling-up fluidized-bed electrochemical reactors. Chem. Eng. J. 79, 203-209.

Hötz, R., Stucki, S., Carcer, B., 1991. Electrochemical waste water treatment using high overvoltage anodes. Part I: Physical and electrochemical properties of SnO_2 anodes. J. Appl. Electrochem. 21, 14-20.

Lafront, A.M., Zhang, W., Ghali, E. and Houlachi, G., 2010. Electrochemical noise studies of the corrosion behavior of lead anodes during zinc electrowinning maintenance. Electrochim. Acta 55, 6665-6675.

Lupi, C. and Pilone, D., 1997. New lead alloy anodes and organic depolarizer utilization in zinc electrowinning. Hydrometallurgy 44, 347-358.

Martins, R., Britto-Costa, P.H. and Ruotolo, L.A.M., 2012. Removal of toxic metals from aqueous effluents by electrodeposition in a spouted bed electrochemical reactor. Environ. Technol. 33, 1123-1131.

Moats, M., Hardee, K. and Brown, C., 2003. Mesh-on-lead anodes for copper electrowinning. JOM 55, 46-48.

Montgomery D.C., 1991. Design and Analysis of Experiments. John Wiley & Sons, USA.

Moskalyk, R.R., Alfantazi, A., Tombalakian, A.S. and Valic, D., 1999. Anodes effect in electrowinning. Miner. Eng. 12, 65-73.

Muresan, L., Varvara, S., Maurin, G. and Dorneanu, S., 2000. The effect of some organic additives upon copper electrowinning from sulphate electrolytes. Hydrometallurgy 54, 161-169.

Olive, H. and Lacoste, G., 1979. Application of volumetric electrodes to the recuperation of metals in industrial effluents-I. Mass transfer in fixed beds of spherical conductive particles. Electrochim. Acta 24, 1109-1114.

Pletcher, D., White, I., Walsh, F.C. and Millington, J.P., 1991. Reticulated vitreous carbon cathodes for metal ion removal from process streams Part II: Removal of copper(II) from acid sulphate media. J. Appl. Electrochem. 21, 667-671.

Ruotolo, L.A.M. and Gubulin, J.C., 2002. Electrodeposition of copper ions on fixed bed electrodes: kinetic and hydrodynamic study. Braz. J. Chem. Eng. 19, 105-118.

Ruotolo, L.A.M. and Gubulin, J.C., 2005. A factorial-design study of the variables affecting the electrochemical reduction of Cr(VI) at polyaniline-modified electrodes. Chem. Eng. J. 110, 113-121.

Ruotolo, L.A.M. and Gubulin, J.C., 2011. A mathematical model to predict the electrode potential profile inside a polyaniline-modified reticulated vitreous carbon electrode operating in the potentiostatic reduction of Cr(VI). Chem. Eng. J. 171, 1170-1177.

Sabacky, B.J. and Evans, J.W., 1979. Electrodeposition of metals in fluidized bed electrodes. J. Electrochem. Soc. 126, 1176-1187.

Salas-Morales, J.C., Evans, J.W., Newman, O.M.G. and Adcock, P.A., 1997. Spouted bed electrowinning of zinc: Part I. Laboratory-scale electrowinning experiments. Metall. Mater. Trans. 28B, 59-68.

San Martin, R.M., Otero, A.F. and Cruz, A., 2005. Use of quillaja saponins (Quillaja saponaria Molina) to control acid mist in copper electrowinning processes Part 2: pilot plant and industrial scale evaluation. Hydrometallurgy 77, 171-181.

Shakarji, R.A., He, Y. and Gregory, S., 2011. Statistical analysis of the effect of operating parameters on acid mist generation in copper electrowinning. Hydrometallurgy 106, 113-118.

Sigley, J.L., Johnson, P.C. and Beaudoin, S.P., 2003. Use of nonionic surfactant to reduce sulfuric acid mist in the copper electrowinning process. Hydrometallurgy 70, 1-8.

Tonini, G.A., Farinos, R.M., Prado, P.F.A. and Ruotolo, L.A.M., 2013. Box-Behnken factorial design study of the variables affecting metal electrodeposition in membraneless fluidized bed electrodes. J. Chem. Technol. Biotechnol. 88, 800-807.

Wiechmann, E.P., Morales, A.S. and Aqueveque, P., 2010. Improving productivity and energy efficiency in copper electrowinning plants. IEEE Trans. Ind. Appl. 46, 1264-1269.

5.3 Conclusões

Este trabalho conclui uma série de estudos sobre o uso de ELP na eletrorrecuperação de cobre. Os resultados mostraram que a eletrodeposição de cobre pode ser realizada neste reator com elevados valores de *EC*, elevado rendimento e baixo consumo energético. Entretanto, primeiro foi necessário otimizar a espessura do eletrodo tridimensional. A espessura ótima foi de 2,4 cm. O uso de uma espessura maior que esta resultou em uma piora do processo de eletrodeposição, enquanto que espessuras menores poderiam levar a problemas hidrodinâmicos e um baixo rendimento espaço-tempo. Em termos de variáveis operacionais, foi encontrado que altas densidades de corrente resultavam em altos valores de *EC* e *Y*, entretanto há restrições relacionadas ao potencial de célula e curto-circuito. O melhor valor de *i* encontrado para o ELP foi de 2600 A m^{-2}. Foi necessário manter o tempo de fluidização no mínimo possível (2 s) para evitar aglomeração de partículas e curto-circuito. Baixas concentrações de ácido foram necessárias para se reduzir a ocorrência de sobrepotenciais anódicos durante a fluidização. Utilizando estas condições experimentais previstas pelos modelos estatísticos, valores de 100% de *EC*, 102 kg m^{-3} h^{-1} de *Y* e 1,7 kWh kg^{-1} de *CE* foram obtidos. No processo convencional os valores geralmente obtidos são 82-92% de *EC*, 5 kg m^{-3} h^{-1} de *Y* e 2,5 kWh kg^{-1} de *CE*. Por este motivo, o ELP objeto de estudo deste trabalho é apresentado como uma alternativa promissora na utilização em eletrorrecuperação de cobre.

6 ELETRORRECUPERAÇÃO DE COBRE UTILIZANDO REATOR ELETROQUÍMICODE LEITO DE JORRO

6.1 Introdução

Neste capítulo empregou-se um eletrodo tridimensional de leito de jorro no estudo da eletrorrecuperação de cobre. O desenvolvimento do trabalho foi realizado visando a determinar as condições experimentais em que elevados valores de eficiência de corrente e rendimento espaço-tempo fossem obtidos aliados a um baixo consumo energético.

O eletrodo de leito de jorro foi escolhido para ser estudado por apresentar características como boa condutividade da fase sólida no *anulus*, sendo que nesta região as partículas estão em movimento contínuo e não sujeitas a aglomerarem, o que poderia resultar em um impedimento da passagem do eletrólito. Diferentemente do ELP, existem trabalhos na literatura sobre a utilização do ELJ em eletrorrecuperação de cobre e zinco, onde foram obtidos resultados promissores para a eletrorrecuperação de cobre. Entretanto, o ELJ apresenta uma região (canal central) em que as partículas estão completamente desprotegidas catodicamente e sujeitas ao ataque do eletrólito ácido, desta forma, a *EC* deste processo é sensível a altas concentrações de ácido sulfúrico. Assim, optou-se por utilizar como eletrólito suporte o sulfato de sódio e então estudar o efeito do pH do eletrólito sobre o processo, sugerindo então uma mudança no processo hidrometalúrgico convencional.

As variáveis independentes estudadas foram a densidade de corrente elétrica, concentração do eletrólito suporte, pH, espessura do eletrodo e temperatura do eletrólito, de modo a se determinar a condição experimental em que se obtém *EC* máxima e consumo energético mínimo, uma vez que este tipo de eletrodo apresenta considerável aumento do rendimento, quando comparado ao reator convencional.

6.2 Desenvolvimento

O desenvolvimento detalhado do Capítulo 6 é apresentado a seguir, no artigo intitulado “ELETRORRECUPERAÇÃO DE COBRE UTILIZANDO REATOR ELETROQUÍMICODE LEITO DE JORRO”, submetido para publicação no periódico Química Nova.

ELETRORRECUPERAÇÃO DE COBRE UTILIZANDO REATOR ELETROQUÍMICO DE LEITO DE JORRO

Pedro H. Britto-Costa [a,*], Luís A. M. Ruotolo [a]

[a]Departamento de Engenharia Química, Universidade Federal de São Carlos, 13.565-905 São Carlos – SP, Brasil

*e-mail: britto_pedro@hotmail.com

Abstract

COPPER ELECTROWINNING USING A SPOUTED-BED ELECTROCHEMICAL REACTOR

In this work the copper electrowinning using a tridimensional spouted-bed electrode (SBE) was studied in order to investigate the effects of current density (*i*), concentration of the supporting electrolyte (C_s), pH, electrolyte temperature, and bed thickness on the process current efficiency (CE), energy consumption (EC) and space-time yield (Y). The results indicated that the SBE can be used successfully for copper electrowinning when high concentration of copper and pHs between 1 and 2. In this case, 100% *CE*, 2.7 kWh kg^{-1} *EC* and 118 kg $L^{-1}h^{-1}$ *Y* can be achieved. It was verified that an increase in the electrolyte temperature caused a decrease of the electrodeposition rate, indicating that, despite the solution conductivity enhancement, the temperature promoted the increase of the anodic dissolution kinetics. Finally, the copper particles were analyzed by scanning electron microscopy and it was verified that a smooth, uniform and compact electrodeposit can be obtained without using any chemical additive.

Keywords: copper; electrowinning; spouted-bed electrode.

INTRODUÇÃO

As indústrias hidrometalúrgicas utilizam eletrodos planos em seus processos de metalurgia extrativa nos quais são aplicadas densidades de corrente da ordem de 300 A m^{-2} [8-10]. Devido à pequena área superficial específica deste tipo de eletrodo, células eletroquímicas extremamente grandes são requeridas para se obter uma elevada produtividade. Além destas limitações, existem outras desvantagens em se utilizar eletrodos planos, como a necessidade de remover o depósito do substrato, a intensa liberação de vapores ácidos devido ao tamanho das células eletroquímicas, que podem oxidar os contatos elétricos ou mesmo causar danos à saúde, além da necessidade de se utilizar um grande número de placas anódicas [9-15]. Os eletrodos de PbO_2, geralmente usados nos processos de eletrorrecuperação, tem como principal desvantagem a baixa resistência à corrosão, principalmente durante a manutenção da célula ou remoção do eletrodepósito em que a solução ácida ataca o eletrodo no momento em que não há passagem de corrente elétrica, diminuindo sua vida útil, além de contaminar o depósito catódico devido à incorporação de chumbo [16,17]. Aditivos químicos geralmente são utilizados na tentativa de minimizar este problema.

Neste contexto, o eletrodo tridimensional, em particular o eletrodo particulado, apresenta-se como uma alternativa para superar alguns dos problemas associados ao processo convencional. Altas densidades de corrente elétrica (até 4466 A m^{-2}) poderiam ser aplicadas nestes reatores particulados [10,13], sem prejudicar a qualidade do depósito, uma vez que estes eletrodos apresentam elevada área superficial, pela qual a corrente elétrica fornecida é distribuída no meio poroso [10,13,18]. Além disto, caso as partículas sejam do mesmo material do metal a ser depositado, a etapa de remoção do depósito seria desnecessária, reduzindo bastante os custos com mão-de-obra e sem a necessidade de interrupções da produção [10]. Devido à significativa redução do volume do reator, uma substituição do ânodo de chumbo por um que seja dimensionalmente estável poderia se tornar viável e reduzir, ou até mesmo eliminar, a necessidade de aditivos químicos [10,19].

A utilização de reatores tridimensionais também soluciona o problema de vapores ácidos, que podem ser facilmente canalizados e neutralizados, evitando sérios danos à saúde dos operários. Dentre os eletrodos de leito particulado, o de leito fixo tem sido muito estudado, particularmente na área de tratamento de efluentes, em que a

concentração de metais é baixa [20-23]. As principais características do leito fixo são a alta condutividade elétrica da fase sólida e o elevado valor do coeficiente de transporte de massa. Essas características promovem altos valores de eficiência de corrente, fazendo com que o leito fixo seja a configuração mais eficiente para a eletrodeposição de metais [22-25]. Entretanto, quando a concentração do metal é muito alta, o entupimento do eletrodo decorrente da deposição do metal nos seus poros ocorre muito rapidamente, impossibilitando a sua utilização em escala industrial[23].

Visando a solucionar os problemas relacionados ao leito fixo, foram propostos eletrodos particulados em que o movimento do fluido resulta no movimento das partículas. Nessa classe de eletrodos encontra-se o de leito de jorro, o qual é caracterizado por um movimento ascendente das partículas no canal de jorro, promovendo então a circulação das partículas. Ao atingir a região da fonte, as partículas sofrem um movimento descendente devido à diminuição da velocidade do fluido, caindo na região do *anulus* e circulando por esta região por efeito da gravidade, atingindo novamente a região de entrada do canal de jorro e permanecendo então em um movimento circular que além de promover altas taxas de transferência de massa também evita a aglomeração das partículas do leito devido ao depósito. Uma descrição mais detalhada do reator de leito de jorro foi feita por Farinos *et al.* (2012) [43]. Assim como no eletrodo de leito fluidizado, o qual já foi estudado por diversos autores [31,44-46], a taxa de reação no eletrodo de leito de jorro é bastante sensível às condições fluidodinâmicas, uma vez que a condutividade da fase sólida, principalmente na região de jorro, depende da frequência estatística de choque entre as partículas [31], a qual é diretamente influenciada pela expansão do leito, por isso, zonas de dissolução dentro do cátodo poroso podem ocorrer, especialmente em soluções muito ácidas [18,30,47].

Estes eletrodos tridimensionais são apresentados como alternativa promissora para a eletrodeposição de metais a partir de soluções diluídas, devido à elevada área superficial e por proporcionarem altas taxas de transferência de massa [10,13,18,21-23,27,31,43,48,49]. Entretanto, pouco tem-se estudado a respeito de sua utilização nos processos hidrometalúrgicos. Embora a limitação destes processos não seja dada pela transferência de massa, devido às altas concentrações deste tipo de eletrólito, a elevada área superficial de eletrodos tridimensionais incrementa consideravelmente o rendimento espaço-tempo (Y) do reator [50]. Desta forma, a utilização do leito de jorro constituído por partículas do

mesmo metal a ser depositado representa uma grande vantagem no processo, uma vez que no método convencional o cobre, depositado nas placas planas, precisa ser removido por um processo demasiadamente trabalhoso, conhecido como colheita. Esta etapa do processo convencional pode ser realizada por equipamentos sofisticados e automatizados, porém que necessitam de manutenção constantemente, ou ainda ser realizado por operadores, em um processo moroso.

Neste trabalho, estudou-se a eletrorrecuperação de cobre em um eletrodo tridimensional de leito de jorro, composto por partículas cilíndricas de cobre visando a determinar as condições experimentais em que se obtenha elevados valores de eficiência de corrente e rendimento espaço-tempo aliados a um baixo consumo energético.

PARTE EXPERIMENTAL

Os experimentos de eletrorrecuperação de cobre foram realizados no sistema experimental esquematizado na Figura 6.1. O eletrólito foi preparado utilizando-se sulfato de cobre pentahidratado ($CuSO_4 \bullet 5H_2O$) como fonte de íons cobre, sulfato de sódio (Na_2SO_4) como eletrólito suporte e ácido sulfúrico para ajuste do pH. Água deionizada foi utilizada no preparo de todas as soluções. Nenhum aditivo químico foi adicionado para melhorar as condições de eletrorrecuperação, comumente utilizados nos processos convencionais.

A Figura 6.2 (a) mostra uma vista frontal do reator eletroquímico de leito de jorro montado e a Figura 6.2 (b), uma visão mais detalhada deste reator. O reator de leito de jorro era formado por placas retangulares que eram justapostas, vedadas por meio de mantas de silicone (3) e fixadas por meio de porcas e parafusos (Figura 6.2b). O contra-eletrodo (6) de $Ti/Ti_{0,7}Ru_{0,3}O_2$ (De Nora do Brasil) era revestido por uma tela de polietileno recoberta com tecido de poliamida (7) para evitar o curto-circuito no reator e utilizou-se uma placa de aço inoxidável AISI 316 como alimentador de corrente, ambos de dimensões 8 cm x 6 cm. As partículas eletroativas que constituíam o cátodo poroso eram de cobre e apresentavam geometria cilíndrica de 1 mm de diâmetro e 1 mm de comprimento. As partículas eram acondicionadas no interior da placa central (4), por onde também escoava o eletrólito, que entrava pela base e saía pelo topo do reator,

retornando ao reservatório (Figura 6.1, item 1). Neste trabalho, foram realizados estudos utilizando duas espessuras de placas centrais, sendo elas de 2,1 cm e 1,3 cm. No centro da placa intermediária estava disposto também o *draft* ou canal central (2), composto por duas placas paralelas de acrílico com distância de 13 mm entre si e encaixadas nas duas placas laterais. Logo acima da entrada do eletrólito no reator e abaixo do leito de partículas eletroativas havia um meio poroso de partículas de polietileno cuja função era evitar caminhos preferenciais do fluxo de eletrólito (5).

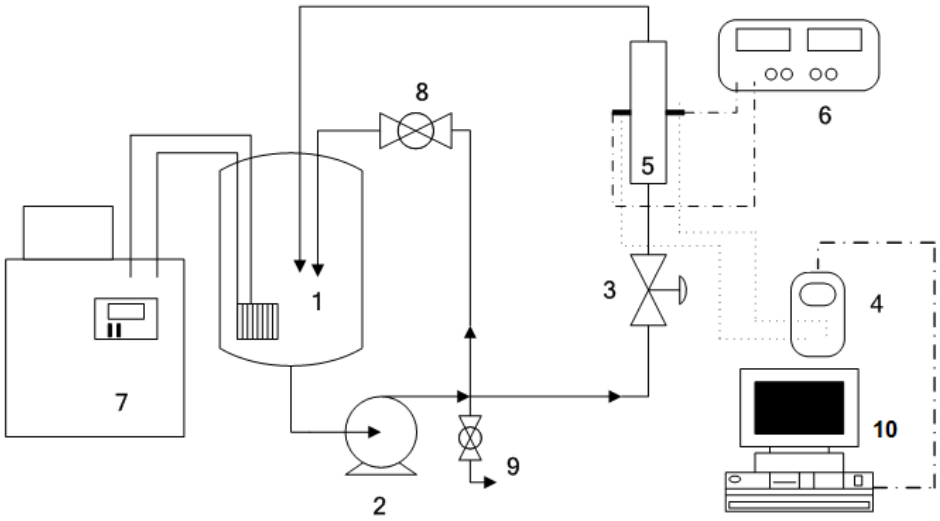

Figura 6.1 - Representação esquemática do sistema experimental. 1) reservatório de eletrólito; 2) bomba centrífuga; 3) válvula de controle da vazão ao reator; 4) voltímetro; 5) reator eletroquímico; 6) fonte de corrente contínua; 7) sistema de controle da temperatura; 8) válvula do *bY-pass*; 9) válvula de esgotamento do sistema e 10) computador para aquisição de dados.

A Tabela 6.1 mostra a sequência de experimentos realizada neste trabalho, de forma que foram estudadas as variáveis concentração de sulfato de sódio, pH, espessura do eletrodo, temperatura do eletrólito, densidade de corrente e massa do cátodo poroso.

Os experimentos foram analisados com base nas variáveis eficiência de corrente (%), consumo energético (kWh kg^{-1}) e rendimento espaço-tempo (kg $m^{-3}h^{-1}$), calculados utilizando as Equações 6.1, 6.2 e 6.3, respectivamente.

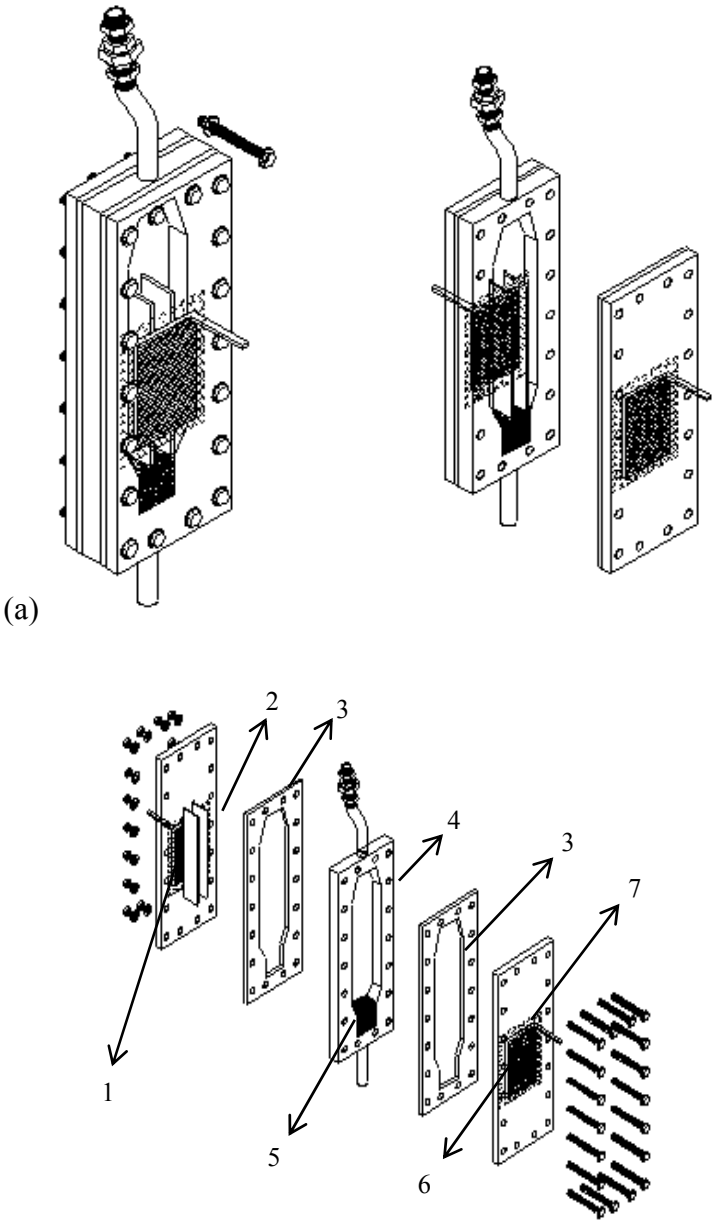

Figura 6.2 - Reator eletroquímico de leito jorro. (a) Vistas frontal e lateral; (b) vista explodida. (1) alimentador de corrente; (2) draft ou canal central; (3) borrachas de silicone; (4) placa central com aberturas de entrada e saída de eletrólito; (5) distribuidor de fluxo; (6) tela de polietileno revestida por tecido de poliamida e (7) contra-eletrodo.

$$EC = \frac{zFV}{MI}\frac{dC}{dt} \tag{6.1}$$

$$CE = \frac{2.78\ x\ 10^{-4} zFE_{cell}}{MCE} \tag{6.2}$$

$$Y = 3.6\frac{V}{V_R}\frac{dC}{dt} \tag{6.3}$$

Tabela 6.1. Matriz de ensaios realizados, variando-se o eletrólito suporte, a espessura do eletrodo, temperatura, corrente elétrica e massa do cátodo.

Ensaio	Na_2SO_4 / mol L^{-1}	pH	espessura / cm	Temp. / ºC	i / A m^{-2}	I / A	$m_{partículas}$ / g
1	0,5	2	2,1	40	3000	9,6	550
2	1	2	2,1	40	3000	9,6	550
3	1	1	2,1	40	3000	9,6	550
4	1,8	2	2,1	40	3000	9,6	550
5	1,8	1	2,1	40	3000	9,6	550
6	1,8	1	2,1	40	1200	3,84	550
7	1,8	1	2,1	40	2500	8	550
8	1,8	1	2,1	40	2000	6,4	550
9	1	2	2,1	60	3000	9,6	550
10	1	2	1,3	60	3000	9,6	400
11	1	2	1,3	40	3000	9,6	400
12	1,8	1	1,3	40	3000	9,6	400
13	1,8	1	1,3	40	2181	6,98	400
14	1,8	1	1,3	40	1856	5,94	400
15	1,8	1	1,3	40	2500	8	400

RESULTADOS E DISCUSSÃO

Eletrorrecuperação galvanostática de cobre

Na Figura 6.3 são apresentados as curvas de concentração normalizada de cobre em função do tempo para todos os experimentos realizados no reator de espessura 2,1 e 1,3 cm. Verifica-se um comportamento linear do decaimento da concentração de cobre ao longo dos experimentos, evidenciando que a cinética do processo está sendo controlada pela transferência de carga, comportamento característico de eletrodeposição em soluções concentradas. Isto significa que existe uma quantidade suficiente de cátions na superfície do cátodo, de modo que um aumento da corrente elétrica aplicada (processo galvanostático) provoca um aumento da taxa de eletrodeposição, se mantidas as demais condições. Os experimentos 04 e 06 apresentaram, respectivamente, a maior e a menor

cinética de reação, entretanto este último apresentou o menor potencial de célula, com valor de 2,12 V. O maior valor de potencial de célula obtido foi do experimento 04, devido a uma menor condutividade da solução, juntamente com elevada densidade de corrente aplicada, resultando em um E_{cel} de 3,54 V.

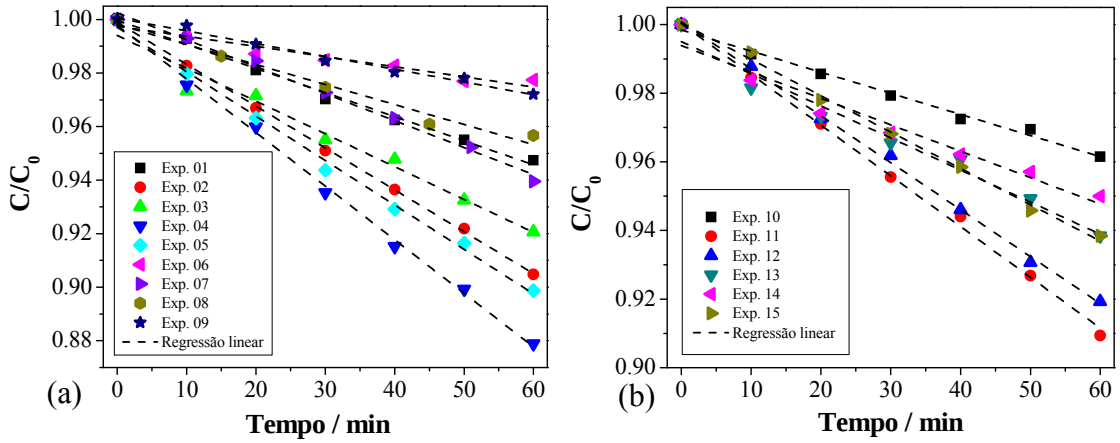

Figura 6.2 – Concentração normalizada de cobre em função do tempo para os experimentos realizados. (a) Eletrorrecuperação em eletrodo de 2,1 cm de espessura, C_0 = 40,00 g L^{-1}; (b) eletrorrecuperação em eletrodo de 1,3 cm de espessura, C_0 = 40,53 g L^{-1}.

Em processos controlados por transferência de carga, a Equação 6.4, de Butler-Volmer, é utilizada para descrever a relação entre a corrente elétrica e o sobrepotencial da reação. Nesta equação, a densidade de corrente elétrica (i) é função do sobrepotencial (η), da densidade de corrente de troca (i_0) e dos coeficientes de transferência de carga (α). α_a e α_c correspondem aos coeficientes de transferência de carga anódico e catódico, respectivamente, R é a constante universal dos gases e T a temperatura do meio.

$$i = i_0 \cdot \left\{ exp\left[\frac{\alpha_a z F}{RT} \cdot \eta\right] - exp\left[\frac{\alpha_c z F}{RT} \cdot \eta\right] \right\} \quad (6.4)$$

Nota-se na Equação 6.4 que na situação de controle por transferência de carga a corrente elétrica não depende da concentração da espécie iônica, nem de parâmetros de transferência de massa, como difusividade dos íons e espessura da camada limite, diferentemente da corrente limite, que é uma característica exclusivamente dependente dos parâmetros de transferência de massa. Assim, analisando-se os resultados mostrados na Figura 6.3 (a), pode-se inferir que a cinética de reação poderia ser aumentada por

variações, dentro dos limites estudados, dos seguintes parâmetros: 1 – aumento da concentração do eletrólito suporte (conclusão da comparação dos experimentos 01, 02 e 04); 2 – aumento do pH (experimentos 02, 03,04 e 05); 3 – redução para temperatura de 40 ºC (experimentos 02 e 09) e 4 – aumento da densidade de corrente para 3000 A m^{-2} (experimentos 05, 06, 07 e 08). Concentrações mais elevadas de sulfato de sódio não puderam ser utilizadas devido à precipitação do sal.

Observando-se os resultados da Figura 6.3 (b) verifica-se que o reator de espessura de 1,3 cm apresentou o mesmo comportamento do reator de maior espessura, porém com menor desempenho na cinética de reação. A influência do aumento da temperatura na cinética de reação de redução de cobre foi verificada por Britto-Costa e Ruotolo (2014) [50] na eletrorrecuperação de cobre em eletrodo de leito pulsante. De forma similar, a causa da diminuição da cinética de eletrodeposição em função do aumento da temperatura pode estar relacionada à competição entre duas reações eletroquímicas, dissolução anódica e eletrodeposição, em que o incremento na dissolução foi mais acentuado do que a influência na reação de eletrodeposição do metal, resultando na diminuição da eficiência do processo. Cifuentes e Simpson (2005) [51] determinaram os parâmetros da equação de Butler-Volmer (Eq. 6.4) para a eletrodeposição de cobre em solução contendo 30 g L^{-1} de Cu^{2+} e 190 g L^{-1} de H_2SO_4, em diferentes temperaturas e os autores verificaram que a temperatura não apresentava nenhuma influência no coeficiente de transferência de carga da eletrodeposição de cobre, no entanto a temperatura causa um aumento da densidade de corrente de troca. Desta forma, pode-se afirmar que a temperatura está realmente ocasionando um aumento da taxa de eletrodeposição, porém um aumento mais intenso da dissolução do metal na região do jorro, faz com que a taxa líquida de eletrodeposição seja menor em temperaturas maiores. Pelo mesmo motivo, este reator apresenta-se pouco eficaz para soluções muito ácidas, uma vez que no canal central as partículas estão desprotegidas catodicamente e em situações em que o metal sofre dissolução acentuada [48].

A partir dos dados de dC/dt, determinados a partir da regressão linear das curvas mostradas na Figura 6.3 foram calculadas as variáveis eficiência de corrente, consumo energético e rendimento espaço-tempo, utilizando as Equações 6.1, 6.2 e 6.3, respectivamente. Os resultados de *EC*, *CE* e *Y* são mostrados nas Figuras 6.4 (a), (b) e (c), respectivamente. Em processos de eletrodeposição controlados por transferência de

carga, o decaimento da concentração do metal em função do tempo é linear, uma vez que a taxa de reação é constante e depende apenas da corrente elétrica aplicada, no caso de um processo galvanostático. Os valores do coeficiente de correlação ao quadrado (R^2) obtidos das regressões lineares das curvas mostradas na Figura 6.3 variaram entre 0,928 e 0,999, o que evidencia a boa linearidade dos pontos experimentais e confirmando que o processo é realmente controlado pela transferência de carga.

Os experimentos 01 a 05 foram realizados com o intuito de analisar a influência da concentração do eletrólito suporte e do pH da solução no processo de eletrodeposição. Verifica-se, analisando a Figura 6.4 (a), que o experimento 02 apresentou 100% de *EC*, o que implicou no consumo de 2,9 kWh kg^{-1}, valor considerado um pouco elevado para a indústria hidrometalúrgica, por implicar diretamente no custo de produção do metal. Adicionalmente, nestes ensaios o reator apresentou rendimento espaço-tempo de 118 kg $h^{-1}m^{-3}$ o que corresponde a um rendimento de aproximadamente 20 vezes superior ao de reatores convencionais de placas planas, que é de aproximadamente 5 kg $h^{-1}m^{-3}$ [50]. Desta forma, do ponto de vista do consumo energético, o processo apresentou-se pouco satisfatório quando comparado com o processo convencional, em que os valores típicos de *CE* estão na faixa de 1,9 a 2,3 kWh kg^{-1} [9,41]. Por outro lado, os valores de *EC* e, principalmente, o *Y* foram bastante superiores aos valores encontrados no processo convencional (82 a 92% de *EC* [9,10,41]). Diante disto, a partir do experimento 02 o foco do trabalho foi diminuir o consumo energético através da diminuição do potencial de célula. Assim sendo, a primeira tentativa foi direcionada à melhoria da condutividade da solução, seguida da diminuição da densidade de corrente elétrica, aumento da temperatura, para favorecer a condutividade da solução e, por último, a diminuição da espessura do eletrodo a fim de amenizar a distribuição do potencial de eletrodo [23].

Verificou-se nos experimentos 05 a 08, que a *EC* sofreu influência da densidade de corrente, de forma que diminuindo-se *i*, diminui-se também a *EC*. Este mesmo comportamento foi observado por Britto-Costa e Ruotolo (2014) [50] no estudo de eletrorrecuperação de cobre utilizando eletrodo de leito pulsante. Os autores concluíram que menores densidades de corrente causavam uma diminuição da proteção catódica das partículas, levando ao surgimento de zonas de dissolução anódica, resultando em um empobrecimento da cinética de reação global. Este resultado foi útil para se determinar a

densidade de 3000 A m^{-2} como ótima, uma vez que densidades maiores que esta iriam apenas aumentar o *CE* do processo.

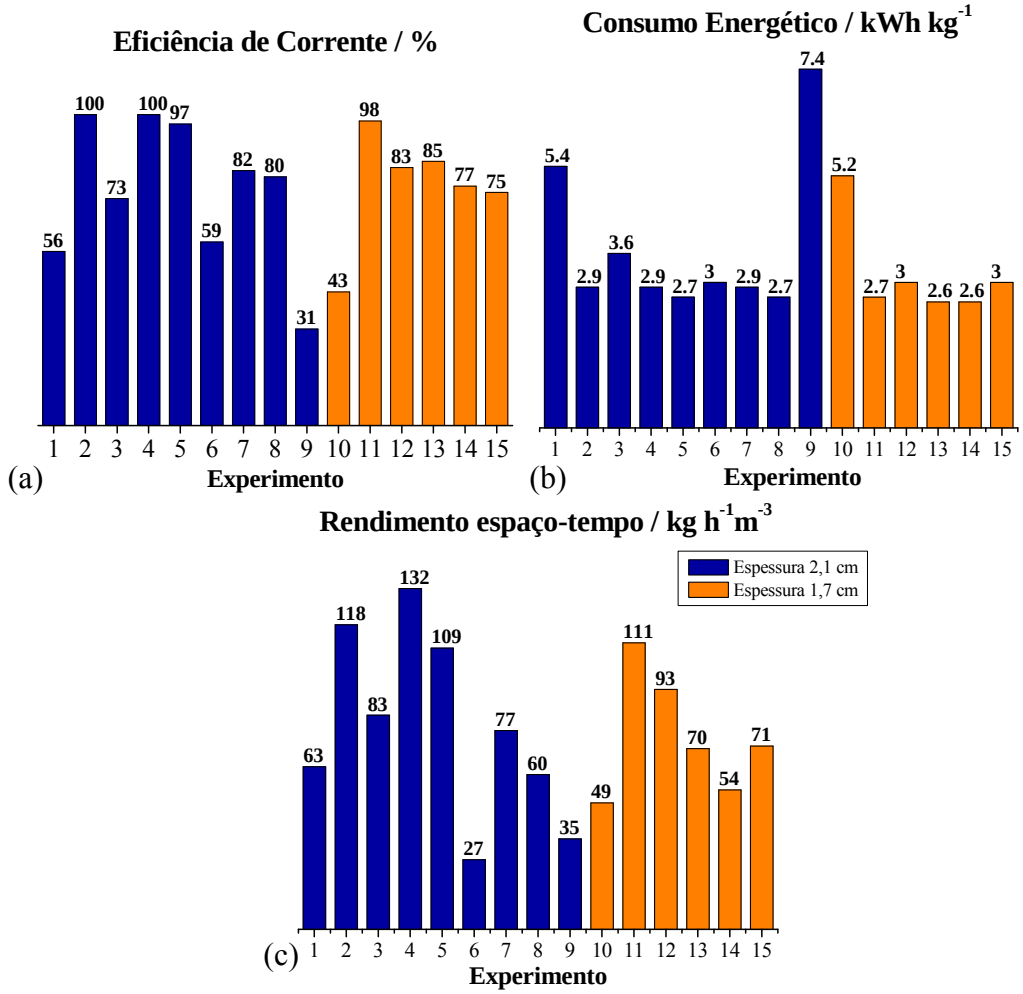

Figura 6.3 – (a) *EC*, (b) *CE* e (c) *Y* em função das condições operacionais para os reatores de espessura 2,1cm (em azul) e 1,3 cm (em laranja).

Desejava-se com a redução da espessura do reator diminuir significativamente o *CE* do processo através da diminuição do potencial de célula e pela redução de possíveis zonas anódicas no interior do cátodo poroso. Entretanto, verificou-se que os resultados do reator de 1,3 cm de espessura não mostraram vantagem alguma comparado ao reator de 2,1 cm de espessura, ou seja, uma redução de 38 % na espessura não foi suficiente para uma redução significativa do consumo energético do processo.

As condições ótimas encontradas por Britto-Costa e Ruotolo (2014)[50] na eletrorrecuperação de cobre em ELP foram 150 g L^{-1} de H_2SO_4, i = 3000 A m^{-2}, 60 s de leito fixo, com fluidização de 2 s, obtendo 77% de *EC*, 2,5 kWh kg^{-1} de *CE* e 61 $kg^{-1}h^{-1}m^{-3}$. Verifica-se que, apesar do ELP apresentar melhores resultados de *CE*, o mesmo é

devido ao fato da condutividade da solução ser bastante superior à utilizada nestes estudos com ELJ, uma vez que a concentração de ácido sulfúrico utilizada nos ensaios do ELP foi muito maior do que a utilizada nestes experimentos. Os autores reportaram ainda problemas de eletrodeposição na tela de separação, o que não foi observado em nenhum experimento com o ELJ, mesmo operando com eletrólito muito menos condutivo. Isto se deve ao fato de que no ELJ as partículas eletricamente carregadas estão em constante movimento, formando um leito móvel, que apresenta características semelhantes às do leito fixo, entretanto não permite, dentro dos limites de *i* estudados, a criação de um depósito dendrítico, responsável por causar curtos-circuitos. Adicionalmente, em nenhum dos experimentos foi evidenciada uma quantidade excessiva de eletrodepósito no alimentador de corrente.

Análise da qualidade do depósito por MEV

Com o intuito de se verificar a qualidade do depósito obtido, foram realizadas microscopias eletrônicas de varredura (MEV) em partículas coletadas antes e após os experimentos de eletrodeposição de cobre. Os resultados são mostrados na Figura 6.5 As Figuras 6.5 (a) e (b) foram realizadas com uma partícula virgem, com aumentos de 250x e 5000x, respectivamente. Verifica-se que se trata de uma superfície que apresenta riscos decorrentes do próprio processo de usinagem do fio de cobre utilizado para a produção das partículas.

A Figura 6.5(c) apresenta a imagem de uma partícula ao final do experimento 9, que foi o ensaio com os piores resultados de *EC* e *CE*. Nota-se que o depósito apresentou grãos muito grandes, em concordância com experimentos de baixa eficiência em ELP. Este tipo de depósito também ocorre nos eletrodos planos convencionais utilizados em indústrias hidrometalúrgicas [50].

As Figuras 6.5(d), (e) e (g), referentes aos experimentos 04, 05 e 11, respectivamente, apresentam características semelhantes entre si, como grãos pequenos e um depósito bastante uniforme, características de depósitos de alta qualidade. Adicionalmente, ao final destes três experimentos, as partículas eram brilhantes e com grande uniformidade entre elas. Com relação a essas três figuras, o depósito mais uniforme foi o do experimento 11, seguido do experimento 04 e por fim o de número 05, de forma que reator de menor espessura apresentou resultado melhor no quesito qualidade

do depósito. Cabe ressaltar que não foi utilizado nenhum aditivo químico visando a melhorar a qualidade do depósito, ou proteger o contra-eletrodo, como ocorre no processo convencional.

A Figura 6.5(f) apresenta a imagem aumentada da partícula ao final do experimento 12, que apesar de ter apresentado resultados satisfatórios, mostra uma piora na qualidade do depósito, devido à ocorrência de grãos maiores e com menor uniformidade, quando comparada ao resultado do experimento 11. Esta diferença foi ocasionada pelo pH do eletrólito, de forma que o eletrólito menos ácido favoreceu a qualidade do depósito, independentemente da condutividade da solução, que foi 47% vezes maior no experimento 12.

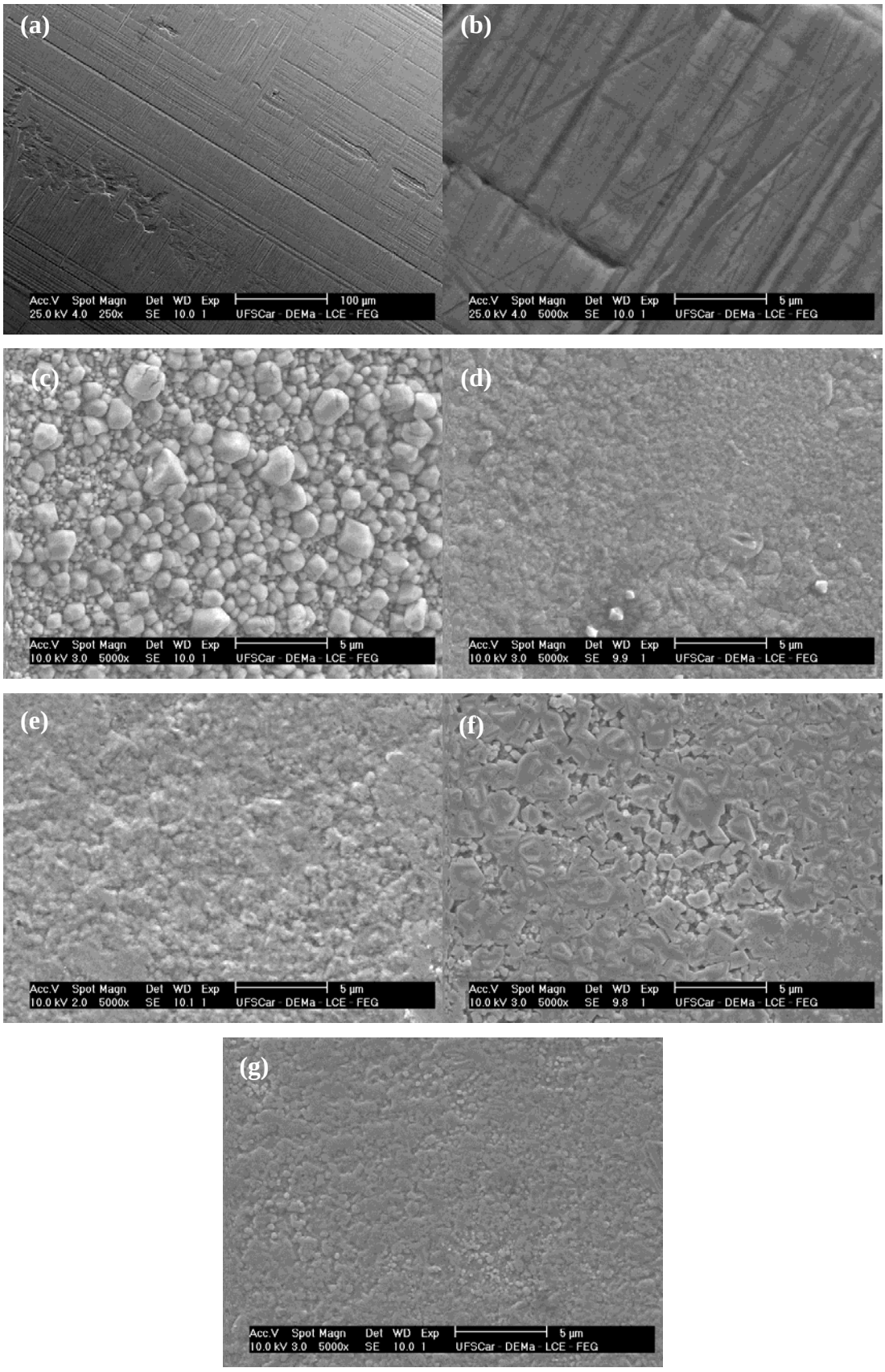

Figura 6.4 – Imagens MEV das partículas de cobrevirgem e ao final de cada experimento. (a) Partícula virgem com aumento de 250x; (b) partícula virgem com 5000x; (c) exp 9; (d) exp. 4; (e) exp. 5; (f) exp. 12; (g) exp. 11.

CONCLUSÕES

O ELJ apresentou boa adequação ao processo de eletrorrecuperação de cobre em solução concentrada, com resultados promissores de eficiência de corrente, rendimento espaço-tempo e qualidade do depósito formado. Apesar do consumo energético de 2,7 kWh kg^{-1} ser considerado relativamente elevado comparado com aquele do processo convencional (1,9 a 2,3 kWh kg^{-1}), dependendo das condições, a economia com aditivos ou mesmo com processos de fundição controlados podem compensar esta diferença no consumo energético. Os melhores resultados obtidos neste trabalho foram nas condições experimentais de maior densidade de corrente (3000 A m^{-2}), solução com maior condutividade (1,8 M Na_2SO_4 e pH 1,0) e temperatura de 40 ºC. Nestas condições foram obtidos valores de 100% de *EC*, 2,7 kWh kg^{-1} de *CE* e rendimento de 118 kg $h^{-1}m^{-3}$, além de um depósito de alta qualidade. Estes resultados quando comparados aqueles relatados para o processo convencional mostram que o ELJ é bastante promissor para a eletrodeposição de cobre.

Agradecimentos

Os autores agradecem ao CNPQ, à FAPESP e à CAPES pelo apoio financeiro que permitiu a realização deste trabalho.

Referências

1. Panda, B.; Das, S. C.; *HYdrometallurgY* **2001**, 59, 55.
2. Wiechmann, E. P.; Morales, A. S.; Aqueveque, P.; *IEEE Trans. Ind. Appl.* **2010**, 46, 1264.
3. Jiricny, V.; Roy, A.; Evans, J. W.; *Metall. Mater. Trans. B* **2002**, 33, 669.
4. Shakarji, R. A.; He, Y.; Gregory, S.; *HYdrometallurgY* **2011**, 106, 113.
5. Cifuentes, L.; Ortiz, R.; Casa, J. M.; *AIChE J.* **2005**, 51, 2273.
6. Evans, J. W.; Ding, R.; Doyle, F. M.; Jiricny, V.; *Scand J. Metall.* **2005**, 34, 363.
7. San Martin, R. M.; Otero, A. F.; Cruz, A.; *HYdrometallurgY* **2005**, 77, 171.
8. Sigley, J. L.; Johnson, P. C.; Beaudoin, S. P.; *HYdrometallurgY* **2003**, 70, 1.
9. Lafront, A. M.; Zhang, W.; Ghali, E.; Houlachi, G.; *ElECtrochim. Acta* **2010**, 55, 6665.
10. Moskalyk, R. R.; Alfantazi, A.; Tombalakian, A. S.; Valic, D.; *Miner. Eng.* **1999**, 12.

11. Coeuret, F.; *J. Appl. ElECtrochem.* **1980**, 10, 687.

12. Lupi, C.; Pilone, D.; *HYdrometallurgY* **1997**, 44, 347.

13. Stankovic, V. D.; Wragg, A. A.; *J. Appl. ElECtrochem.* **1995**, 25.

14. Olive, H.; Lacoste, G.; *ElECtrochim. Acta* **1979**, 24, 1109.

15. El-Shakre, M. E.; Saleh, M. M.; El-Anadouli, B. E.; Ateya, B. G.; *J. ElECtrochem. Soc.* **1994**, 141, 441.

16. Ruotolo, L. A. M.; Gubulin, J. C.; *Braz. J. Chem. Eng.* **2002**, 19, 105.

17. Pletcher, D.; White, I.; Walsh, F. C.; Millington, J. P.; *J. Appl. ElECtrochem.* **1991**, 21, 667.

18. Widner, R. C.; Sousa, M. F. B.; Bertazzoli, R.; *J. Appl. ElECtrochem.* **1998**, 28.

19. Farinos, R. M.; Britto-Costa, P. H.; Ruotolo, L. A. M.; *Environ. TEChnol.* **2012**, 33, 1123.

20. Sabacky, B. J.; Evans, J. W.; *J. ElECtrochem. Soc.* **1979**, 126, 1176.

21. Hadzismajlovic, D. Z. E.; Popov, K. I.; Pavlovic, M. G.; *Powder TEChnol.* **1996**, 86, 145.

22. Kazdobin, K.; Shvab, N.; Tsapakh, S.; *Chem. Eng. J.* **2000**, 79, 203.

23. Thilakavathi, R.; Balasubramanian, N.; Ahmed Basha, C.; *J. Hazard. Mater.* **2009**, 162.

24. Hutin, D.; Coeuret, F.; *J. Appl. ElECtrochem.* **1977**, 7, 463.

25. Bareau, J. Y.; Coeuret, F.; *J. Appl. ElECtrochem.* **1979**, 9, 737.

26. Coeuret, F.; Paulin, M.; *J. Appl. ElECtrochem.* **1988**, 18, 162.

27. Farinos, R. M., UFSCar, 2010.

28. Tonini, G. A.; Farinos, R. M.; Prado, P. F. A.; Ruotolo, L. A. M.; *J Chem TEChnol BiotECHnol* **2013**, 88, 800.

29. Britto-Costa, P. H.; Pereira-Filho, E. R.; Ruotolo, L. A. M.; *HYdrometallurgY* **2014**, 144-145, 15.

30. Cifuentes, L.; Simpson, J.; *Chem. Eng. Sci.* **2005**, 60, 4915.

31. Beukes, N. T.; Badenhorst, J.; *J. S. Afr. I. Min. Metall.* **2009**, 109, 343.

6.3 Conclusões

O ELJ apresentou bons resultados para a eletrorrecuperação de cobre a partir de soluções concentrada, com resultados promissores de eficiência de corrente, rendimento espaço-tempo e qualidade do depósito formado. Se comparados os resultados entre o ELJ e o ELP, verifica-se que o ELP apresentou menor consumo energético devido ao menor potencial de célula proveniente de uma solução com maior concentração de ácido e, consequentemente, mais condutiva. Entretanto, dependendo da aplicação, o ELJ pode ser escolhido por ter apresentado maior rendimento espaço-tempo e melhor qualidade no depósito. Neste estudo a condição ótima obtida foi: 1,8 mol L^{-1}de Na_2SO_4; pH 1,0; T = 40 ºC e e = 2,1 cm, que proporcionou 97% de EC, 2,7 kWh kg^{-1} de CE e 109 kg $m^{-3}h^{-1}$ de Y.

7 CONCLUSÕES E SUGESTÕES PARA TRABALHOS FUTUROS

7.1 Conclusões

As melhorias do processo de eletrorrecuperação de cobre proporcionadas pelos eletrodos tridimensionais utilizados neste trabalho, quando comparados ao eletrodo convencional, mostram que os eletrodos tridimensionais não proporcionam apenas a vantagem de diminuir a espessura da camada limite, portanto sendo eficazes apenas em soluções diluídas. Neste trabalho, ficou claro o potencial deste tipo de reatores em processos de eletrodeposição a partir de soluções concentradas, que visam ao aumento da produtividade. O processo de eletrorrecuperação de cobre em eletrodo de leito pulsante foi otimizado de modo que resultados de *EC* e *CE* foram ainda melhores que no processo convencional e sem a necessidade de se utilizar aditivos que melhorariam a qualidade do depósito. Neste reator, as conclusões obtidas das variáveis estudadas foram:

- A variável tempo de leito fluidizado apresentou efeito negativo no processo, devendo ser diminuída ao mínimo do valor necessário para realizar a homogeneização do meio particulado e impedir o curto-circuito;
- O tempo de leito fixo deve ser mantido entre 54 e 60 s, de forma que valores maiores provocam o curto-circuito do reator e valores menores diminuem a eficiência de corrente;
- Dentre as espessuras estudadas, 2,4 cm foi o valor ótimo de espessura do eletrodo, por proporcionar melhores resultados devido a uma melhor distribuição do sobrepotencial de eletrodo no interior da matriz porosa;
- Os valores ótimos de densidade de corrente estudados foram 3000 A m^{-2} para o reator de maior espessura e 2600 A m^{-2} para o de menor espessura. Verificou-se que a densidade de corrente apresentou efeito positivo para o processo, entretanto valores maiores do que 3000 A m^{-2} acarretam em um curto-circuito do reator nos primeiros 30 min de experimento;
- A concentração de ácido sulfúrico apresentou efeito negativo para a eficiência de corrente, porém reduziu o potencial de célula, consequentemente, reduzindo o consumo energético. Como o seu efeito na *EC* foi mais significativo do que no

potencial de célula, a variável apresentou melhores resultados em valores mais baixos, entre 100 e 116 g L^{-1}.

A condição ótima obtida para a eletrorrecuperação de cobre em ELP foi de 2600 A m^{-2} de *i*, 54 s de t_p, 116 g L^{-1} de H_2SO_4 e espessura de 2,4 cm, proporcionando 100% de *EC*, 1,7 kWh kg^{-1} de *CE* e 76 kg $m^{-3}h^{-1}$ de *Y*, valores muito superiores aos obtidos no processo convencional da indústria hidrometalúrgica.

O eletrodo de leito de jorro se mostrou melhor do que o ELP em soluções de menor condutividade sem ocorrer o curto-circuito, como ocorreu com o ELP para soluções com menos do que 100 g L^{-1} de H_2SO_4 e isto é devido ao fato das partículas no *anulus* estarem em constante movimento. O ELJ mostrou ser ainda superior ao ELP com relação ao rendimento espaço-tempo e qualidade do depósito, entretanto não foi possível reduzir o consumo energético à faixa de valores do processo convencional. Neste reator, as conclusões obtidas das variáveis estudadas foram:

- Melhores condições foram obtidas com um aumento da densidade de corrente, de forma que 3000 A m^{-2} foi o valor ótimo. Ressalta-se que este valor de densidade é o mesmo que o ELP de 3,4 cm de espessura, ou seja, é possível de se aplicar densidades de corrente mais altas do que no ELP sem ocorrer entrave do curto-circuito;
- A condutividade da solução favorece o processo, entretanto, valores de pH muito baixos acarretam em uma diminuição da *EC*, portanto, deve-se operar com uma solução de maior condutividade possível e pH acima de 1. Neste trabalho, não foi possível de se trabalhar com mais do que 1,8 mol L^{-1}de Na_2SO_4 por problemas de precipitação do sal;
- A temperatura do eletrólito foi desfavorável ao processo por aumentar a dissolução de cobre no canal central, onde as partículas estão desprotegidas do ataque ácido, sendo 40 ºC a melhor temperatura estudada;
- A diminuição da espessura do eletrodo não proporcionou, diferentemente do ELP, melhorias no processo, de forma que o melhor resultado foi obtido para a maior espessura. Esperava-se, de acordo com experiência obtida com o ELP, que uma redução da espessura do eletrodo iria melhorar a distribuição de sobrepotencial de eletrodo e diminuir o potencial de célula, entretanto isto não ocorreu.

A condição ótima obtida para a eletrorrecuperação de cobre em ELJ foi: 1,8 mol L^{-1}de Na_2SO_4; pH 1,0; T = 40 ºC e *e* = 2,1 cm, que proporcionou 97% de *EC*, 2,7 kWh kg^{-1} de *CE* e 109 kg $m^{-3}h^{-1}$ de *Y*.

7.2 Sugestões para trabalhos futuros

As sugestões para trabalhos futuros são:

- Realizar um estudo de eletrorrecuperação de cobre em ELP em escala piloto;
- Realizar um estudo sobre a eletrorrecuperação de zinco em ELP, uma vez que 80% do zinco tem sido obtido via rota hidrometalúrgica;
- Realizar um estudo da eletrorrecuperação de zinco em ELJ;
- Realizar um estudo do processo completo: lixiviação, flotação, purificação e eletrorrecuperação para avaliar novas condições operacionais.

REFERÊNCIAS BIBLIOGRÁFICAS

ALAM, M. S.; TANAKA, M.; KOYAMA, K. et al. Electrolyte purification in energy-saving monovalent copper electrowinning processes. **Hydrometallurgy**, 87, p. 36-44, 2007.

ARGONDIZO, A. **Remoção de íons cobre de soluções aquosas diluídas em eletrodo de leito pulsante**. 131, Tese de Doutorado Tese, Universidade Federal de São Carlos, São Carlos-SP, Brasil, 2001.

BAREAU, J. Y. ; COEURET, F. The anodic dissolution of copper in a fluidized bed electrode. **Journal of Applied Electrochemistry**, 9, p. 737-743, 1979.

BEUKES, N. T. ; BADENHORST, J. Copper electrowinning: theoretical and practical design. **Journal of the Southern African Institute of Mining and Metallurgy**, 109, p. 343-356, 2009.

BRITTO-COSTA, P. H. ; RUOTOLO, L. A. M. Mass transfer study on the electrochemical removal of copper ions from synthetic effluents using reticulated vitreous carbon. **Environmental Technology**, 34(4), p. 437-444, 2013.

CIFUENTES, L.; ORTIZ, R. ; CASA, J. M. Electrowinning of copper in a lab-scale squirrel-cage cell with anion membrane. **American Institute of Chemical Engineers Journal**, 51(8), p. 2273-2284, 2005.

COEURET, F. The fluidized bed electrode for the continuous recovery of metals. **Journal of Applied Electrochemistry**, 10, p. 687-696, 1980.

COEURET, F. ; PAULIN, M. Experiments on copper recovery in a pulsed granular fixed bed electrode. **Journal of Applied Electrochemistry**, 18, p. 162-165, 1988.

DOHERTY, T.; SUNDERLAND, J. G.; ROBERTS, E. P. L. et al. An improved model of potential and current distribution within a flow-through porous electrode. **Electrochimica Acta**, 41, p. 519-526, 1996.

EL-SHAKRE, M. E.; SALEH, M. M.; EL-ANADOULI, B. E. et al. Applications of porous flow-through electrodes. **Journal of the Electrochemistry Soc.iety**, 141(2), p. 441-447, 1994.

EVANS, J. W.; DING, R.; DOYLE, F. M. et al. Copper electrodeposition onto extended surface area electrodes and the treatment of copper containing waste streams. **Scandinavian Journal of Metallurgy**, 34, p. 363-368, 2005.

GARFIAS-VASQUEZ, F. J.; DUVERNEUIL, P. ; LACOSTE, G. Behaviour, modelling and simulation of a pulsed three-dimensional radial electrode with continuous solid flow: Part I. **Journal of Applied Electrochemistry**, 34, p. 417-426, 2004.

GOODRIDGE, F. ; SCOTT, K. **Electrochemical Process Engineering**. New York, Plenum Press, 1995. p.

GUBULIN, J. C. Transferência de Massa Em Sistemas Particulados: Aplicações A Sistemas Eletroquímicos. **Tópicos Especiais em Sistemas Particulados**. J. T. Freire. São Carlos-SP, Gráfica da UFSCar, 1998.

HABASHI, F. A short history of hydrometallurgy. **Hydrometallurgy**, 79, p. 15-22, 2010.

HADZISMAJLOVIC, D. Z. E.; POPOV, K. I. ; PAVLOVIC, M. G. The visualization of the electrochemical behavior of metal particles in spouted, fluidized and packed beds. **Powder Technology**, 86, p. 145-148, 1996.

HERRERO, D.; ARIAS, P. L.; GÜEMEZ, B. et al. Hydrometallurgical processes development for the production of a zinc sulphate liquor suitable for electrowinning. **Minerals Engineering**, 23, p. 511-517, 2010.

JIRICNY, V.; ROY, A. ; EVANS, J. W. Copper electrowinning using spouted-bed electrodes: part I. Experiments with oxygen evolution or matte oxidation at the anode. **Metallurgy and Materials Transactions B**, 33, p. 669-676, 2002.

LAFRONT, A. M.; ZHANG, W.; GHALI, E. et al. Electrochemical noise studies of the corrosion behavior of lead anodes during zinc electrowinning maintenance. **Electrochimica Acta**, 55, p. 6665-6675, 2010.

LUPI, C. ; PILONE, D. New lead alloy anodes and organic depolarizer utilization in zinc electrowinning. **Hydrometallurgy**, 44, p. 347-358, 1997.

MOSKALYK, R. R.; ALFANTAZI, A.; TOMBALAKIAN, A. S. et al. Anodes effect in electrowinning. **Minerals Engineering**, 12(1), p., 1999.

NEWMAN, J. S. **Electrochemical Systems**. London, Prentice-Hall, 1973. p.

NORGATE, T. ; JAHANSHAHI, S. Low grade ores – smelt, leach or concentrate? **Minerals Engineering**, 23, p. 65-73, 2010.

OLIVE, H. ; LACOSTE, G. Application of volumetric electrodes to the recuperation of metals in industrial effluents-I. Mass transfer in fixed beds of spherical conductive particles. **Electrochimica Acta**, 24, p. 1109-1114, 1979.

PANDA, B. ; DAS, S. C. Electrowinning of copper from sulfate electrolyte in presence of sulfurous acid. **Hydrometallurgy**, 59, p. 55-67, 2001.

PLETCHER, D. ; WALSH, F. C. **Industrial Electrochemistry**. Cambridge, Chapman and Hall, 1990. p.

PLETCHER, D.; WHITE, I.; WALSH, F. C. et al. Reticulated vitreous carbon cathodes for metal ion removal from process streams Part II: Removal of copper(II) from acid sulphate media. **Journal of Applied Electrochemistry**, 21, p. 667-671, 1991.

PONTE, M. J. J.; PONTE, H. A. ; GUBULIN, J. C. **Distribuição de sobrepotenciais em eletrodo de leito fluidizado**. Anais do XXI ENEMP, Ouro Preto-MG, 1994.

RAJESHVAR, K. ; IBANEZ, J. G. **Environmental Electrochemistry**. London, Harcourt Brace, 1997. p.

RUOTOLO, L. A. M. **Estudo cinético e hidrodinâmico da eletrodeposição de íons cobre em eletrodos tridimensionais de leito fixo**, Dissertação de Mestrado, UFSCar, São Carlos-SP, 1998.

RUOTOLO, L. A. M. ; GUBULIN, J. C. Electrodeposition of copper ions on fixed bed electrodes: kinetic and hydrodynamic study. **Brazilian Journal of Chemical Engineering**, 19(1), p. 105-118, 2002.

SALAS-MORALES, J. C.; EVANS, J. W.; NEWMAN, O. M. G. et al. Spouted bed electrowinning of zinc: Part I. Laboratory-scale electrowinning experiments. **Metallurgy and Materials Transactions B**, 28B, p. 59-68, 1997.

SAN MARTIN, R. M.; OTERO, A. F. ; CRUZ, A. Use of quillaja saponins (Quillaja saponaria Molina) to control acid mist in copper electrowinning processes Part 2: pilot plant and industrial scale evaluation. **Hydrometallurgy**, 77, p. 171-181, 2005.

SHAKARJI, R. A.; HE, Y. ; GREGORY, S. Statistical analysis of the effect of operating parameters on acid mist generation in copper electrowinning. **Hydrometallurgy**, 106, p. 113-118, 2011.

SIGLEY, J. L.; JOHNSON, P. C. ; BEAUDOIN, S. P. Use os nonionic surfactant to reduce sulfuric acid mist in the copper electrowinning process. **Hydrometallurgy**, 70, p. 1-8, 2003.

SILVA-MARTÍNEZ, S. ; ROY, S. Copper recovery from tin stripping solution: galvanostatic deposition in a batch-recycle system. **Separation and Purification Technology**, 118, p. 6-12, 2013.

SILVA, A. P. **Eletrosseparação de íons cobre, em eletrodo de escala piloto, em escala industrial**, Tese de Doutorado, UFSCar, São Carlos-SP, 2000.

STANKOVIC, V. D. ; WRAGG, A. A. Modelling of time-dependent performance criteria in a three-dimensional cell system during batch recirculation copper recovery. **Journal of Applied Electrochemistry**, 25, p., 1995.

TICIANELLI, E. A. ; GONZÁLEZ, E. R. **Eletroquímica, Princípios e Aplicações**. São Paulo-SP, EDUSP, 1998. p.

VETTER, K. J. **Electrochemical Kinetics**. London, Academic Press, 1967. p.

WIDNER, R. C.; SOUSA, M. F. B. ; BERTAZZOLI, R. Electrolytic removal of lead using a flow-through cell with a reticulated vitreous carbon cathode. **Journal of Applied Electrochemistry**, 28, p., 1998.

WIECHMANN, E. P.; MORALES, A. S. ; AQUEVEQUE, P. Improving productivity and energy efficiency in copper electrowinning plants. **IEEE Transactions on Industrial Applications**, 46, p. 1264-1269, 2010.